

Title	STRUCTURE AND STABILITY OF BENICE JONES PROTEINS
Author(s)	Azuma, Takachika
Citation	大阪大学, 1974, 博士論文
Version Type	VoR
URL	https://hdl.handle.net/11094/1574
rights	
Note	

Osaka University Knowledge Archive : OUKA

<https://ir.library.osaka-u.ac.jp/>

Osaka University

STRUCTURE AND STABILITY OF BENCE JONES PROTEINS

TAKACHIKA AZUMA

Department of Biology, Faculty of Science, Osaka University

CONTENTS

I	Introduction	1
II	Experimental	11
II-1	Materials	11
(1)	Bence Jones proteins	
(2)	Other reagents	
II-2	Methods	13
(1)	Amino acid analysis	
(2)	Potentiometric titration	
(3)	Spectrophotometric titration	
(4)	Difference absorption spectroscopy	
(5)	Optical rotation	
(6)	Circular dichroism	
(7)	Acetylation with N-acetylimidazole	
(8)	Reaction with 2-hydroxy-5-nitrobenzyl bromide	
(9)	Reduction of disulfide bonds	
(10)	Modification with fluorescein mercuric acetate	
III	Results	21
III-1	States of ionizable groups	21
III-2	States of tyrosyl and tryptophyl residues	24
III-3	Modification with fluorescein mercuric acetate	28
III-4	Denaturation by guanidine hydrochloride	40

	III-5	Denaturation by urea	58
	III-6	pH Dependent conformational changes	74
IV		Discussion	94
	IV-1	States of ionizable groups	94
	IV-2	States of tyrosyl and tryptophyl residues	104
	IV-3	Domain structure	109
	IV-4	Stability against denaturants	112
	IV-4-1	Denaturation by guanidine hydrochloride	112
	IV-4-2	Denaturation by urea	121
	IV-4-3	pH Dependent conformational changes	125
V		Conclusion	130
		Acknowledgement	133
		References	134

ABBREVIATIONS

CD	Circular dichroism
DTN	5,5'-Dithiobis-(2-nitrobenzoic acid)
DTT	Dithiothreitol
FMA	Fluorescein mercuric acetate
GuHCl	Guanidine hydrochloride
HNB bromide	2-Hydroxy-5-nitrobenzyl bromide
NAI	N-Acetylimidazole
ORD	Optical rotatory dispersion

I INTRODUCTION

Immunoglobulins are proteins of animal origin endowed with known antibody activity, and also include certain proteins related to antibodies in chemical structure and antigenic specificity. Structural studies have shown that all the immunoglobulins are multichain proteins which consist of a four-chain unit containing two light and two heavy chains (1). These proteins are usually heterogeneous and a family of proteins in the γ -globulin fraction of the blood. Therefore, it is difficult to carry out the chemical analysis even on preparation of highly purified antibody to a single hapten antigen.

A group of proteins called Bence Jones protein is found in the urine of patients who suffer from multiple myeloma. Henry Bence Jones described this urinary protein at first, so that it was named after him (2). Since the disease of multiple myeloma is usually associated with malignant proliferation of plasma cells, large amount of proteins (myeloma protein) are secreted into the serum and Bence Jones proteins excreted in the urine. Myeloma proteins are homogeneous and classified as immunoglobulins because of their similarity in site of synthesis, polypeptide chain structure, and antigenic specificity. Edelman and Gally (3) demonstrated that Bence Jones proteins are homogeneous light chains of the myeloma proteins not incorporated into whole molecules.

On the basis of antigenic analysis, Bence Jones proteins have been

classified into two types, χ and λ (4, 5). The light chains are classified into two types and determine the antigenic type of their parent immunoglobulins either χ or λ (6). The heavy chains determine the class of immunoglobulins (6-10).

Because the Bence Jones proteins are homogeneous, available in large amounts and smaller than a whole immunoglobulin molecule, they have been studied in detail. However, there are some difficulties in the studies of Bence Jones proteins. One is related to the variation of amino acid sequences for each patient (as described below). This variation is thought to be related to antibody specificity (11). It is difficult to find out the common properties to all Bence Jones proteins so far as one or two specimens were studied, because each specimen reveals to individual specific properties which are derived from different amino acid sequences from specimen to specimen. Another difficulty in the studies of Bence Jones proteins arises from the limitation of the amount of samples. The patients of multiple myeloma die ordinarily within one or two years, or if happily recovered, they do not excrete Bence Jones proteins again. Thus, no two Bence Jones proteins which have precisely the same properties are obtainable.

Most Bence Jones proteins have sedimentation coefficients of about 3.5 S, which correspond to the molecular weight of about 45,000 (12). Edelman and Gally (3) showed that the light chains of myeloma proteins have the molecular weight of approximately 20,000, therefore, 3.5 S

Bence Jones proteins exist as dimers of light chains. The dimer of Bence Jones proteins occurs in two forms; dissociable dimer in which the chains are linked by non-covalent interaction, and stable dimer in which the chains are linked by non-covalent interaction and disulfide bond. Both dissociable dimers and reduced stable dimers dissociate into monomers in 1 M propionic acid or 6 M guanidine hydrochloride solution (13, 14). Some Bence Jones proteins do occur naturally as 1.8-2.5 S units (monomer)(15).

The shape of Bence Jones proteins has been studied by low angle X-ray scattering and hydrodynamic measurements by Holasek et al. (16, 17). The hydrodynamic data showed that the molecular weight was 43,000, partial specific volume (\bar{v}); 0.736 ml/mg, sedimentation coefficient ($s_{20,w}$); 3.6 S, diffusion constant ($D_{20,w}$); 7.71 cm²/sec, frictional coefficient ratio (f/f_0); 1.19. Since the f/f_0 value of the typical globular proteins lies in the range of 1.10 to 1.25, the Bence Jones protein appears to be a globular protein. Low angle X-ray scattering data showed that the molecular weight was 43,000, particle volume; 75,200 Å³, radius of gyration; 26.3 Å, specific surface; 0.190 Å⁻¹, the three average major particle axes ; 21.0 Å, 48.3 Å, 74.8 Å, which correspond respectively to axial ratio 1 : 2.3 : 3.6.

Optical rotatory dispersion (ORD) measurements of Bence Jones proteins, carried out by Hamaguchi and Migita, yield low values of the Moffitt-Yang parameter b_0 , suggesting the absence of α -helix (18).

Jirgensons et al.(19) studied ORD spectra in the ultraviolet regions and suggested the presence of β -structure. Ikeda et al.(20) studied the circular dichroism (CD) of Bence Jones proteins and found a negative maximum at 216 nm corresponding to β -structure. They also suggested that Bence Jones proteins can be classified into either κ or λ antigenic type on the basis of the CD bands at 216, 230, and 300 nm, though there were a few exceptions in their results (20). The CD and ORD spectra of immunoglobulins also showed the presence of β -structure (21-24).

Bence Jones proteins have been known for their unusual thermal solubility properties of precipitation when heated to about 50°C, dissolution at near boiling, and reprecipitation on cooling (2). Neet and Putnam (25) studied on the thermal denaturation of Bence Jones proteins by ultracentrifugation. They found that the polymerization and depolymerization processes at various temperatures corresponded to the precipitation reactions.

Hamaguchi and Migita (26) studied denaturations of Bence Jones proteins by 2-chloroethanol, guanidine hydrochloride, and lithium salts. They found the different changes of Moffitt-Yang parameter b_0 between κ and λ proteins in 2-chloroethanol solution. They also suggested that the antigenic types of Bence Jones proteins can be identified on the basis of the ratio ΔOD_{293} to ΔOD_{286} of the difference absorption spectra produced by the addition of guanidine

hydrochloride (26, 27).

Studies on amino acid sequences show that Bence Jones proteins have unusual structural features (28). One unique structural characteristic of Bence Jones proteins is that both κ and λ chains are divisible into an amino-terminal variable region (residues 1 to 108) and a carboxyl-terminal constant region (residues 109 to 214). Variable regions of different proteins have diverse amino acid sequences, while constant regions differ in only a few residues. The amino acid substitution was observed in only one position (position 191) in the constant region of κ proteins, which was associated with the Inv genetic factor. In the case of λ proteins, the substitution occurred at positions of 144, 155, 172, and 190. The position at 190 is related with the Gm genetic factor. The significance of other variations in the constant regions of λ proteins is not understood yet (28). As mentioned above, the diversity of amino acid sequences of variable regions is observed in both antigenic type proteins. The sequence differences observed between any two proteins have ranged from 16 to 60. On the average, the substitution occurred in about 40 of the first 108 residues. Bence Jones proteins differ not only in sequence but also in length in the variable region. The length of the proteins vary from 213 to 221 residues.

Another feature shared by all Bence Jones proteins is the presence of two intrachain disulfide bonds, each forming a loop of about 60

amino acid residues. These are symmetrically distributed; one is within the variable region and the other in the constant region of the chain (11). It is supposed that this apparent symmetry results in a gross similarity in the conformation of two regions.

Another general feature is the presence of a cysteine residue at the constant regions, which provides a link to a heavy chain or a light chain. This cysteine residue is the last residue in κ proteins and is the penultimate residue in λ proteins.

Although the locations in the primary structure is not so precisely conservative as that of disulfide bonds, the tryptophyl residues are present in the relatively fixed positions. In most κ proteins, two tryptophyl residues are present at position 35 in the variable region and 148 in the constant region. In the case of λ proteins, three tryptophyl residues at position 34 (in the variable region), 150, and 187 (in the constant region) are invariant. The tryptophyl residue at position 90 in some λ proteins is replaced by a tyrosyl or arginyl residues in other λ proteins. The locations of tyrosyl residues are also less frequently substituted than other residues (28).

Hamaguchi et al.(27) studied the spectrophotometric titrations of Bence Jones proteins and showed that the ionization of tyrosyl residues was abnormal. It is interesting to investigate the states of these residues of Bence Jones proteins in the three dimensional structure of the protein molecule.

The author studied the states of amino acid residues by means of hydrogen ion equilibria, chemical modifications and difference absorption spectra. The studies of hydrogen ion equilibria afford information about the location of the amino acid residues with ionizable groups. The titration data showed that all of the carboxyl and α - and ϵ -amino groups are available for titration with normal pK values. One of two histidyl and eight of nine tyrosyl residues are not titrated in the pH region between 4 and 10.2. The reactivity of tyrosyl residues was studied by use of N-acetylimidazole (NAI) and found the presence of one or two highly NAI-reactive tyrosyl residue(S) in Bence Jones proteins. The most NAI-reactive tyrosyl residue was estimated to be Tyr-173 in the constant regions of κ Bence Jones proteins. The states of tryptophyl residues were investigated by means of difference absorption spectra and chemical modifications with 2-hydroxy-5-nitrobenzyl bromide. It was found that all the tryptophyl residues (two) of a κ protein and two of three residues of a λ protein are buried in the interior of the protein molecule. One tryptophyl residue exposed on the surface was estimated to be Trp-186 in the constant region of λ proteins.

In 1969, Edelman (28, 29) proposed that the constant and variable regions of Bence Jones proteins are folded into a compact domain, on the basis of amino acid sequence studies described above. Previously, the smaller polypeptides than the monomer of Bence Jones proteins

were found in the urine of some patients (30-34). In most cases, these polypeptides were identified to be the variable region (half) of the Bence Jones proteins. Solomon and McLaughlin (35) demonstrated that Bence Jones proteins can be cleaved into the constant and variable halves by proteolytic enzymes. Björk et al. (36) and Ghose and Jirgensons (37) studied on the conformation of Bence Jones proteins by use of the constant and variable halves obtained by limited proteolysis by means of ORD and CD spectra, and supported the domain hypothesis. Concurrently, the author studied the domain structure of Bence Jones proteins by use of another approach. As described above, the stable dimer of Bence Jones proteins has four intrachain and one interchain disulfide bonds. The interchain disulfide bond is much more susceptible to reduction than the intrachain disulfide bonds. The organic mercury compound (in the present experiment, fluorescein mercuric acetate (FMA) was used) was conjugated with the cysteine residue produced by the selective reduction. It is known that absorption bands of a chromophoric groups which are optical inactive when it is free in solution are rendered optically active by interaction with an asymmetric environment of the protein molecule and the extrinsic Cotton effects thus generated serve as subtle probe of the local conformation of the protein molecule (38-41). Since the interchain disulfide bond is located at the carboxyl-terminus in the κ proteins and at the penult in the λ proteins (28), the extrinsic Cotton effect

of FMA introduced at this position was expected to reflect the local conformation of the carboxyl terminal half of the protein molecule. The FMA-Bence Jones protein conjugates of κ proteins showed similar CD spectra with one another in signs and positions of the bands. These results suggested that the constant region of Bence Jones proteins folded independently with little effect of the variable region.

Recently, X-ray crystallographic studies on κ and λ Bence Jones proteins showed that the constant and variable halves folded independently and they were connected with each other by more extended polypeptide stretch (42, 43).

It is interesting to examine whether the stability of the constant and variable domains of the Bence Jones proteins toward denaturants is different from each other or not. The author has studied the denaturation of Bence Jones proteins by guanidine hydrochloride, urea, and acid. The denaturations of Bence Jones proteins do not proceed in the simple two-state transition between the native and denatured states. The different stability of the constant and variable halves was observed in the denaturations. The results of difference absorption spectra and CD spectra measurements suggest that the constant half is less stable than the variable half.

As described above briefly, the author reports the studies on the structure and stability of Bence Jones proteins in the present paper. The immunoglobulins consist of much more domains than Bence Jones

proteins. The findings in the studies of Bence Jones proteins would contribute to understanding of the structural properties of immunoglobulins.

II EXPERIMENTAL

II-1 Materials

(1) Bence Jones Proteins----- Urine samples containing Bence Jones proteins were obtained from patients with multiple myeloma. The urine specimen decolorized (not perfectly) with charcoal was precipitated with 60 to 80 % saturated ammonium sulfate at pH 5-6. The precipitate was dialyzed against distilled water, then against 0.02 M phosphate buffer at pH 7-8. The crude Bence Jones protein sample contains some components such as albumin, glycoprotein, transferrin, and γ -globulin of which amounts differ specimen to specimen. The isolation of major component was achieved by means of gel filtration (Sephadex G-100) and ion-change chromatography (DEAE-Sephadex A-50 or DEAE-cellulose). The buffer systems used in ion-exchange chromatography were 0.02 M phosphate buffer solutions at pH 7-8 with increasing molarity of sodium chloride up to 1 M. Rechromatography on Sephadex G-100 or Sephadex G-75 was carried out, if necessary. The homogeneity of isolated Bence Jones protein was analyzed by use of polyacrylamide gel electrophoresis and immunoelectrophoresis. The purified Bence Jones protein was dialyzed against distilled water and lyophilized. The antigenic type of Bence Jones protein was determined by the Ouchterlony method or immunoelectrophoresis, using rabbit antisera to type κ and λ Bence Jones proteins. Most of the Bence Jones proteins were provided by Professor Migita, Kanazawa University.

Bence Jones proteins used in the present experiments were stable dimers. Bence Jones proteins are referred to by symbols indicating the individual patient (e.g. Ta, Ni,).

(2) Reagents————— N-Acetylimidazole (NAI), 2-hydroxy-5-nitrobenzyl bromide (HNB bromide), fluorescein mercuric acetate (FMA) were purchased from Nakarai Pure Chemicals Co. Dithiothreitol (DTT) and 5,5'-dithiobis-(2-nitrobenzoic acid) (DTN) were purchased from Wako Pure Chemicals Co.

Urea was obtained from Nakarai Pure Chemicals Co. and recrystallized from 80 % ethanol. Guanidine hydrochloride (GuHCl) was purchased from Nakarai Pure Chemicals Co. and recrystallized from ethanol-benzene and again from water (44). Tris (hydroxymethyl) aminomethane was obtained from Sigma Chemicals Co. and recrystallized from 70 % ethanol or 80 % methanol.

Rabbit antisera against human IgG and human serum proteins were purchased from the Research Institute for Microbial Diseases, Osaka University. Rabbit antisera against a type χ and λ Bence Jones proteins were kindly donated from Professor Migita, Kanazawa University.

All other chemicals were reagent grade and used without further purification.

II-2 Methods

(1) Amino Acid Analysis-----Samples (Ta protein, type K) were hydrolyzed in 6 N HCl for 15, 24, 48, 72, and 96 hr at 110°C and analyzed in a Hitachi automatic amino acid analyzer, model KLA-3B. The procedure of analysis followed with this instrument was essentially the same as that of Spackman et al.(45). In calculating the amino acid composition, correction was made for moisture content of the lyophilized samples by using the value of 214 for the total numbers of residues of the type χ Bence Jones proteins as a monomer form.

Tryptophan content was estimated from tyrosine to tryptophan ratio determined by the spectrophotometric method of Goodwin and Morton (46).

(2) Potentiometric Titration-----Solutions containing 0.5 to 0.8 g of protein per 100 ml of 0.15 M KCl prepared with boiled deionized water were dialyzed against 100 volumes of the same 0.15 M KCl in capped flask for at least 48 hr with four changes of the outer solution. The pH of the inner protein solution thus obtained was found to be 6.3-6.5. A continuous titration was carried out under wet and CO₂-free nitrogen in a water-jacketed cell at 25 ± 0.1°C on Radiometer pH meter type PHM 4d using a G2222B glass electrode and a K4112 calomel electrode. Radiometer standard buffers, pH 4.65, 6.48, and 9.18 at 25°C, were used to standardize the pH meter. If the difference in the value of pH of the buffer before and after the titration exceeded 0.02 pH unit,

the run was discarded. In each experiment, 5.0 ml of the protein solution in 0.15 M KCl after dialysis was placed in the titration cell, thermostated at 25.0°C, and the system was stirred for 30 min in atmosphere of nitrogen for temperature equilibration. Then either HCl or KOH was added from a microburette of 1.000 ml capacity. After the solution was stirred for 3 to 5 min with a glass-enclosed stirring bar on a magnetic stirrer and the pH was stabilized, the pH was measured. Similar titration was performed on 5.0 ml of the solvent blank (0.15 M KCl). The titration curve of the protein was obtained by subtracting the value of the solvent blank from that of the protein solution.

(3) Spectrophotometric Titration-----Ultraviolet absorption was measured with a Hitachi-Perkin Elmer spectrophotometer model 139, using 1 cm quartz cell, at 25°C. The absorbance of an alkaline solution of the protein was read against a neutral protein solution. The difference spectra for the ionization of the tyrosyl groups have two maxima: one at 295 nm and the other at 245 nm. In the present experiments, the titration was performed at 245 nm. The buffers used for the titration were as follows: Tris-HCl (pH 7-8.7), glycine-KOH (pH 9-12.5). The ionic strength of these buffer solutions was adjusted with KCl. Measurements of pH were made on Toa-Dempa pH meter model HM-8 at 25°C.

(4) Difference Absorption Spectra-----Difference spectra were

recorded with a Hitachi automatic recording spectrophotometer, model EPS-3T or model 124. The absorbance of a solution of Bence Jones protein at a given pH or at a given denaturant concentration was read against a solution of the protein of a reference pH or in the absence of denaturants. The ionic strength of the solutions was adjusted with KCl. The concentrations of Bence Jones proteins used for the spectral measurements were in the range of 0.02 to 0.05 %. All the solutions were allowed to stand for 20 hr at room temperature before measurements.

(5) Optical Rotation————— Measurements of optical rotation were carried out using a Jasco spectropolarimeter, model J-20. The measurements were made at a protein concentration of about 0.05 % in a 1.0 cm cell. The optical rotation was expressed in terms of the mean residue rotation, $[m']$, defined as

$$[m']_{\lambda} = \frac{3}{n^2 + 2} \cdot \frac{M_0}{100} \cdot [\alpha]_{\lambda} \quad (1)$$

where $[\alpha]_{\lambda}$ is the specific rotation at wavelength λ , M_0 is the average residue weight and n is the refractive index of the solvent at wavelength λ . The refractive indices as a function of wavelength were obtained from those tabulated by Fasman (47). The refractive index of GuHCl solution at 250 nm, as a function of the concentration, was obtained by approximating that $(n^2 + 2)$ for GuHCl solutions remains

in a fixed ratio to $(n^2 + 2)$ for pure water. The refractive indices of GuHCl solutions at 589 nm were taken from the results of Kielly and Harrington (48). The refractive index of urea solution at 250 nm as a function of the concentration, was obtained by the same procedure as that of GuHCl solutions. The refractive indices of urea solutions at 589 nm were taken from the table given by Fasman (47). GuHCl and urea solutions were always freshly prepared before measurements.

(6) Circular Dichroism———CD measurements were carried out with a Jasco automatic recording spectropolarimeter, model J-20 or model ORD/UV-5, equipped with a CD attachment. The instrument was calibrated with d-10-camphorsulfonic acid (49, 50). The mean residue ellipticity, $[\theta]$, was obtained by the equation,

$$[\theta] = 3,300 (\epsilon_L - \epsilon_R) \quad (2)$$

where $(\epsilon_L - \epsilon_R)$ is the difference between the molar extinction coefficients for left and right circularly polarized light. The average residue weight was used in calculation of $(\epsilon_L - \epsilon_R)$ with the exception of FMA-conjugated with Bence Jones protein. In the case of FMA-Bence Jones protein conjugates, molecular ellipticities were expressed in units of degrees cm^2 per dmole of FMA. Cell path-length and protein concentrations were chosen so that the total absorbance

was always less than 2 over the region. The temperature was controlled by use of a thermostatically controlled cell holder at 25°C.

In the experiments of denaturation, all the solutions were allowed to stand in a thermostat at 25°C for about 20 hr before spectral measurements.

(7) Acetylation with NAI-----Acetylation of the tyrosyl groups of Bence Jones proteins were carried out by the method of Riordan et al.(51). To 4 mg of a Bence Jones protein per ml of 0.01 M Tris buffer containing 0.15 M KCl at pH 7.5 or 0.05 M sodium borate buffer at pH 7.5, was added 30- to 300-fold molar excess of NAI, and the reaction was allowed to continue for one hour. The reaction mixture was then dialyzed for 20 hr against several changes of 0.15 M KCl at 5°C.

The extent of modification of the tyrosyl residues was determined from the decrease in the absorbance at 278 nm using a factor of 1,160 cm^{-1} per mole of tyrosyl residue (51). The number of tyrosyl residues acetylated is expressed on the basis of the molecular weight of 22,500. Deacetylation of the modified protein was carried out with 1 M hydroxylamine at pH 7.5, 25°C for an hour.

(8) Reaction with HNB Bromide-----Modification of tryptophyl residues of Bence Jones proteins was carried out according to the method of Koshland, Jr. et al.(52, 53). To 3 ml of a protein solution of about 1 % in 0.15 M KCl, or in a urea solution containing 0.15 M KCl, both at pH 5, was added 50-fold molar excess of HNB bromide at

25°C. The pH was maintained at 5 during the reaction by adding small increment of 1 N KOH (54). Because of the insolubility of Bence Jones proteins in aqueous organic solvents, HNB bromide powders were added directly to the protein solution. The reaction was carried out for one or two hours. After a small amount of precipitates formed during the reaction had been filtered off, the modified protein was separated from the reagent by gel filtration on a Sephadex G-25 column (1.5 x 50 cm), equilibrated with the same solvent as used for the modification. The protein solution eluted was dialysed overnight against two changes (two liters each) of 0.05 M KCl at 4°C. The extent of modification of tryptophyl residues was estimated from the absorbance at 410 nm at pH 11.5-12, assuming a molar extinction coefficient of $18,900 \text{ cm}^{-1} \text{ M}^{-1}$ (52).

(9) Reduction of Disulfide Bonds-----The reduction of the disulfide bonds of Bence Jones proteins was performed with DTT. To 2.5 ml of about 1 % Bence Jones proteins in a urea solution at pH 8.0 adjusted with KOH, was added 0.1 ml of DTT solution (0.5 M). The reduction was continued for an hour at 25°C. The pH was maintained at 8.0 by use of a pH stat through the reaction. After the reduction, the pH of the reaction mixture was lowered to 2 to 3 by adding 1 N HCl and then subjected to gel filtration on a column of Sephadex G-25 and eluted with 6 M urea solution at pH 2. The number of disulfide bonds reduced was determined at pH 8.0 by adding DIN to an aliquot of

the eluted solution. A molar extinction coefficient for the reduced DTN of 13,000 was used to convert the absorbance at 412 nm to sulfhydryl content (55). The protein concentration was estimated from the absorbance at 280 nm for the native protein, since absorbance change at this wavelength with urea denaturation was very small.

(10) Modification with FMA———Organic mercury compounds combine specifically with sulfhydryl group (56-58). The stable dimer of Bence Jones protein has four intrachain and one interchain disulfide bonds. The interchain disulfide bond of the stable dimer of the protein is much more susceptible to reduction than the intrachain disulfide bonds. A low concentration of DTT reduces only the interchain disulfide bond at pH 8 and 25°C. All the intrachain disulfide bonds remain intact under these conditions. Reduction of the interchain disulfide bond of a Bence Jones protein (4×10^{-4} M) was carried out with DTT (2.2×10^{-3} M) in Tris buffer at pH 8 and 25°C for one hour in a glass stoppered vessel. FMA powders were then added. The amount of FMA added was in molar ratio to DTT of 1.2 to 1.5 excess. The reaction mixture was stirred gently for two hours at 25°C until an appreciable amount of FMA dissolved. The reaction was allowed to continue further for ten hours at 4°C. After a small amount of precipitate formed during the reaction had been filtered off, the filtrate was dialyzed against Tris buffer at pH 8.2, and then passed through a Sephadex G-25 column equilibrated with the same buffer. The modified protein solution eluted

was again dialyzed against 0.1 M KCl at 4°C and used as a stock solution. All the procedures were carried out in the dark. The number of FMA attached to the protein was estimated from the absorbance at the absorption maximum of modified protein in 0.1 N NaOH assuming a molar extinction coefficient of $7.8 \times 10^4 \text{ cm}^{-1} \text{ M}^{-1}$ at 499 nm (57). The molar absorptivity of FMA conjugated with N-acetyl-L-cysteine in alkali was found to agree with this value.

Protein Concentration-----The concentrations of unmodified Bence Jones proteins were estimated from the absorbance at 280 nm, assuming $E_{1\text{cm}}^{1\%} = 14.2$ (26). The concentrations of modified proteins were determined by the method of Lowry-Folin (59). Unmodified protein was employed as a standard. A molecular weight of 22,500 was used for calculation of the molar concentrations of Bence Jones proteins.

pH Measurement-----Measurements of pH were carried out with a Hitachi-Horiba pH meter, model F-5 except for the titration experiments.

III RESULTS

III-1 States of Ionizable Groups

Amino Acid Composition-----The results of the amino acid analyses of Ta protein (type K) are given in Table I. The values are expressed as the number of residues per molecular weight of 22,500. The values for threonine and serine were corrected by making extrapolation to zero hydrolysis time. The values for valine and isoleucine were corrected by making extrapolation to a longer time hydrolysis.

Direct Titration-----Figure 1 shows the results of the titration of Ta protein in 0.15 M KCl at 25.0°C. The ordinate \bar{Z} represents the algebraic sum of H^+ ions bound to and released from a protein molecule. It is impossible to experimentally determine the isoionic point of Ta protein owing to insolubility of the protein in deionized water. Therefore, the point $\bar{Z} = 0$ was obtained on the titration curve by finding the point that the amount of acid needed to bring the titration curve to sufficiently low pH from the isoionic point is equal to the total number of the basic groups, which is found to be twenty four from the data of the amino acid analysis. The isoionic point of Ta protein thus obtained was found to be 10.3. Since there are no binding data of ions other than H^+ ion, the value of \bar{Z} is assumed to be equal to the number of the mean net charges of the protein molecule.

On back-titration after exposure to pH 2.0, solution of Ta protein became turbid near pH 3.7 and redissolved above pH 11. On the other

TABLE I.

Amino acid composition

Amino acid	Residues per 22,500 g						
	Hours of hydrolysis					Average or extrapolated value	Nearest integer
	15	24	48	72	96		
Lysine	(8.4)	9.3	9.8	9.9	9.9	9.7	10
Histidine	(1.6)	2.3	2.0	2.0	2.1	2.1	2
Ammonia	25.5	20.3	21.5	22.9	24.8	23.0	23 ⁽¹⁾
Arginine	(10.5)	12.0	11.4	11.9	11.9	11.8	12
Aspartic acid	16.5	17.5	16.5	16.8	17.5	17.0	17
Threonine	20.4	20.0	18.8	18.8	18.0	21.0	21
Serine	27.8	27.4	25.0	22.3	21.3	30.5	31
Glutamic acid	22.6	23.4	22.7	22.3	23.1	22.8	23
Proline	12.4	12.3	12.3	12.3	12.3	12.2	12
Glycine	13.3	13.4	13.1	12.8	13.3	13.2	13
Alanine	9.8	10.0	9.8	9.8	9.9	9.9	10
Half-cystine	4.4	5.0	(3.9)	(3.9)	4.3	4.6	5
Valine	16.0	16.3	16.6	16.5	16.9	16.9	17
Methionine		0.8	0.9	(0.3)	0.9	0.9	1
Isoleucine	4.4	4.9	5.5	5.6	5.8	5.8	6
Leucine	16.0	16.3	16.0	16.0	16.0	16.0	16
Tyrosine	9.0	8.8	8.6	8.4	8.3	9.2	9
Phenylalanine	6.9	7.0	6.9	7.0	7.0	7.0	7
Tryptophan							2 ⁽²⁾
Total							214

The values in parentheses are omitted from average or extrapolation.

(1) Not included in the total.

(2) Determined by the method of Goodwin and Morton.

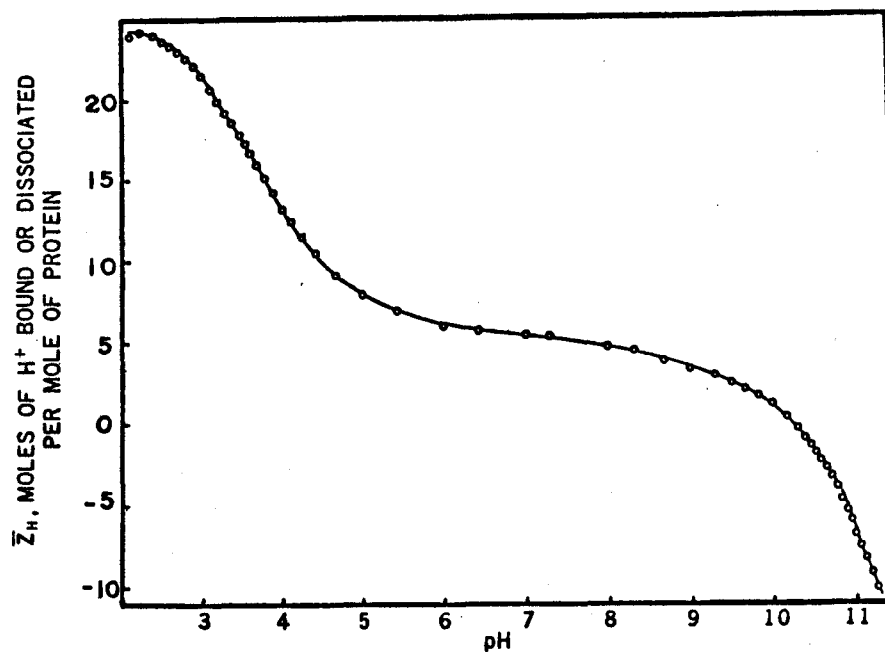


Fig. 1. Titration curve of Bence Jones protein (Ta) at ionic strength 0.15, 25°C. The solid line represents the values calculated by Eq. (3) using the parameters shown in Table V. Below pH 4.0 and above pH 10.2 the values of w shown in Fig. 53 were used.

hand, on back-titration from pH 12 the solution became turbid near pH 9.5 and redissolved below pH 2.5. These back-titration data are not shown here, since the reproducibility was not so satisfactory as that of the forward titration.

Spectrophotometric Titration——Figure 2 shows the results of spectrophotometric titration of Ta protein at 245 nm. Between pH 8.5 and 10.2 the titration curve did not change with time. Above pH 10.2 the curve obtained after exposure to each pH for 24 hr was slightly higher than the initial curve. The total change of the molar extinction coefficient at 245 nm was about 95,000 which means 10,500 per tyrosyl residue, since there are nine tyrosyl residues in the Ta protein molecule (Table I). This is an expected value for the ionization of one tyrosyl residue.

III-2 States of Tyrosyl and Tryptophyl Residues

Reaction with NAI——The extent of acetylation of type χ proteins (Ta and Ya) and that of type λ proteins (Fu, Sh, As, and Ko) are given in Figs. 3 and 4, respectively. Acetylation with NAI of four (Ya, Ta, Fu, and Ko) out of six Bence Jones proteins studied proceeded in two stages. At relatively low concentration of NAI, 1.5 tyrosyl residues were acetylated, except for Ta protein. In the case of As protein, however, the first stage of acetylation was not observed, but the number of tyrosyl residues acetylated was the same as those (three)

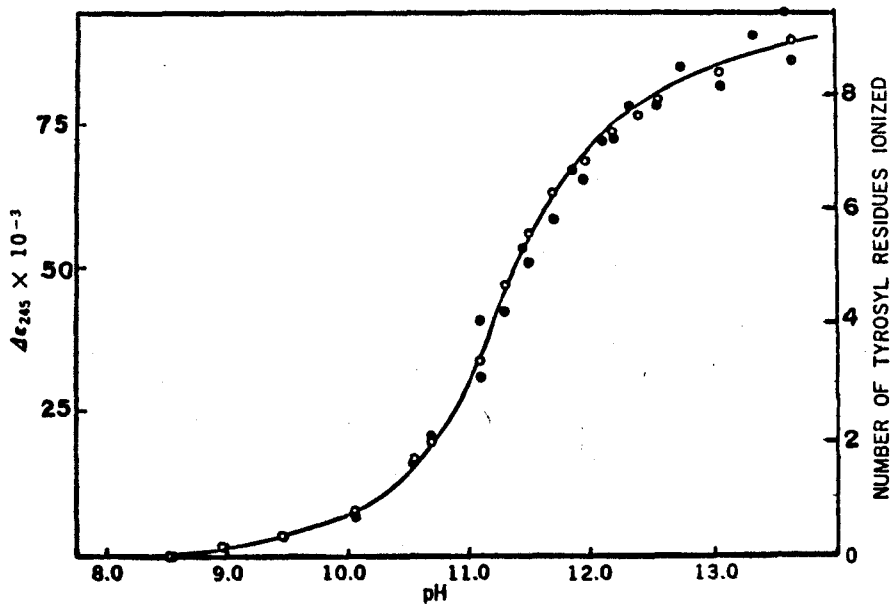


Fig. 2. Spectrophotometric titration of Bence Jones protein (Ta) at 245 nm, 25°C, ionic strength 0.15.

- ◐ , After exposure to each pH for 5 min,
- , After exposure to each pH for 10 min,
- , After exposure to each pH for 24 hr.

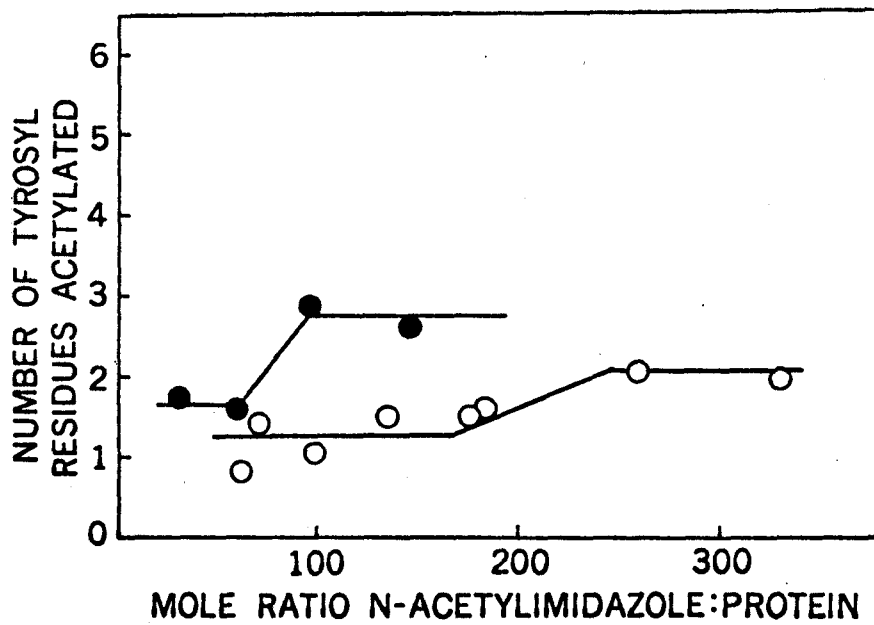


Fig. 3. Acetylation of tyrosyl residues in type X Bence Jones proteins with NAI at pH 7.5, 25°C. ○, Ta protein; ●, Ya protein.

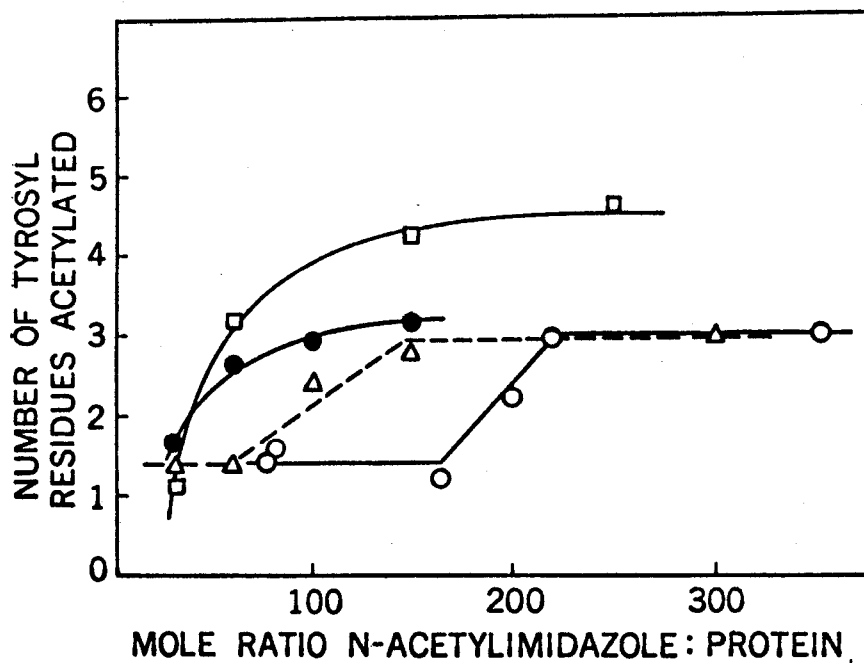


Fig. 4. Acetylation of tyrosyl residues in type λ Bence Jones proteins with NAI at pH 7.5, 25°C. ○, Fu protein; □, Sh protein; △, Ko protein; ●, As protein.

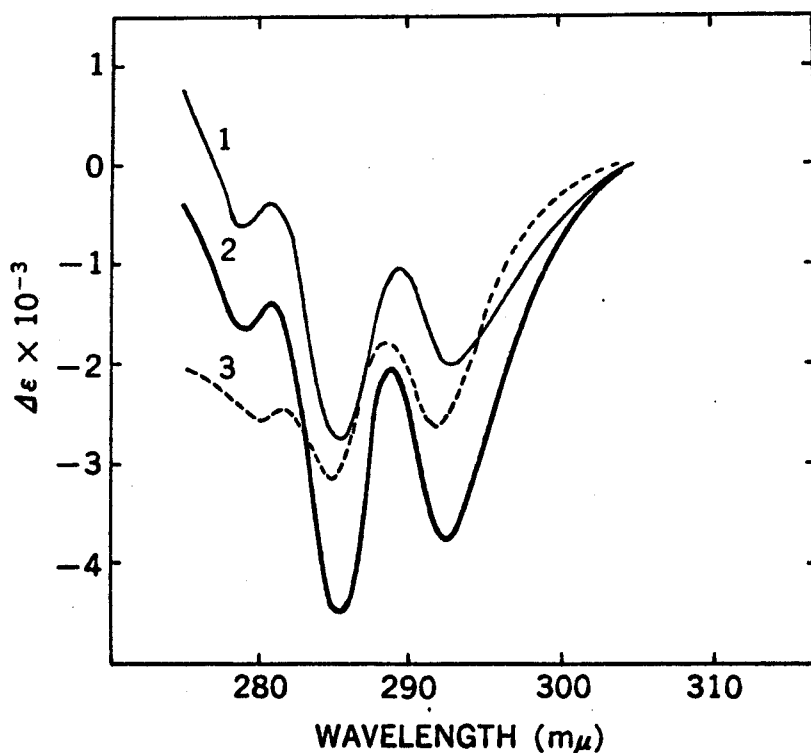


Fig. 5. Difference absorption spectra of type X Bence Jones protein (Ta). (1), acid-denatured (in 0.1 N HCl, pH 2, ionic strength 0.15) vs. native Ta protein (in 0.15 M KCl, pH 6); (2) urea-denatured (in 6.3 M urea, pH 4.3, ionic strength 0.15) vs. native Ta protein; (3), urea-denatured (in 6.3 M urea, pH 4.3, ionic strength 0.15) vs. acid-denatured Ta protein (in 0.1 N HCl, pH 2, ionic strength 0.15)

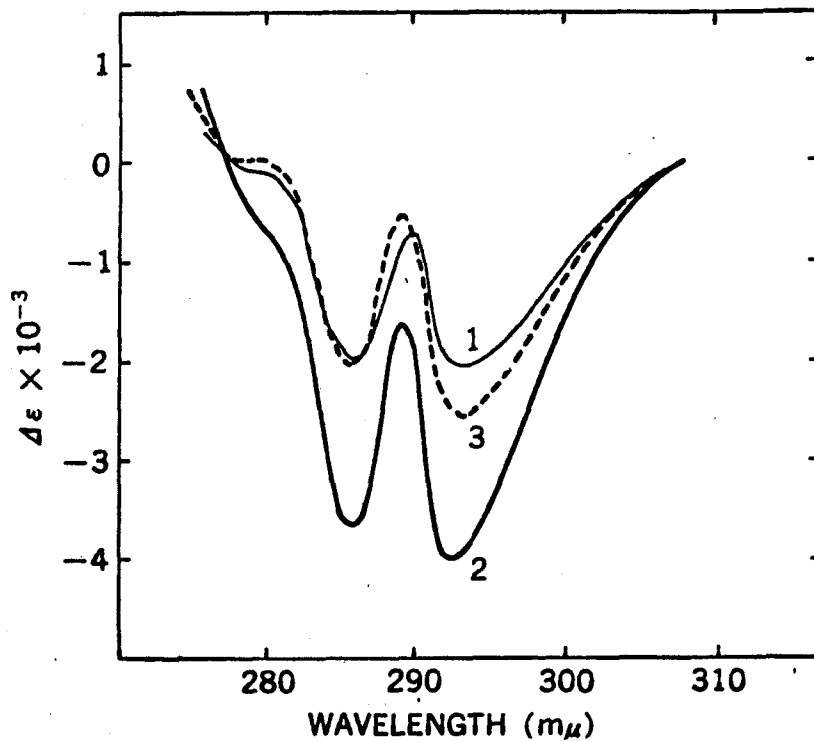


Fig. 6. Difference absorption spectra of type A Bence Jones protein (Fu). (1), acid-denatured (in 0.2 N HCl, pH 0.6) vs. native Fu protein (in 0.15 M KCl, pH 6); (2), urea-denatured (in 6.3 M urea, pH 4.2, ionic strength 0.15) vs. native Fu protein; (3), urea-denatured (in 6.3 M urea, pH 4.2, ionic strength 0.15) vs. acid-denatured Fu protein (in 0.2 N HCl, pH 0.6).

for Ya, Ko, and Fu proteins. The number of tyrosyl residues acetylated for Sh protein was 4.5, being higher than the value for the other proteins.

Reaction with HNB Bromide——Table II shows the results of modification of the tryptophyl residues of Ta (type χ) and Fu (type λ) proteins with HNB bromide. As shown in this table, HNB bromide modified no tryptophyl residue in Ta protein in 0.15 M KCl at pH 5. In the case of Fu protein, however, one tryptophyl residue was modified under the same conditions. In 6 M urea, two and three tryptophyl residues of Ta and Fu proteins, respectively, were modified with the reagent.

Difference Absorption Spectra——Figure 5 shows the difference spectra of acid-denatured vs. native Ta protein, urea-denatured vs. native Ta protein, and urea-denatured vs. acid-denatured Ta protein. The solutions of acid- and urea-denatured proteins were allowed to stand for at least 20 hr before measurements. Similar data for Fu protein are shown in Fig. 6. The changes in the molar absorptivity at 293 nm in the various denaturation processes for Ta and Fu proteins are summarized in Table III.

III-3 Modification with FMA

Reaction with FMA——The numbers of FMA molecule reacted with the reduced Bence Jones proteins are shown in Table IV. It is found that

TABLE II. Modification of tryptophyl residues of Bence Jones proteins with HNB bromide.

Proteins	Antigenic type	Conditions	Moles of modified Trp per mole of protein
Ta	κ	0.15 M KCl, pH 5	< 0.05
		6.0 M urea, pH 5	1.9-2.1
Fu	λ	0.15 M KCl, pH 5	0.9
		6.0 M urea, pH 5	2.9-3.0

TABLE III. Data of difference spectrophotometry for Ta and Fu proteins.

Difference spectra	$\Delta \epsilon$ at 293 nm	Number of Trp residues exposed
Ta protein (Two buried and no exposed Trp)		
Acid-denatured vs. native protein	-2050	1
Urea-denatured vs. acid-denatured protein	-2700	1
Urea-denatured vs. native protein	-3800	2
Fu protein (Two buried and one exposed Trp)		
Acid-denatured vs. native protein	-2100	1
Urea-denatured vs. acid-denatured protein	-2600	1
Urea-denatured vs. native protein	-4100	2

approximately one mole of FMA reacted with one mole of Bence Jones protein monomer, except for Fu protein in which considerable amount of precipitate formed during the reaction with FMA. This shows that one FMA molecule reacted with one sulfhydryl group of the reduced Bence Jones protein monomer, since organic mercury compounds combine specifically with sulfhydryl groups. Karush et al.(57) reported that one mercury atom of FMA is utilized for the reaction with glutathione and ribonuclease in alkali on the basis of the results of fluorescence spectroscopy. Since the Bence Jones proteins conjugated with FMA showed no change in the CD spectra in the wavelength region of 200 to 230 nm which reflect backbone conformation, no serious changes in the protein conformation occur.

Absorption and CD spectra——The absorption spectra of FMA conjugated with Ta (type χ) and Ni (type λ) proteins (FMA-Ta and FMA-Ni) at two pH values are shown in Fig. 7a. The spectra of FMA-N-acetyl-L-cysteine conjugate (FMA-Cys) used as a reference compound are also shown in this figure. An absorption maximum for FMA-Cys appeared at 495 nm at pH 7.7. In the case of FMA-protein conjugates, the absorption spectra measured at pH 7.5 are similar to each other in shape, with a maximum at 510 nm and a shoulder between 480 and 450 nm, but they differ in intensity.

The CD spectra of FMA-Ta and FMA-Ni are shown in Fig. 7b. No CD bands were observed for FMA-Cys. In contrast, FMA conjugated with

TABLE IV. Modification of Bence Jones proteins with FMA

Proteins	Antigenic type	Moles of FMA per mole of Bence Jones protein monomer*
Ta	κ	0.7
Ha	κ	0.8
Ya	κ	1.1
Ni	λ	1.0
Fu	λ	0.5
Sh	λ	0.7
As	λ	1.0

* Average values of two to four experiments

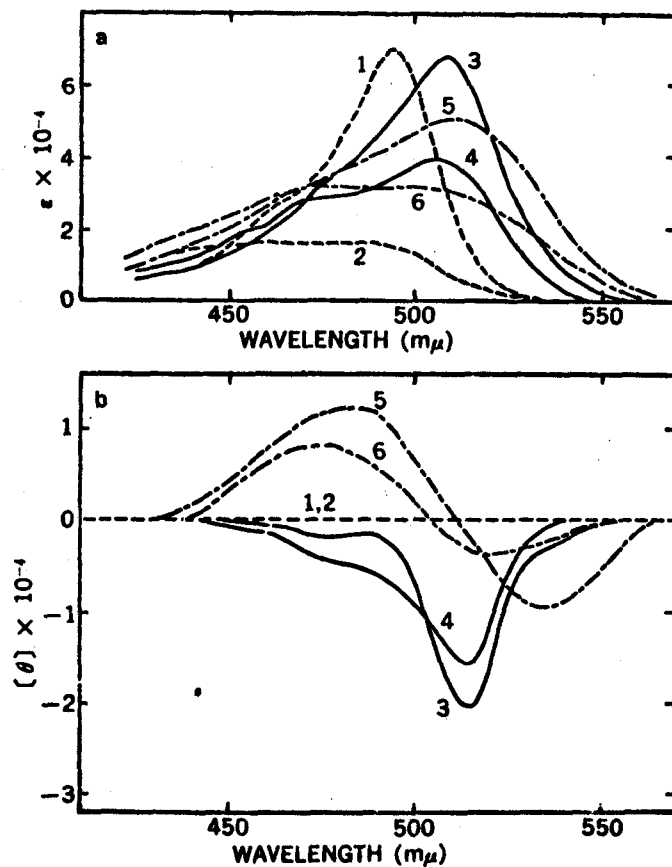


Fig. 7. Absorption (a) and CD (b) spectra of FMA conjugated with N-acetyl-L-cysteine and Bence Jones proteins. 1, FMA-Cys, pH 7.7; 2, FMA-Cys, pH 6.2; 3, FMA-Ta, pH 7.2; 4, FMA-Ta, pH 6.0; 5, FMA-Ni, pH 7.5; 6, FMA-Ni, pH 6.0.

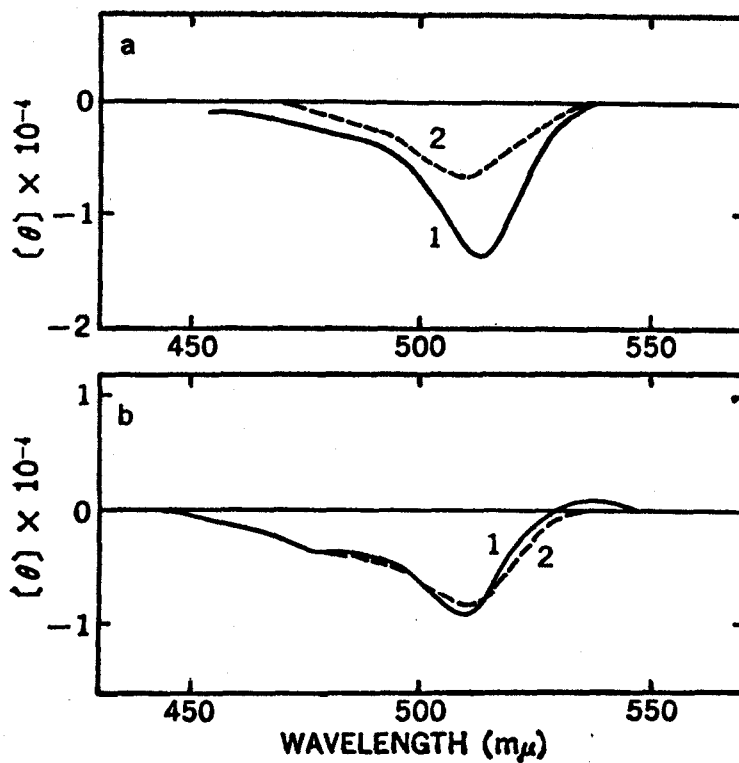


Fig. 8. CD Spectra of FMA conjugated with λ Bence Jones proteins.
 (a) FMA-Ya: 1, pH 7.4; 2, pH 6.0. (b) FMA-Ham: 1, pH 7.4; 2, pH 6.1.

Bence Jones proteins generated extrinsic Cotton effects. The extrinsic Cotton effects disappeared on exposure to 6 M GuHCl. Although the absorption spectra of FMA-protein conjugates were similar to each other, the extrinsic Cotton effects characteristic of FMA were different from each other. These facts suggest that the characteristic extrinsic Cotton effects of FMA reflect the differences in the conformation of each carrier protein. A negative CD band centered at 515 nm, which corresponded to the principal absorption maximum at 510 nm, was observed for FMA-Ta (type χ) at pH 7.2 and 6.0. The ellipticity, $[\theta]$, at 515 nm at pH 7.2 was found to be -2×10^4 degrees $\text{cm}^2 \text{dmole}^{-1}$. The magnitude of the ellipticity decreased slightly by lowering the pH of the solution to 6.0. On the other hand, FMA-Ni (type η) exhibited a negative CD band centered at 535 nm and a positive band centered near 485 nm at pH 7.5. The positive maximum corresponded to the shoulder at around 480 nm in the absorption spectrum. The positive and negative maxima shifted toward shorter wavelength by 10 to 15 nm and the ellipticities decreased slightly by lowering the pH to 6.0. The values of $[\theta]$ at 535 and 485 nm at pH 7.5 were found to be -1×10^4 and 1.2×10^4 degrees $\text{cm}^2 \text{dmole}^{-1}$, respectively.

The CD spectra of FMA conjugated with χ Bence Jones proteins (Ham and Ya) are shown in Fig. 8. A negative CD band was observed at 513 nm for FMA-Ya and 510 nm for FMA-Ham. The CD spectra of these conjugates were very similar to those of FMA-Ta in Fig. 7b, except for a

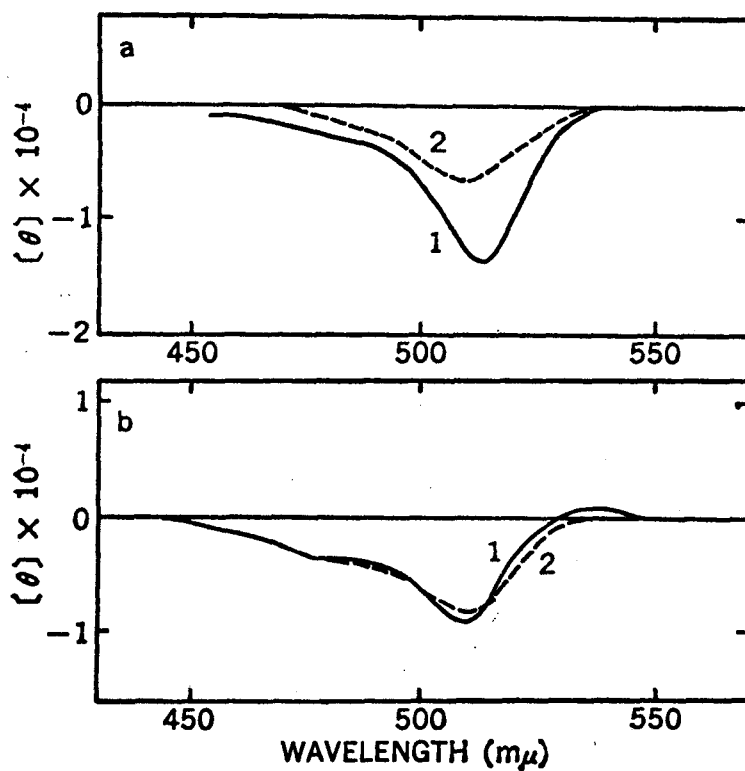


Fig. 8. CD Spectra of FMA conjugated with κ Bence Jones proteins.
 (a) FMA-Ya: 1, pH 7.4; 2, pH 6.0. (b) FMA-Ham: 1, pH 7.4; 2, pH 6.1.

small positive band near 540 nm observed for FMA-Ham. The value of $[\theta]$ at the negative maximum was -1.5×10^4 for FMA-Ya and -1.0×10^4 for FMA-Ham. The magnitude of $[\theta]$ for FMA-Ya decreased to -0.7×10^4 by lowering the pH to 6.0, while the CD spectra of FMA-Ham changed only slightly at pH 6.1.

The extrinsic Cotton effects characteristic of FMA conjugated with λ proteins (As, Fu, and Sh) are shown in Fig. 9. The spectra were different from specimen to specimen in their spectral locations, signs, and magnitudes of the CD bands. The negative maxima appeared at 530 and 470 nm for the CD spectrum of FMA-As at pH 7.4 (Fig. 9). The values of $[\theta]$ at 530 and 470 nm were -1.8×10^4 and -0.8×10^4 degrees $\text{cm}^2 \text{dmole}^{-1}$, respectively. In the case of FMA-N1, a positive CD band appeared at 530 nm (Fig. 7b). The CD maxima of FMA-As shifted to shorter wavelength by lowering the pH to 6.1. The CD spectrum of FMA-Fu at pH 7.5 exhibited positive maxima at 530 and 490 nm and a negative maximum at 450 nm (Fig. 9). The magnitudes of these bands were smaller than those for the other proteins. Because of the low solubility of FMA-Fu in the acidic media, the measurements of CD spectra below pH 7 could not be made. The CD spectra of FMA-Sh at pH 7.4 showed positive maxima at 545 and 440 nm and a negative maximum at 490 nm. No appreciable differences were observed between the spectrum at pH 7.4 and that at pH 6.1.

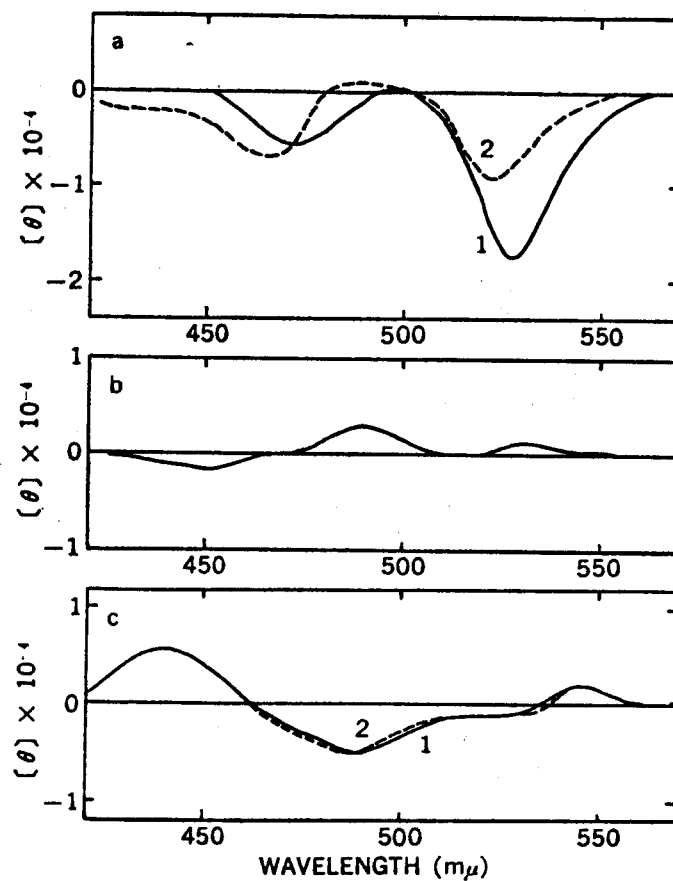


Fig. 9. CD Spectra of FMA conjugated with λ Bence Jones proteins.

(a) FMA-As: 1, pH 7.4; 2, pH 6.1 (b) FMA-Fu: pH 7.5

(c) FMA-Sh; 1, pH 7.4, 2, pH 6.1.

III-4 Denaturation by GuHCl

Type λ Bence Jones Proteins—Figure 10 shows the results of optical rotation measurements at 250 nm as a function of GuHCl concentration for type λ proteins (Fu, Tod, and Ni). The measurements were made at a protein concentration about 0.05 % in a 1.0 cm cell. The pH of solutions was adjusted to 5.8–6.0 by use of 0.1 M potassium phosphate buffer. The transitions began to occur above 0.9 M GuHCl. It can be seen that the transition curves of Tod and Ni proteins consist of two processes, while the transition of Fu protein appeared to occur in a single stage. The change in the value of $[m']$ at 250 nm in the first stage of the transition for Ni and Tod proteins was about a half the total change in the value of $[m']$ at 250 nm.

Figure 11 shows the CD spectra of Ni protein in the region of 250 nm to 325 nm at various GuHCl concentrations. The spectrum in the absence of GuHCl had positive maxima at 315, 289, 278, and 271 nm and negative maxima at 293 and 286 nm. At a GuHCl concentration as low as 0.6 M, the positive ellipticities at 289, 278, and 271 nm decreased and the negative ellipticities at 293 and 285 nm increased with accompanying no change in the band position and shape of the spectrum (Fig. 11a). The shape of the CD spectrum changed above 1.2 M GuHCl. The ellipticities in the region of 280 to 250 nm were almost constant between 1.2 and 1.8 M GuHCl (Fig. 11b). A further increase in the GuHCl concentration gradually reduced the CD bands and became

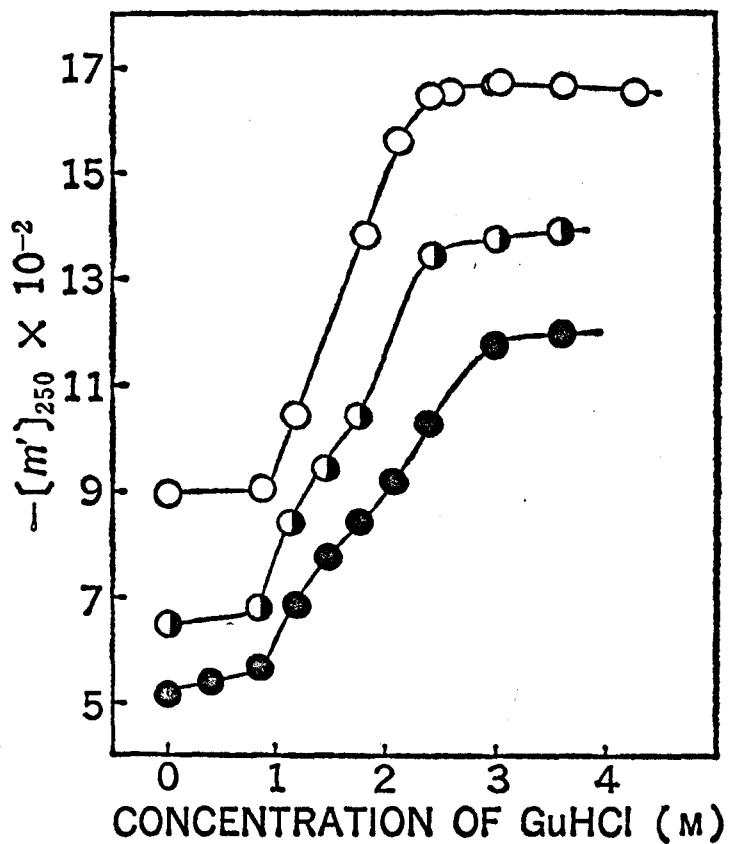


Fig. 10. Dependence of the value of $[m']$ at 250 nm of type λ Bence Jones proteins as a function of GuHCl concentration. 25°C, pH 5.8-6.0.

● , Ni protein; ◐ , Tod protein; ○ , Fu protein.

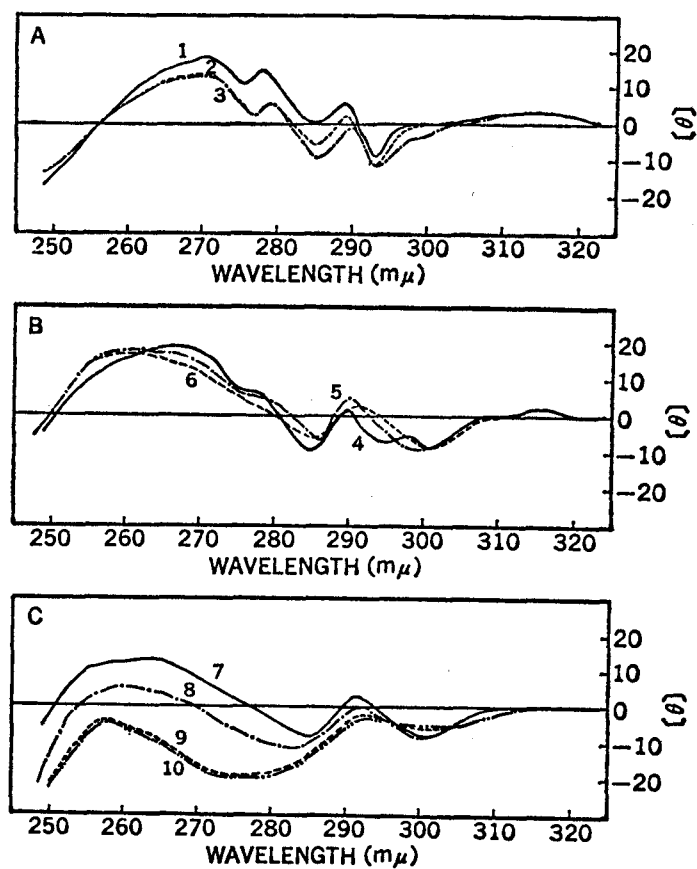


Fig. 11. CD Spectra in the region of 250 to 320 nm of Ni protein at various GuHCl concentrations. 25°C, pH 5.8-6.0. 1, 0 M; 2, 0.6 M; 3, 0.9 M; 4, 1.2 M; 5, 1.5 M; 6, 1.8 M; 7, 2.1 M; 8, 2.4 M; 9, 3.0 M; 10, 3.6 M

negative at 3.0 and 3.6 M GuHCl. There was essentially no difference between the CD spectrum at 3.0 M and that of 3.6 M GuHCl (Fig. 11c).

Figure 12 shows the CD spectra of Ni protein in the region of 245 to 210 nm at various GuHCl concentrations. In the absence of GuHCl, there were small positive maximum at 237 nm ($[\theta] = +30$) and a negative maximum at 218 nm. At 0.6 M GuHCl, the value of $[\theta]$ at 237 nm increased to +100, while no change in the negative band at 218 nm occurred. Above 1.2 M GuHCl, the positive band shifted from 237 to 233 nm. The band at 233 nm increased up to 1.5 M GuHCl and decreased again above 1.8 M. In this concentration range, the negative ellipticities at 218 nm were reduced.

The values of $[\theta]$ at 237-233 and 218 nm are plotted against GuHCl concentration in Fig. 13. The value of $[\theta]$ at 237-233 nm reached a maximum at 1.5 M GuHCl. A plateau was observed in the change in the value of $[\theta]$ at 218 nm near 1.8 M GuHCl.

Figures 14 and 15 show the CD spectra of Tod protein at various GuHCl concentrations. The CD spectrum in the absence of GuHCl had positive maxima at 299, 288 and 279 nm and negative maxima at 293 and 218 nm. As in the case of Ni protein, addition of GuHCl to 0.6 M reduced the spectrum in the region of 225 to 310 nm with accompanying no change in the shape of the spectrum, while the negative maximum at 218 nm remained unchanged. In the presence of 0.9 M GuHCl, a further reduction of the spectrum in the region of 250 to 320 nm occurred

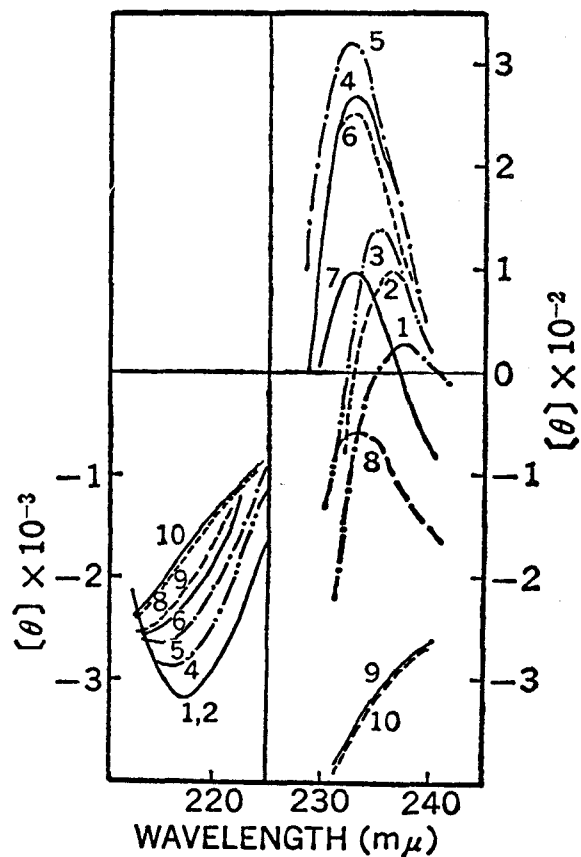


Fig. 12. CD Spectra in the region of 210 to 240 of Ni protein at various GuHCl concentrations. 25°C, pH 5.8-6.0. 1, 0 M; 2, 0.6 M; 3, 0.9 M; 4, 1.2 M; 5, 1.5 M; 6, 1.8 M; 7, 2.1 M; 8, 2.4 M; 9, 3.0 M; 10, 3.6 M.

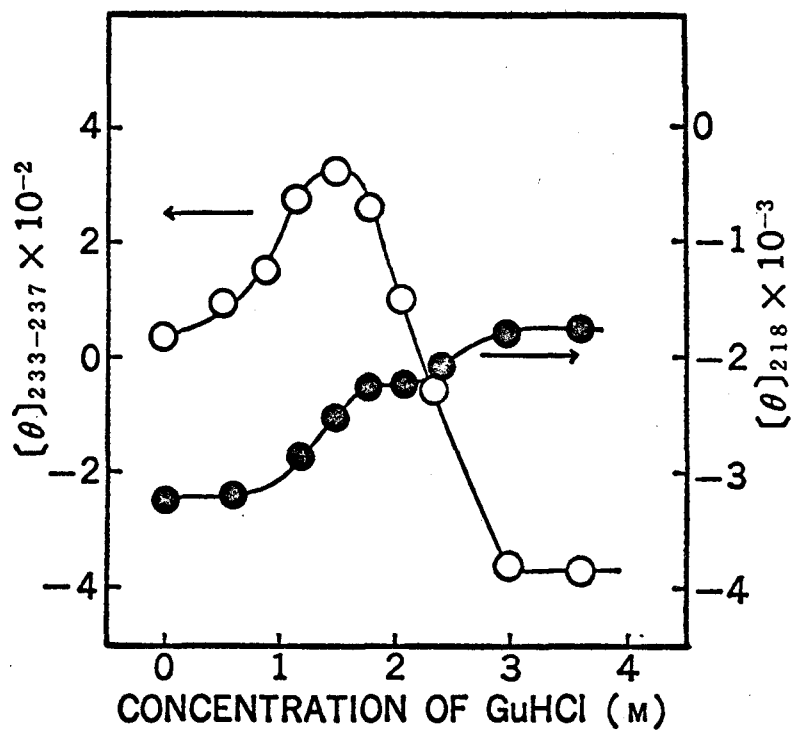


Fig. 13. Dependence of the values of $[\theta]$ at 218 nm (●) and at 233-237 nm (○) of Ni protein as a function of GuHCl concentration. 25°C, pH 5.8-6.0.

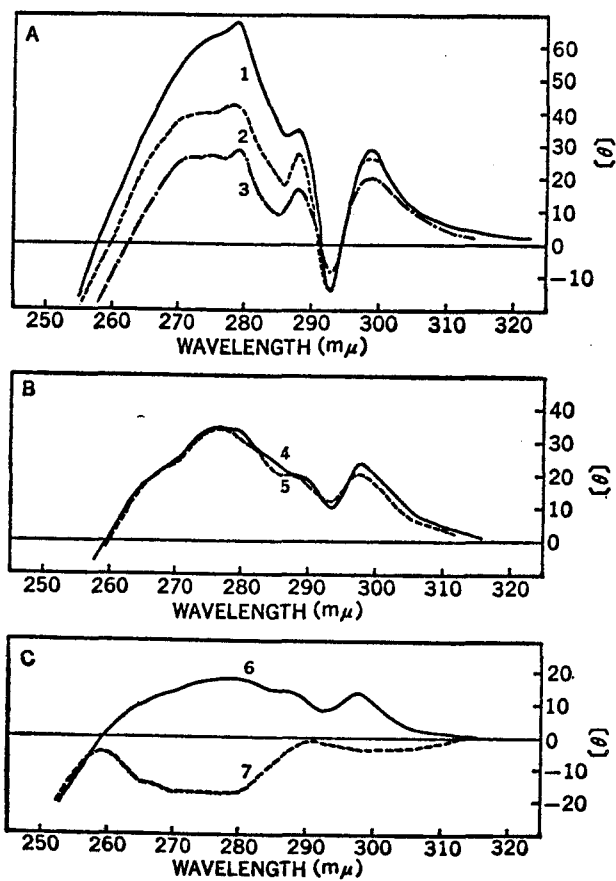


Fig. 14. CD Spectra in the region of 250 to 320 nm of Tod protein at various GuHCl concentrations. 25°C, pH 5.8-6.0. 1, 0 M; 2, 0.6 M; 3, 0.9 M; 4, 1.2 M; 5, 1.5 M; 6, 1.8 M; 7, 3.0 M.

with accompanying no change in the shape of the spectrum. At this GuHCl concentration, however, a slight reduction in the CD band at 218 nm was observed. At 1.2 M GuHCl, the negative maximum at 293 nm changed greatly, but no significant change was observed at the positive bands at 298 to 280 nm when compared to the spectrum at 0.9 M GuHCl. The spectrum at 1.2 M GuHCl resembles that at 1.5 M GuHCl (Fig. 14b). A further increase in the GuHCl concentration to 1.8 M reduced the ellipticities of the CD bands in the magnitude. The CD spectrum of Tod protein at 3.0 M GuHCl was very similar to that of Ni protein at 3.0 or 3.6 M GuHCl.

Figures 16 and 17 show the CD spectra of Fu protein at various GuHCl concentrations. The CD spectrum in the absence of GuHCl had positive maxima at 299, 289, and 280 nm and a negative maximum at 218 nm. On addition of GuHCl to 0.6 M, a slight but reproducible reduction of the positive maxima occurred with accompanying no change in the negative maximum at 218 nm. An increase in the GuHCl concentration to 1.2 M had no effect on the ellipticities of the CD bands at 289 and 299 nm, while the trough at 293 nm became shallower and the negative ellipticity at 218 nm became smaller. At 1.8 M GuHCl, the positive ellipticities at 289 and 299 nm were reduced but the position at these bands remained unchanged. The spectrum at 3.6 M GuHCl was similar to those of Ni and Tod proteins at 3.6 M GuHCl.

Type X Bence Jones Proteins—Figure 18 shows the results of

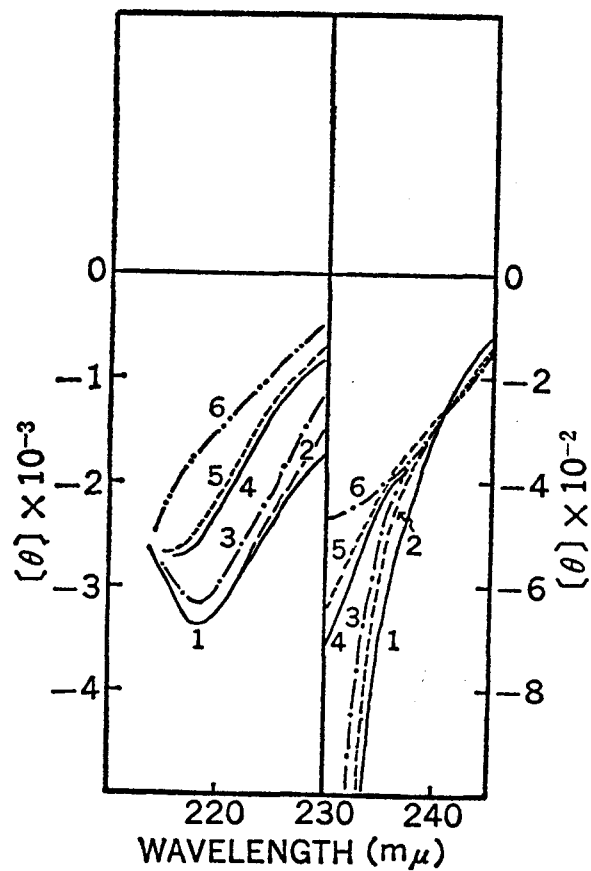


Fig. 15. CD Spectra in the region of 250 to 245 nm of Tod protein at various GuHCl concentrations. 25°C, pH 5.8-6.0. 1, 0 M; 2, 0.6 M; 3, 0.9 M; 4, 1.2 M; 5, 1.5 M; 6, 3.0 M.

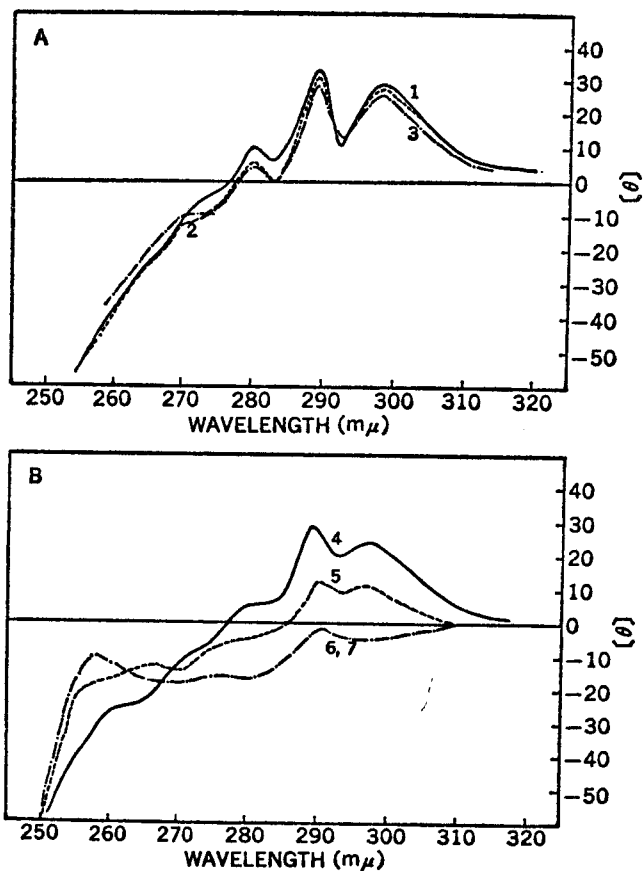


Fig. 16. CD Spectra in the region of 250 to 320 of Fu protein at various GuHCl concentrations. 25°C, pH 5.8-6.0. 1, 0 M; 2, 0.6 M; 3, 0.9 M; 4, 1.2 M; 5, 1.8 M; 6, 2.4 M; 7, 3.6 M.

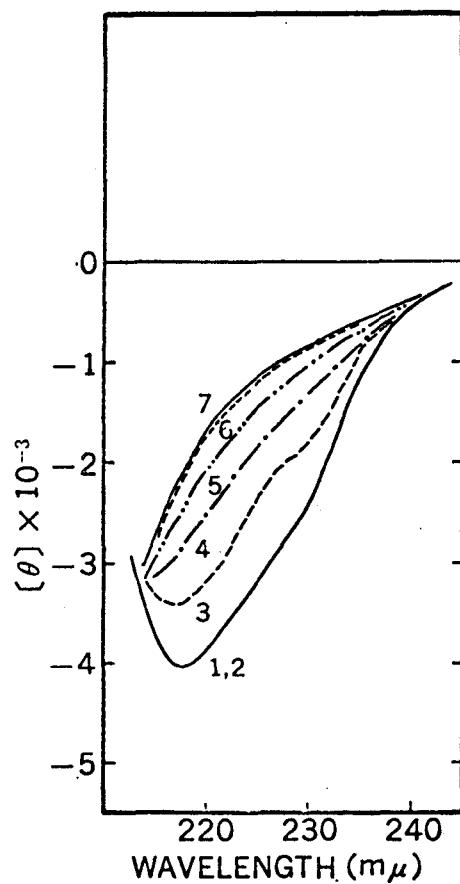


Fig. 17. CD Spectra in the region of 210 to 245 nm of Fu protein at various GuHCl concentrations. 25°C, pH 5.8-6.0. 1, 0 M; 2, 0.6 M; 3, 1.2 M; 4, 1.8 M; 5, 2.4 M; 6, 3.0 M; 7, 3.6 M.

optical rotation measurements as a function of GuHCl concentration for type X proteins (Ta and Ham). The levorotation of both Ta and Ham proteins increased at the GuHCl concentrations above 0.8 M. The changes in the rotation occurred in two stages, one of which lies between 0.8 and 2.0 M GuHCl and the other above 2.0 M GuHCl. The values of $[\alpha]'$ at 250 nm for the native and unfolded conformations of the both proteins were different from one another, but the total changes in the value of $[\alpha]'$ at 250 nm on going from the native to denatured form were the same.

Figure 19 shows the CD spectrum of Ta protein at various GuHCl concentrations. The spectrum in the absence of GuHCl had positive maxima at 292, 271, and 228 nm and a negative maximum at 215 nm. The CD spectrum in the region of 250 to 320 nm was unaffected by the presence of GuHCl up to 0.7 M. A drastic change in the CD spectrum occurred between 1 and 2.1 M GuHCl. At the latter GuHCl concentration, all the CD bands became negative. A further increase in the GuHCl concentration from 2.1 to 4.2 M reduced the magnitudes of the negative bands. The positive band at 228 was very sensitive to the presence of GuHCl. The ellipticity at this wavelength decreased even in the presence of 0.35 M GuHCl and became negative at the concentrations above 1.26 M. The CD spectra in the region of 210 to 225 nm, which reflect the conformation of the polypeptide backbone, were independent of GuHCl concentration up to 0.7 M, this being similar to

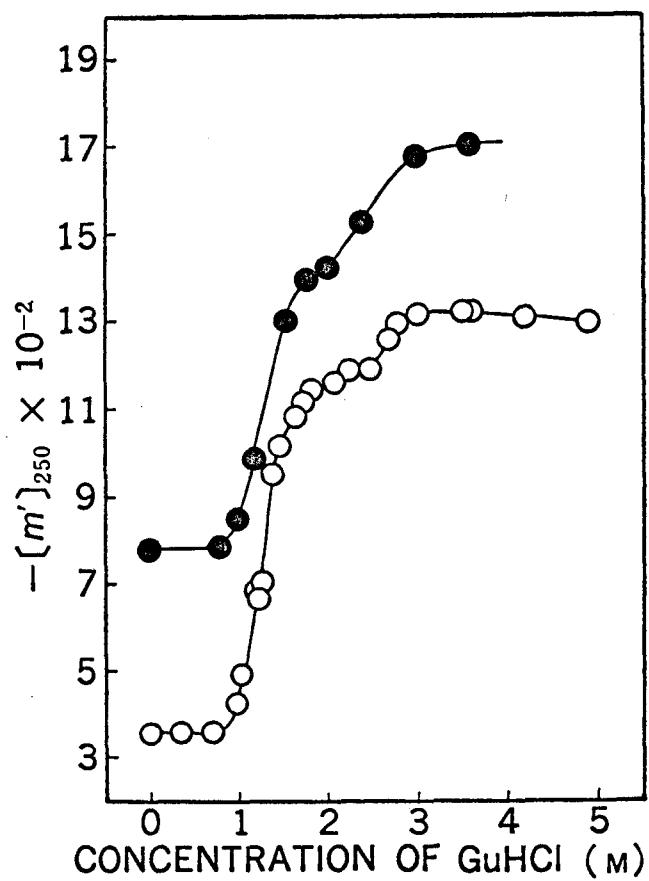


Fig. 18. Dependence of the value of $[m']$ at 250 nm of type χ Bence Jones proteins as a function of GuHCl concentration. 25°C, pH 5.8-6.0.

○ , Ta protein; ● , Ham protein.

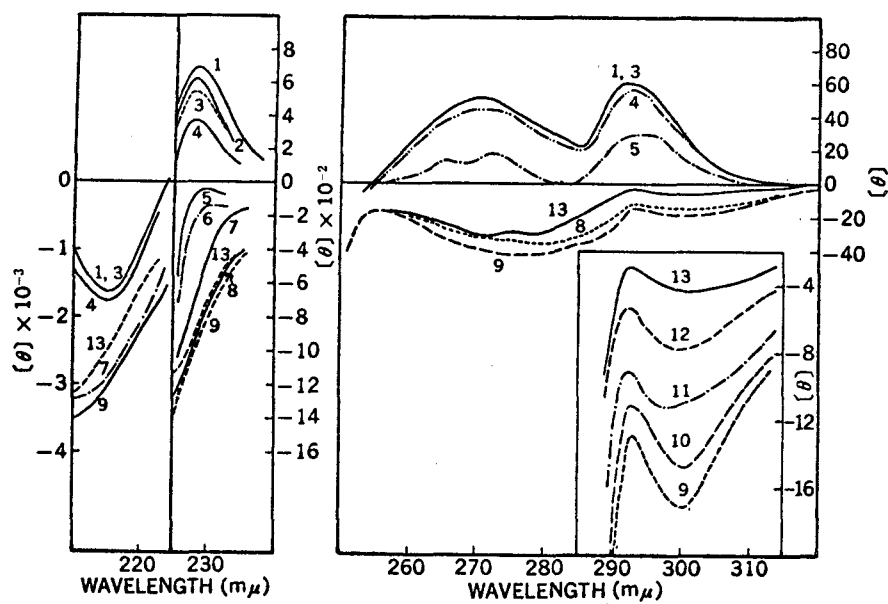


Fig. 19. CD Spectra of Ta protein at various GuHCl concentrations. 25°C, pH 5.8-6.0. 1, 0 M; 2, 0.35 M; 3, 0.7 M; 4, 1.0 M; 5, 1.25 M; 6, 1.26 M; 7, 1.4 M; 8, 1.5 M; 9, 2.1 M; 10, 2.25 M; 11, 2.7 M; 12, 3.0 M; 13, 4.2 M.

that observed in the CD spectra above 250 nm. The negative maximum at 215 nm was deepened at 1 M GuHCl and disappeared above 1.4 M GuHCl. A further increase in the GuHCl concentration from 2.1 to 4.2 M decreased the negative ellipticity at 215 nm. The facts described above are illustrated more clearly in Fig. 20 in which the values of $[\theta]$ at 293, 228, and 215 nm are plotted as a function of GuHCl concentration. The results shown in this figure as well as those in Fig. 19 demonstrate that the transition of Ta protein by GuHCl does not proceed in one stage.

Figure 21 shows the CD spectra of Ham protein at various GuHCl concentrations. The CD spectrum in the absence of GuHCl had positive maxima at 295 and 290 nm, negative maxima at 270 and 218 nm and a shoulder near 237 nm. The positive maxima at 295 and 290 nm became negative on adding 2.1 M GuHCl. A further increase in the GuHCl concentration to 3.6 M reduced the amplitudes of the spectrum, as was observed for the CD spectra of Ta protein (Fig. 19). The shoulder near 237 nm was changed by the addition of GuHCl to 0.8 M and then disappeared at 1.2 M. In the GuHCl concentration range of 1.2 to 2.1 M, no change in the spectrum in the region of 230 to 245 nm was observed. When the GuHCl concentration increased further, a shoulder appeared again in the vicinity of 232 nm. The negative maximum at 218 nm remained unchanged up to 0.8 M GuHCl. The changes in the ellipticities at 218 and 235 nm are plotted against GuHCl concentration in

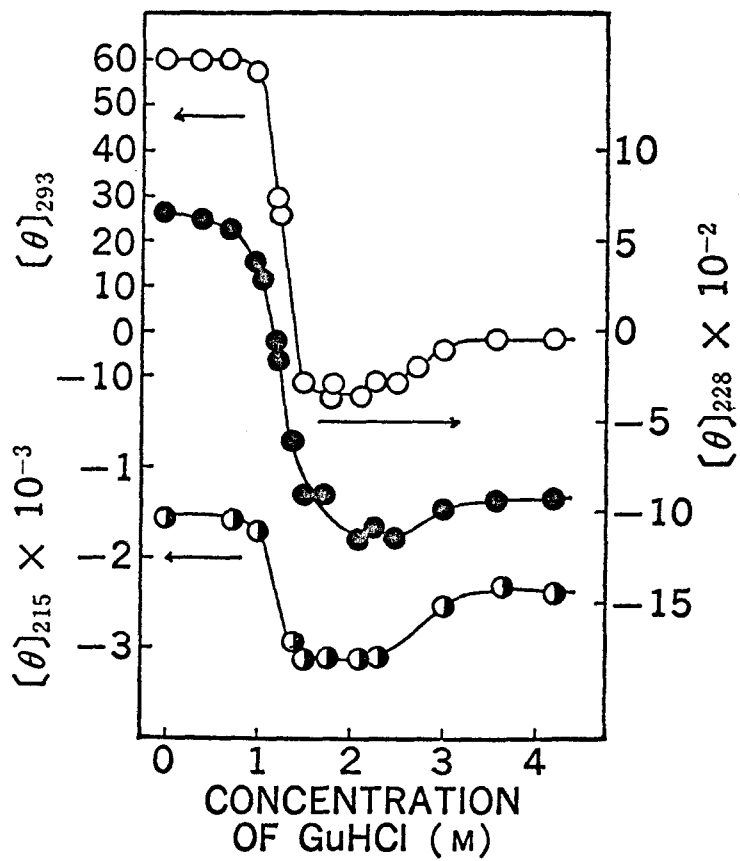


Fig. 20. Dependence of the values of $[\theta]$ at 293 nm (○), 228 nm (●), and 215 nm (◐) of Ta protein as a function of GuHCl concentration. 25°C, pH 5.8-6.0.

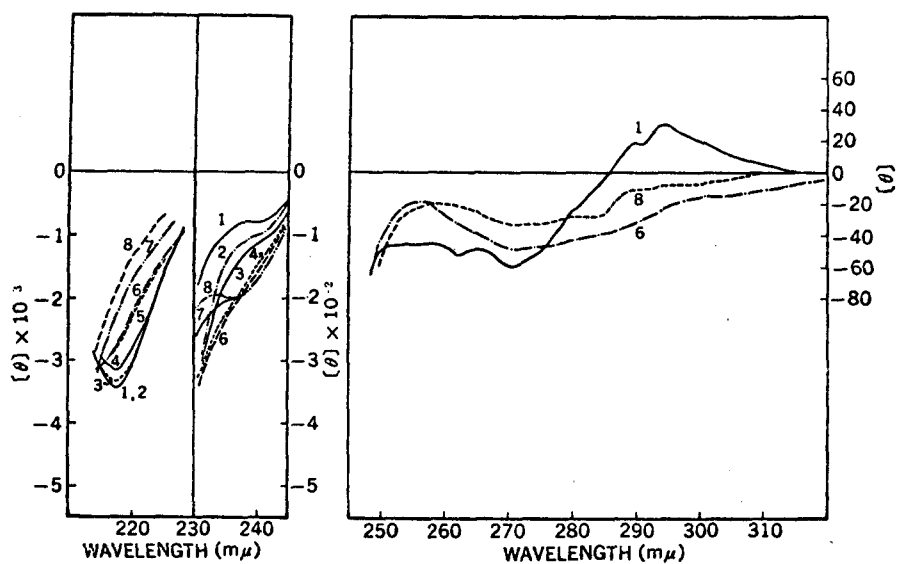


Fig.21. CD Spectra of Ham protein at various GuHCl concentrations.
 25°C, pH 5.8-6.0. 1, 0 M; 2, 0.8 M; 3, 1.0 M; 4, 1.2 M; 5, 1.8 M;
 6, 2.1 M; 7, 3.0 M; 8, 3.6 M.

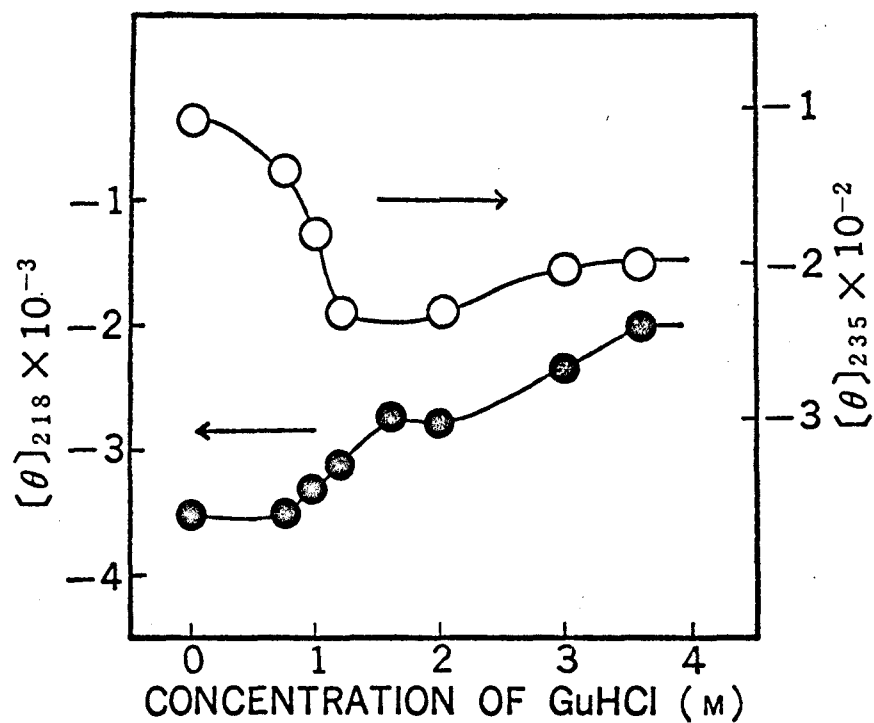


Fig. 22. Dependence of the values of $[\theta]$ at 235 nm (○) and 218 nm (●) of Ham protein as a function of GuHCl concentration. 25°C, pH 5.8-6.0.

Fig. 22. Although the changes in the ellipticities at 218 and 235 nm were not exactly parallel with each other, a plateau was observed at the concentrations between 1.2 and 2.1 M GuHCl in each transition. The data of Figs. 21 and 22 show that Ham protein does not obey the two-state approximation.

III-5 Urea Denaturation

Figure 23 shows the results of optical rotation measurements at 250 nm as a function of urea concentration for a type λ Bence Jones protein (Ta) at different pH values. Since the pH of the urea solution increased slightly with an increase in urea concentration, the pH in this figure represents the value near the center of the transition. The ionic strength of buffer and urea solutions was adjusted to 0.15 with KCl. The measurements were made at protein concentrations of about 0.05 % in a 1.0 cm cell. At pH 5.5, 8.0, and 9.4, a sharp increase in levorotation was observed between 2 and 4 M urea. There was then a further progressive increase in levorotation. The transition curve at pH 6.8 shifted to higher urea concentrations. At pH 2.1, where the transition by acid had been completed (see the section of acid denaturation), the addition of urea further increased the levorotation. The pH dependence of the value of $[m']$ at 250 nm of Ta protein in 3.5 M urea is shown in Fig. 24.

Figure 25 shows the CD spectra of Ta protein at various urea

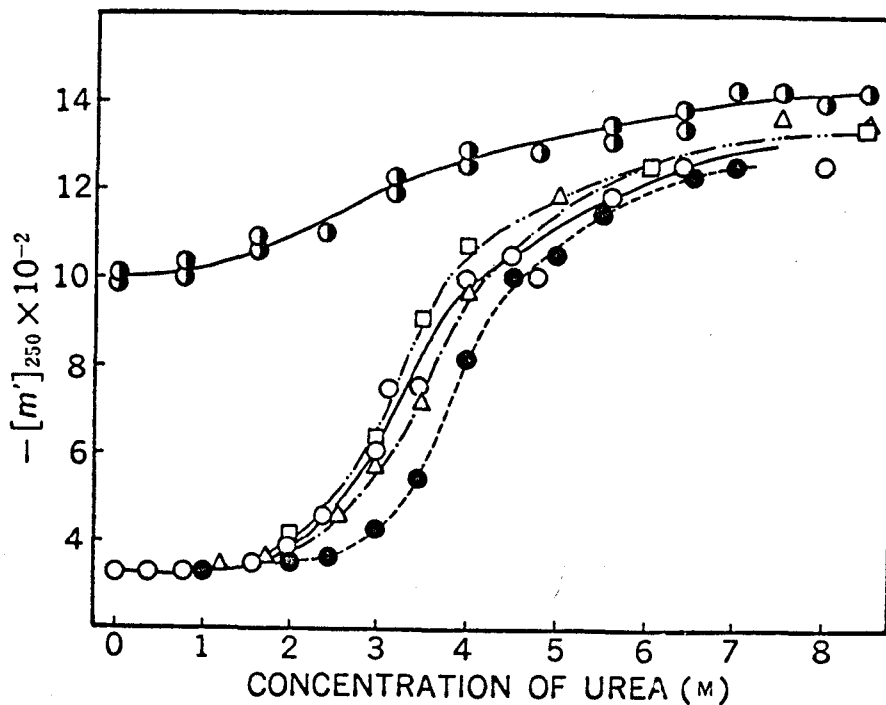


Fig. 23. The effect of urea concentration on the optical rotation at 250 nm of Ta protein, at various pH values. Ionic strength 0.15, 25°C. □ , pH 9.4; △ , pH 8.0; ● , pH 6.8; ○ , pH 5.5; ⊙ , pH 2.1.

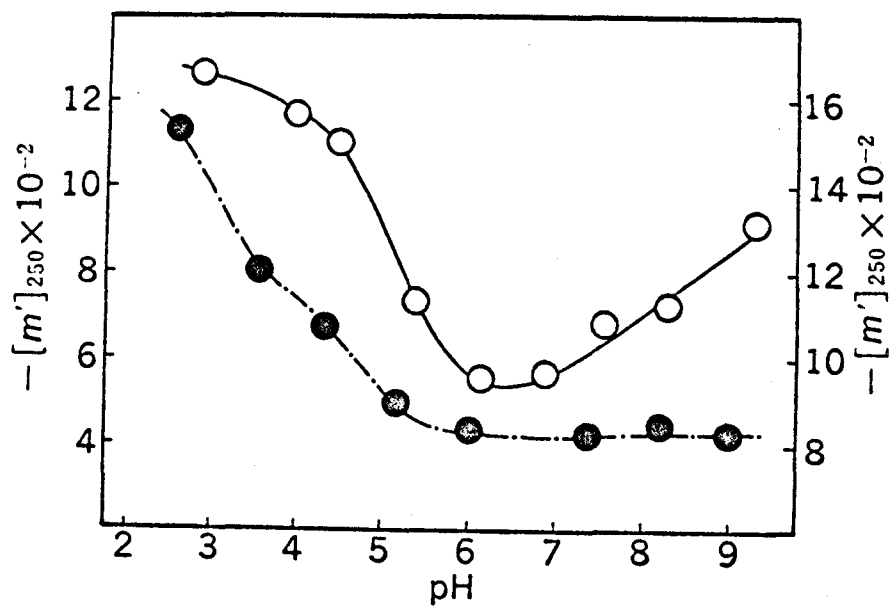


Fig. 24. The pH dependence of the value of $[m']$ at 250 nm for Ta protein in 3.5 M urea (\bigcirc) and for Fu protein in 2.5 M urea (\bullet). Ionic strength 0.15, 25°C.

concentrations at pH 5.5. The spectrum in the absence of urea had positive maxima at 292, 271, and 228 nm and a negative maximum at 215 nm. A drastic change in the CD spectrum occurred between 2 and 4.5 M urea, all the CD bands in the region of 250 to 310 nm became negative. A further increase in urea concentration increased the negative ellipticities of the CD bands. The positive band at 228 nm decreased in magnitude in a way similar to that observed in the CD spectra above 250 nm and became negative at 4 M urea. The CD spectra in the region of 210 to 225 nm, which reflect the conformation of the polypeptide backbone, were independent of urea concentrations up to 2 M. The negative maximum at 215 nm deepened and shifted to shorter wavelength at 4.5 M urea and disappeared above 5 M urea. These observations are illustrated in Fig. 26, in which the values of $[\theta]$ at 293, 228, and 215 nm are plotted as a function of urea concentration.

Figure 27 shows the difference spectra of Ta protein at selected urea concentrations. These are typical of denaturation difference spectra, with negative peaks at 293, 286, and 279 nm.

Figure 28 shows the values of $\Delta \epsilon$ at 293 nm, which reflect the change in the state of tryptophyl residues, plotted against urea concentrations. The value of $\Delta \epsilon$ decreased sharply between 3 and 6 M urea.

The Bence Jones protein (Ta) dimer contains one interchain disulfide bond and four intrachain disulfide bonds. Ta protein contains

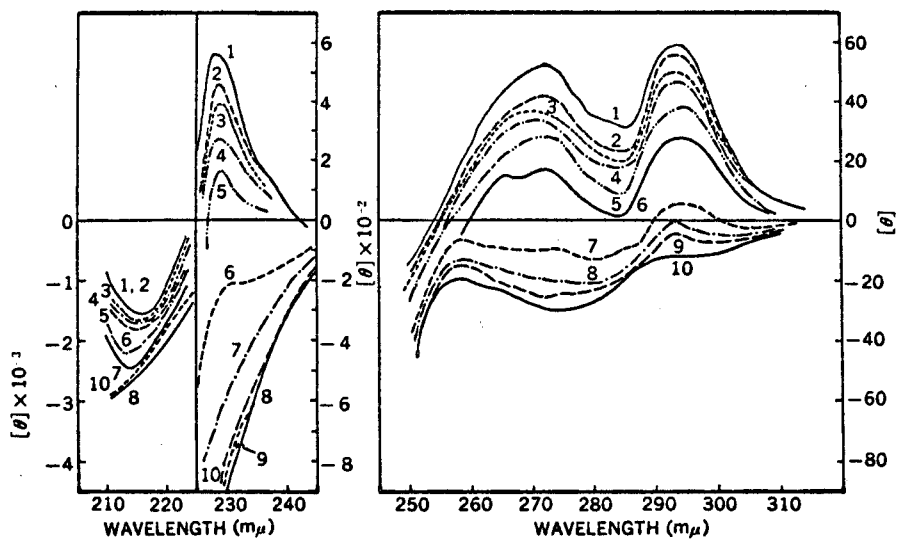


Fig. 25. CD Spectra of Ta protein at various urea concentrations. pH 5.5, ionic strength 0.15, 25°C. 1, 0 M; 2, 2.0 M; 3, 2.5 M; 4, 3.0 M; 5, 3.5 M; 6, 4.0 M; 7, 4.5 M; 8, 5.0 M; 9, 6.0 M; 10, 7.0 M urea.

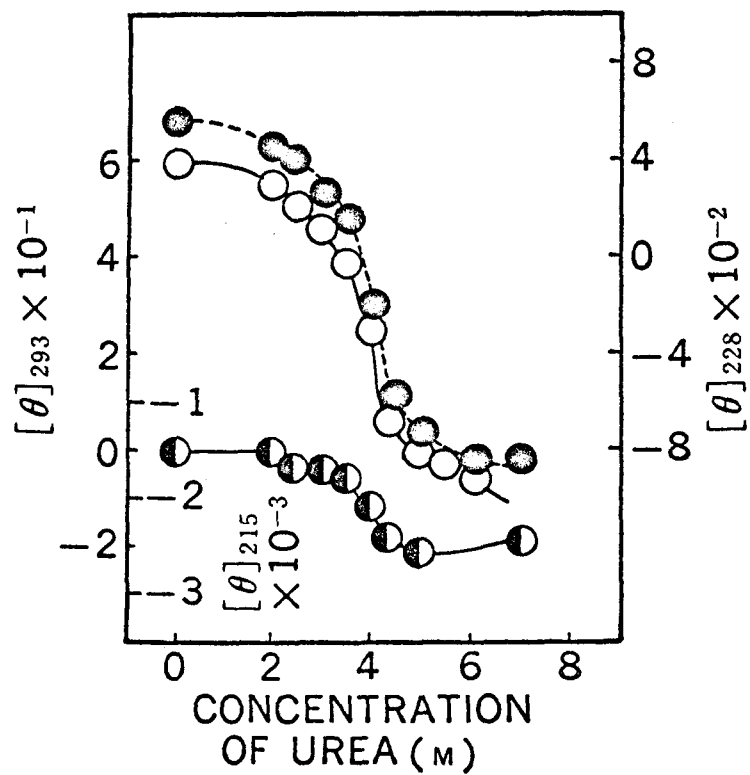


Fig. 26. Changes with urea concentration in the values of $[\theta]$ at 215 nm (\bullet), 228 nm (\bullet), and 293 nm (\circ) for Ta protein.

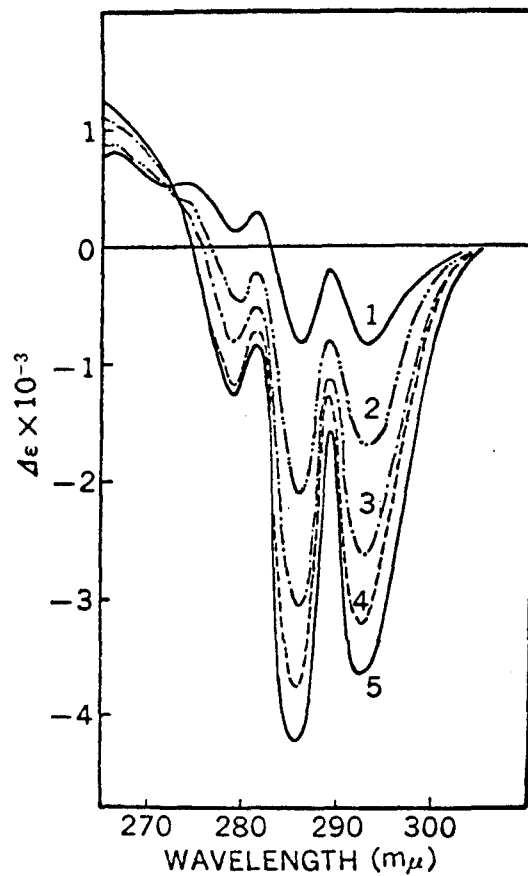


Fig. 27. Difference absorption spectra of Ta protein produced by urea. pH 6.5, ionic strength 0.15, 25°C. 1, 4.0 M; 2, 4.5 M; 3, 5.0 M; 4, 6.0 M; 5, 7.0 M urea.

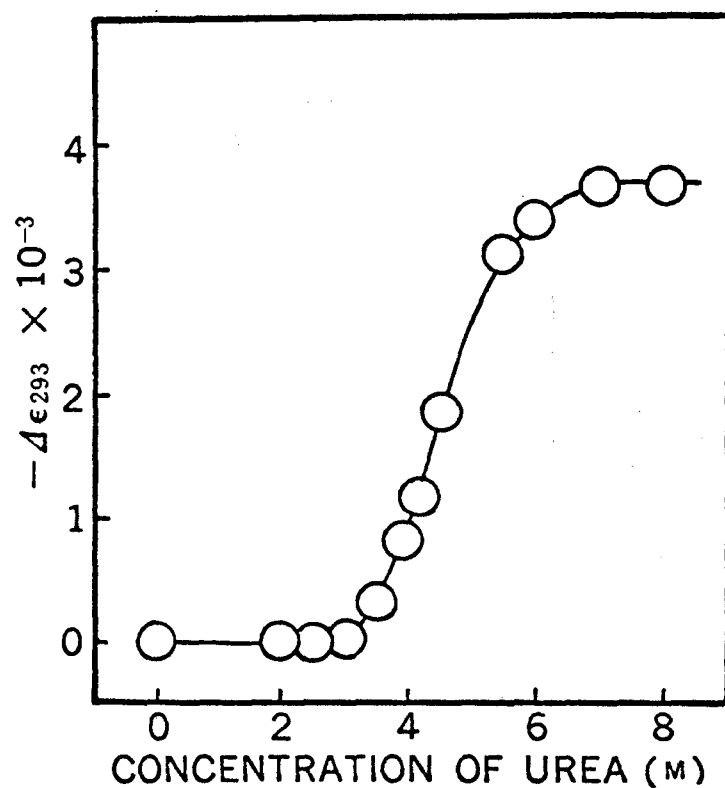


Fig. 28. Change with urea concentration in the value of $\Delta\epsilon$ at 293 nm for Ta protein. pH 6.5, 25°C.

two tryptophyl residues per monomer. Figure 29 shows the reactivities of the disulfide bonds at pH 8.0 and tryptophyl residues at pH 5.0 of Ta protein as a function of urea concentration. The number of disulfide bonds reduced is expressed as a dimer units. A disulfide bond which is reduced in the absence of urea is known to be the interchain bond. At urea concentrations below 2 M, only the interchain disulfide bond was cleaved. The cleavage of intrachain disulfide bonds began to occur above 2 M urea and in the vicinity of 4 M urea, there appeared a plateau which corresponds to the cleavage of two intrachain disulfide bonds per dimer unit. There was then a further increase in the number of disulfide bonds reduced above 5 M urea, with a rather broad profile. The reduction was incomplete even in 8 M urea. Whereas no tryptophyl residues reacted with HNB bromide below 2 M urea, both the tryptophyl residues were modified above 4 M urea.

Figure 30 shows the CD spectra of a type λ protein, Ni, at various urea concentrations at pH 6.5. The spectrum in the absence of urea had maxima at 315, 289, and 271 nm and negative maxima at 298, 286, and 218 nm. At a urea concentration as low as 2 M, no appreciable change was observed in the CD spectrum. The shape and magnitude of the CD bands changed above 2.5 M urea. With an increase in urea concentration up to 4 M, the CD spectrum between 250 and 265 nm increased and the ellipticity at 237 nm increased with a shift to 233 nm. Above 5.0 M urea, the band at 233 nm decreased again. The neg-

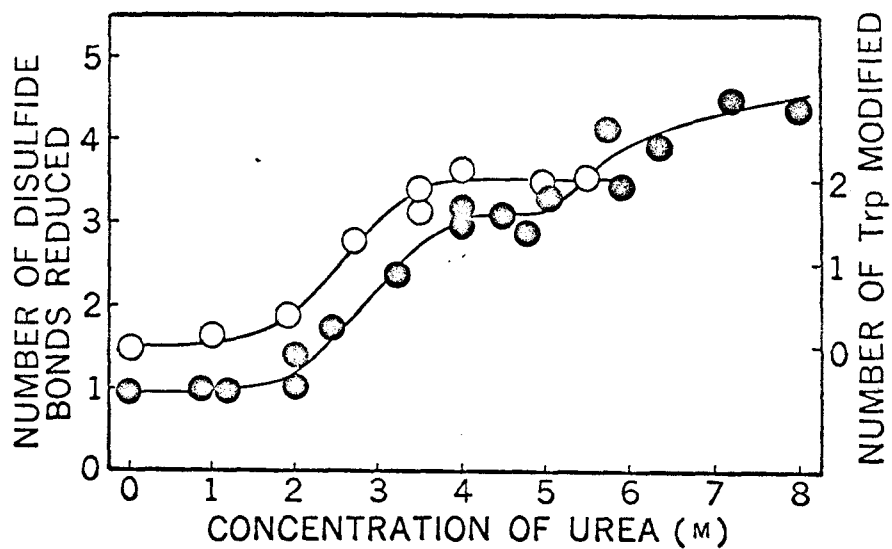


Fig. 29. Reactivities of disulfide bonds toward DTT at pH 8.0 (●) and of tryptophyl residues toward HNB bromide at pH 5.0 (○) in Ta protein as a function of urea concentration. The number of disulfide bonds reduced is expressed as dimer units and the number of tryptophyl residues modified as monomer units.

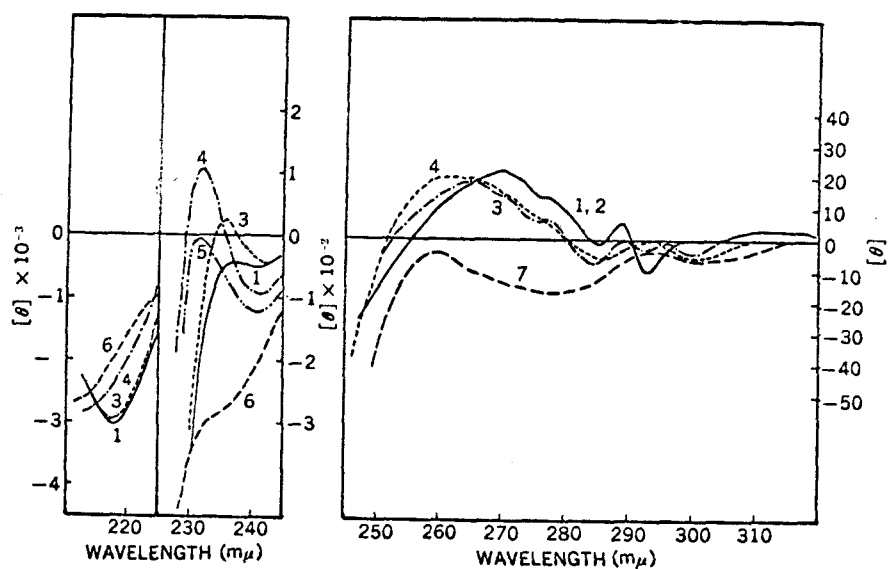


Fig. 30. CD Spectra of Ni protein at various urea concentrations. pH 6.5, ionic strength 0.15, 25°C. 1, 0 M; 2, 2.0M; 3, 2.5 M; 4, 4.0 M; 5, 5.0 M; 6, 6.3 M; 7, 7.0 M urea.

ative ellipticity at 218 nm was reduced above 2.5 M urea. The changes in the values of $[\theta]$ at 237-233 and 218 nm with urea concentration are illustrated in Fig. 31. The value of $[\theta]$ at 237-233 nm reached a maximum at 4 M urea.

Figure 32 shows the difference spectra of type λ proteins, Ni and Fu, produced by urea. Negative peaks at 293 and 286 nm and a shoulder at about 279 nm were observed for the spectra of both proteins. In addition, there was a positive peak at 305 nm for the spectrum of Ni protein but not in that of Fu protein.

In Fig. 33, the values of $\Delta \epsilon$ at 293 nm, $[m']$ at 250 nm and the number of disulfide bonds reduced for Ni protein are plotted against urea concentrations. The levorotation and the value of $\Delta \epsilon$ at 293 nm began to change above 2 M urea. These changes are seen to consist of more than one process and were incomplete even at 7 M urea. In the transition as observed by optical rotation measurements, there was a small but distinct plateau in the vicinity of 4 M urea. On the other hand, the number of disulfide bonds reduced by DTT increased with increasing urea concentration from 0 to 2 M, where no change in the values of $[m']$ at 250 nm and $\Delta \epsilon$ at 293 nm occurred, and one intrachain disulfide bond was reduced between 2 and 3 M urea. Above 3 M urea, a further increase in the reactivity was observed.

Figure 34 shows the changes with urea concentration in the value of $[m']$ at 250 nm, $\Delta \epsilon$ at 293 nm and the reactivity of the disulfide

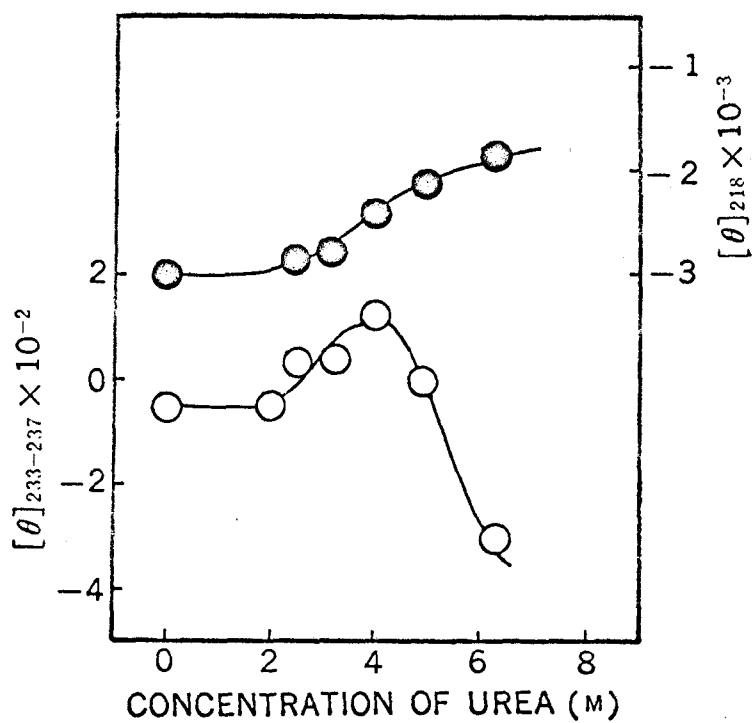


Fig. 31. Changes with urea concentration in the values of $[\theta]$ at 218 nm (●) and 233-237 nm (○) for Ni protein. pH 6.5.

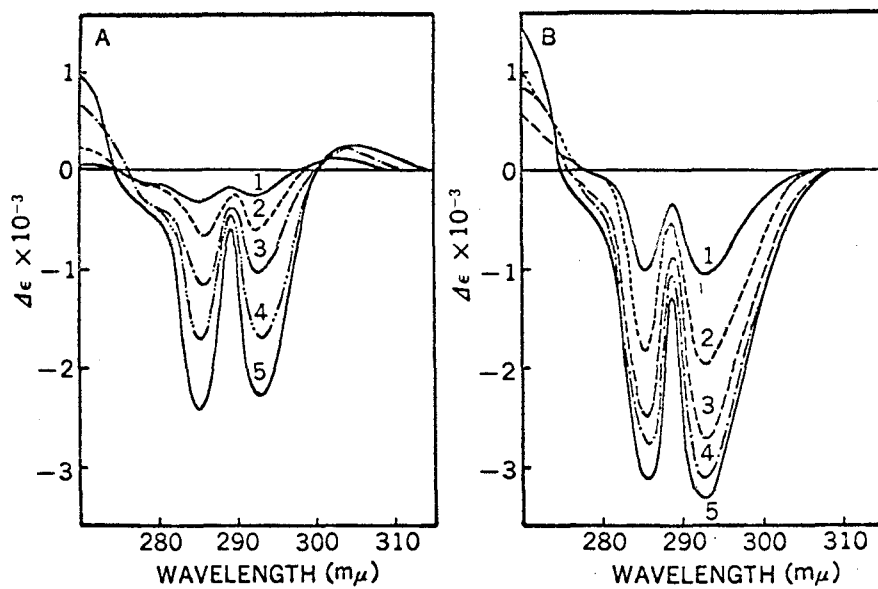


Fig. 32. Difference absorption spectra of Ni protein (A) and Fu protein (B) produced by urea. pH 6.5, ionic strength 0.15, 25°C.
 (A) 1, 2.4 M; 2, 3.0 M; 3, 3.5 M; 4, 5.0 M; 5, 7.0 M urea.
 (B) 1, 3.0 M; 2, 3.5 M; 3, 4.0 M; 4, 5.0 M; 5, 6.0 M urea.

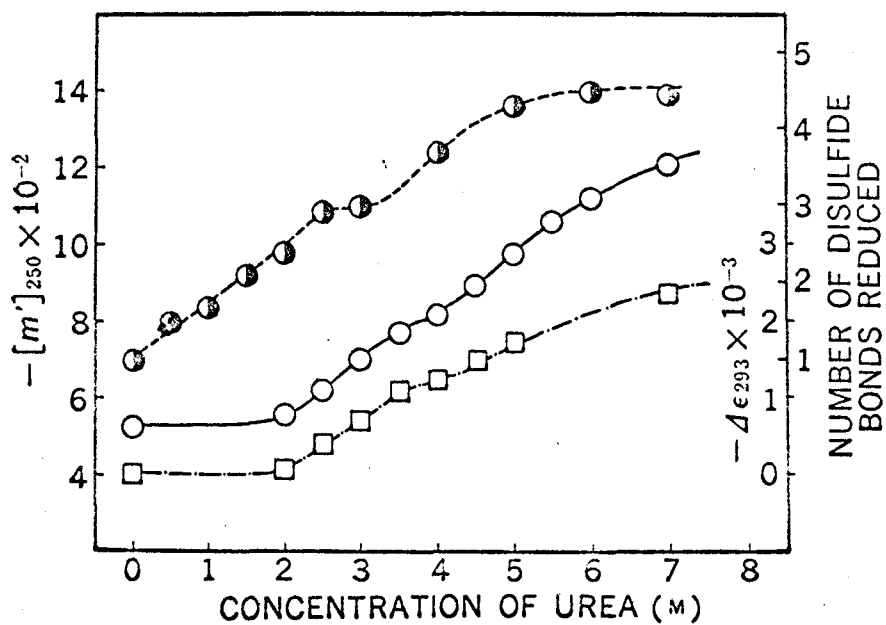


Fig. 33. The effect of urea concentration on the values of $[m']$ at 250 nm at pH 6.5 (\odot), $\Delta\epsilon$ at 293 nm at pH 6.5 (\square) and on the reactivity of disulfide bonds at pH 8.0 (\bullet) for Ni protein. Ionic strength 0.15, 25°C.

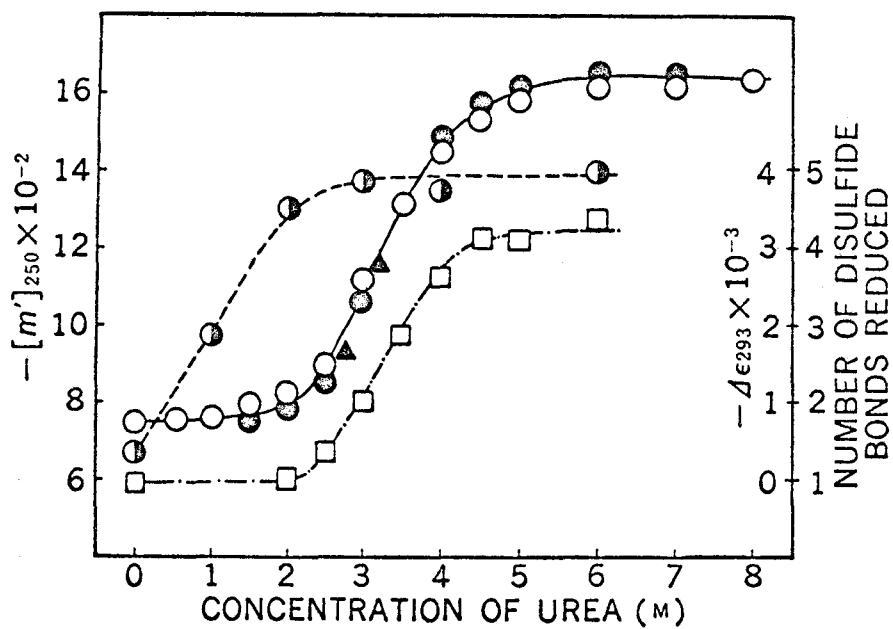


Fig. 34. The effect of urea concentration on the values of $[m']$ at 250 nm at pH 8.2 (\bigcirc) and pH 5.2 (\bigcirc), $\Delta\epsilon$ at 293 nm at pH 6.5 (\square) and on the reactivity of disulfide bonds at pH 8.0 (\bullet) for Fu protein. Closed triangles show data at pH 8.2 obtained by dilution from 8 M urea. Ionic strength 0.15, 25°C.

bonds toward DTT for another type λ protein, Fu. As in the case of Ni protein, the optical rotation began to change above 2 M urea. However, in contrast to the transition for Ni protein, the change in the optical rotation for Fu protein appeared to occur in a single stage. The transition was reversible: the results obtained after exposure to 8 M urea at pH 8.2 fell on the same curve as data obtained by addition of urea to aqueous Fu protein solution. The change in the value of $\Delta \epsilon$ at 293 nm in the difference spectra was seen to parallel the change in the optical rotation. The three tryptophyl residues were reacted with HNB bromide in the presence of 4.5 M urea. The reactivity of the disulfide bonds toward DTT increased with increasing urea concentration and all the disulfide bonds were reduced above 3 M urea. The pH dependence of the value of $[m']$ at 250 nm of Fu protein in 2.5 M urea is shown in Fig. 24.

III-6 pH Dependent Conformational Change

Figure 35 shows the results of optical rotation measurements as a function of pH for type λ proteins (Fu and Ni) and a type κ protein (Ta). The levorotation of all the proteins increased as the pH of the solution was lowered below 4. The changes in the rotation for Fu and Ni proteins occurred in two stages, one of which lies between pH 4 and 2.5 and the other below pH 2.5. For Ta protein, on the other hand, the transition with pH appeared to occur in only one stage.

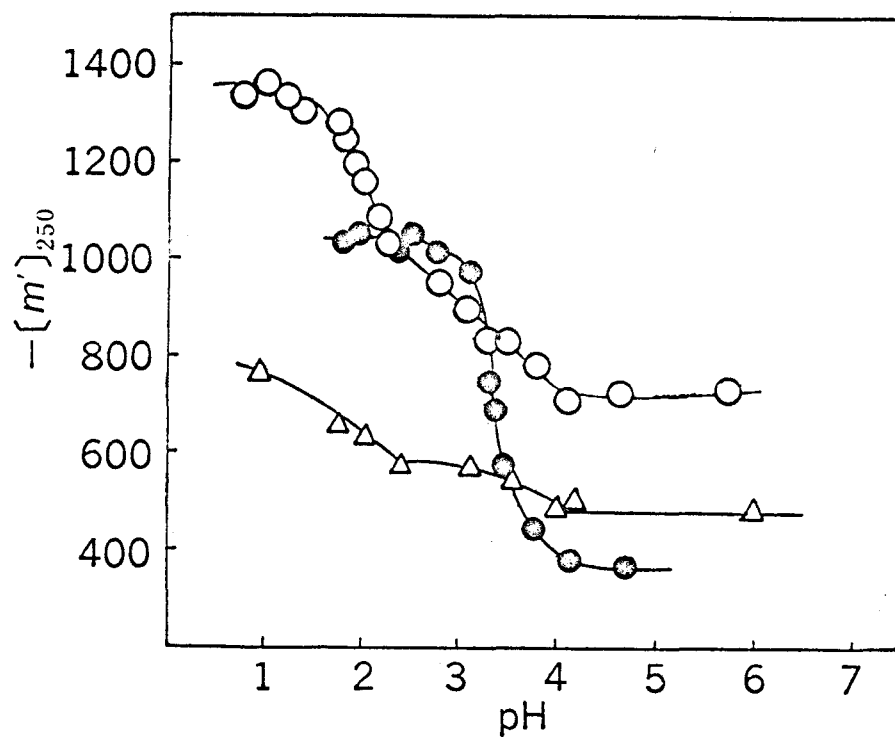


Fig. 35. The pH dependence of the values of $[m']$ at 250 nm. 25°C, ionic strength 0.15. ○, Fu protein; △, Ni protein; ●, Ta protein.

Figure 36 shows typical difference spectra of a type K Ta protein (reference, between pH 1.02 and 1.33). Three peaks appeared at 279, 286, and 293 nm. It is to be noted that the height of the peak at 286 nm relative to 293 nm increased with increasing pH.

Figure 37 shows the values of $\Delta \epsilon$ at 286 and 293 nm as a function of pH. The value of $\Delta \epsilon$ decreased steeply below pH 4 and the height of the peak at 293 and 286 nm became the same as the pH was lowered below pH 2.7.

The reversibility of the acid denaturation of Ta protein was studied. Ta protein (0.071 %) in 0.08 N HCl and 0.02 M KCl (pH 1.2) was allowed to stand for 20 hr at 25°C. Appropriate buffers were added to aliquots of this solution for the purpose of raising the pH (final protein concentration, 0.014 %). After additional 20 hr of incubation at 25°C, the difference spectra were measured against a protein solution at pH 1.20. The spectra obtained was identical with those obtained with protein that had not been exposed to acid prior to measurements. The value of $\Delta \epsilon$ at 286 and 293 nm obtained from these spectra are given in Fig. 37.

Figure 38 shows the CD spectra of Ta protein at various acidic pH's. The CD spectrum of this protein at pH 6.0 had positive maxima at 228, 271, and 292 nm and a negative maximum at 215 nm. Between pH 6 and 3.2, the CD spectrum in the region of 255 to 310 nm remained unchanged, while the spectrum in the region of 210 and 255 nm changed

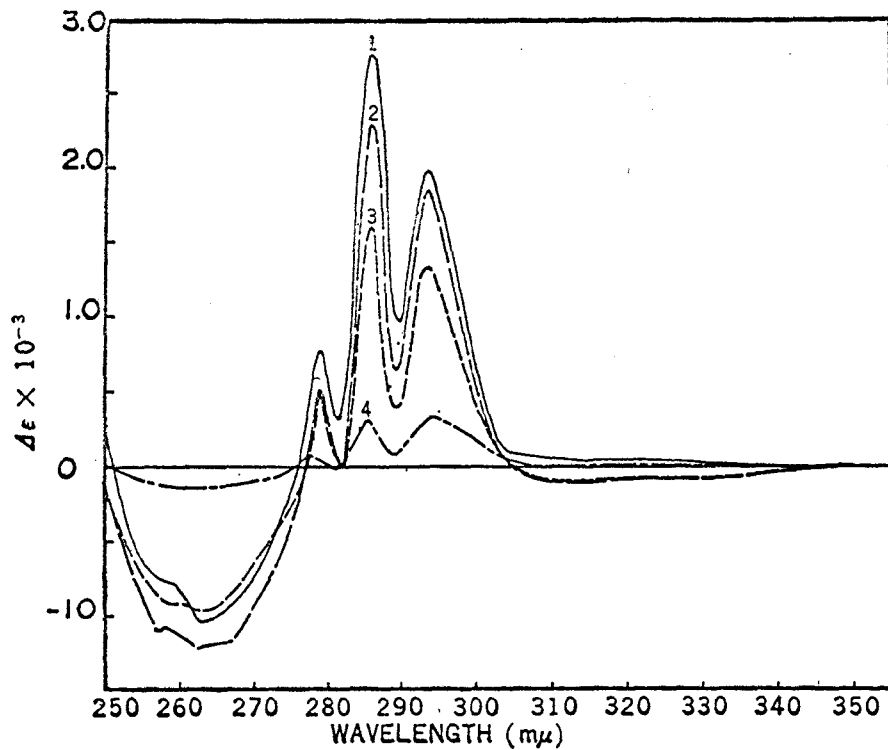


Fig. 36. Acid difference spectra of Bence Jones protein (Ta) at 25°C, ionic strength 0.1. Reference: Ta protein in 0.08 N HCl and 0.02 M KCl (pH 1.3).

1 pH 5.96; 2, pH 3.46; 3, pH 3.00; 4, pH 2.50.

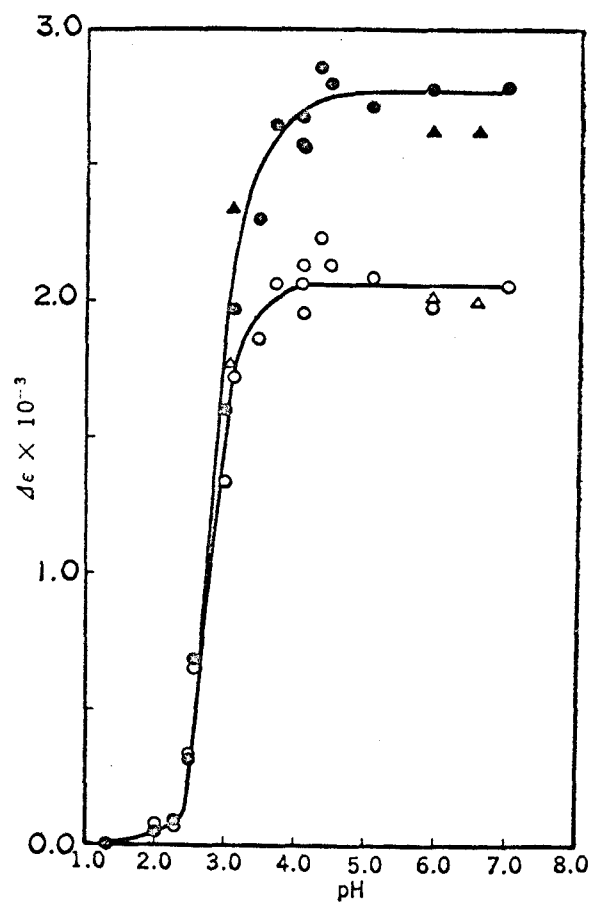


Fig. 37. $\Delta \epsilon$ at 293 nm (○) and 286 nm (●) as a function of pH. The values of $\Delta \epsilon$ at 293 nm and 286 nm measured at a given pH after exposure to pH 1.20 are shown by open and closed triangles, respectively.

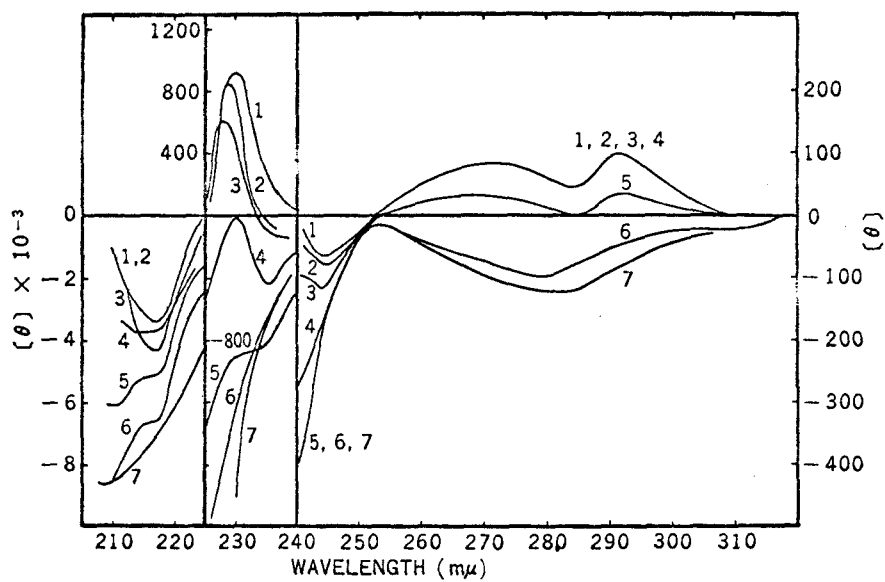


Fig. 38. CD Spectra of Bence Jones protein (Ta) at various acidic pH's. 1, pH 6.0; 2, pH 4.1; 3, pH 3.8; 4, pH 3.2; 5, pH 2.7; 6, pH 2.3; 7, pH 1.2.

below pH 4. At pH's below 2.3 a negative maximum appeared at around 280 nm.

Figure 39 shows the CD spectra of Ta protein at various alkaline pH's. At alkaline pH's a positive extremum appeared at 250 nm. The ellipticity of the negative CD band at 215 nm increased at pH 11.9 and then decreased with further increase in pH.

In Fig. 40 the values of $[\theta]$ at 215, 228, 250, and 292 nm are plotted against pH. The positive extremum at 228 nm the negative extremum at 215 nm were unchanged between pH 4 and 10. Below pH 4 and above 10 these extrema changed steeply. The value of $[\theta]$ at 250 nm increased above 10.

Figure 41 shows the CD spectra of Fu protein (type λ) at various pH values. The CD spectra in the region of 210 to 240 nm were independent of pH between pH 4.1 and 7.2 and had a negative maximum at 218 nm and a shoulder at around 228 nm. Lowering pH from 4.1 to 2.5 shifted the negative maximum to shorter wavelength but the magnitude of the maximum remained unchanged. Further decrease in pH to 1.1 deepened the negative maximum. In the region of 320 to 250 nm, the CD spectra of Fu protein showed pH dependence between pH 4.1 and 7.2 but are similar in shape with each other. These spectra had maxima at 300, 289, and 280 nm and minima at 293 and 284 nm. At pH 5.2, the CD spectrum changed and had positive maxima at 296 and 290 nm and a negative maximum at 281 nm. At pH 1.1, the CD spectrum changed markedly. In Fig. 42 the values of $[\theta]$ at 210 and 300 nm are plotted against pH.

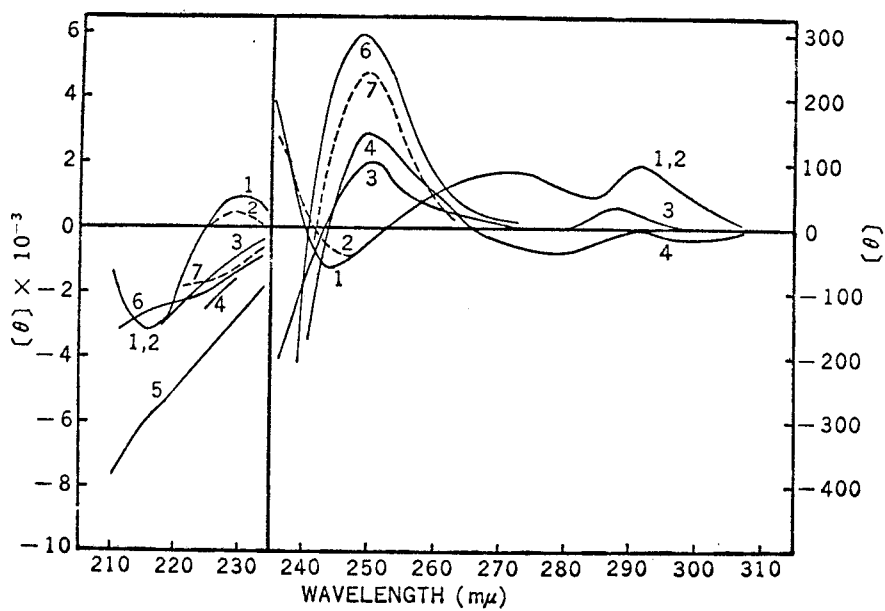


Fig. 39. CD Spectra of Bence Jones protein (Th) at various alkaline pH's. 1, pH 6.0; 2, pH 10.2; 3, pH 10.6; 4, pH 10.7; 5, pH 11.9; 6, pH 12.7; 7, pH 13.3.

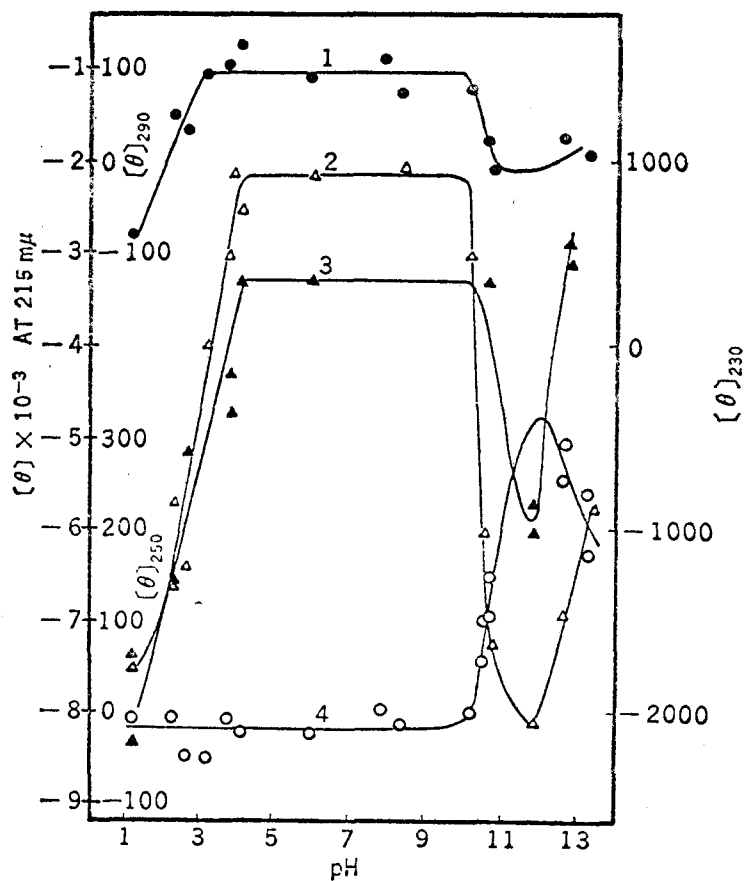


Fig. 40. Changes in the values of $[\theta]$ at 290 nm (curve 1), 230 nm (curve 2), 215 nm (curve 3), and 250 nm (curve 4) with pH.

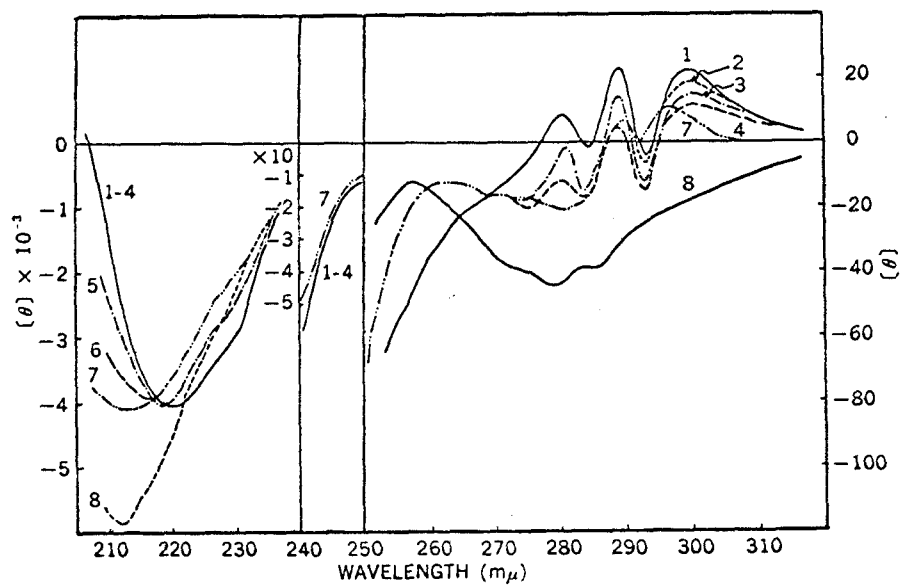


Fig. 41. CD spectra of Fu protein at various pH values. 25°C, ionic strength 0.15. 1, pH 7.2; 2, pH 6.0; 3, pH 5.1; 4, pH 4.1; 5, pH 3.5; 6, pH 3.0; 7, pH 2.5; 8, pH 1.1.

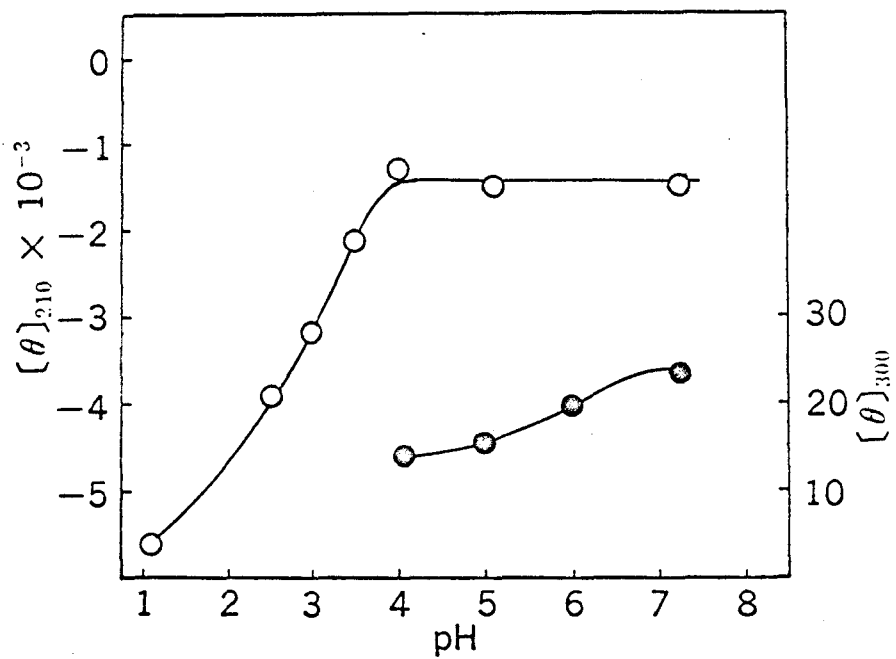


Fig. 42. The pH dependence of the values of $[\theta]$ at 210 nm (○) and 300 nm (●) for Fu protein.

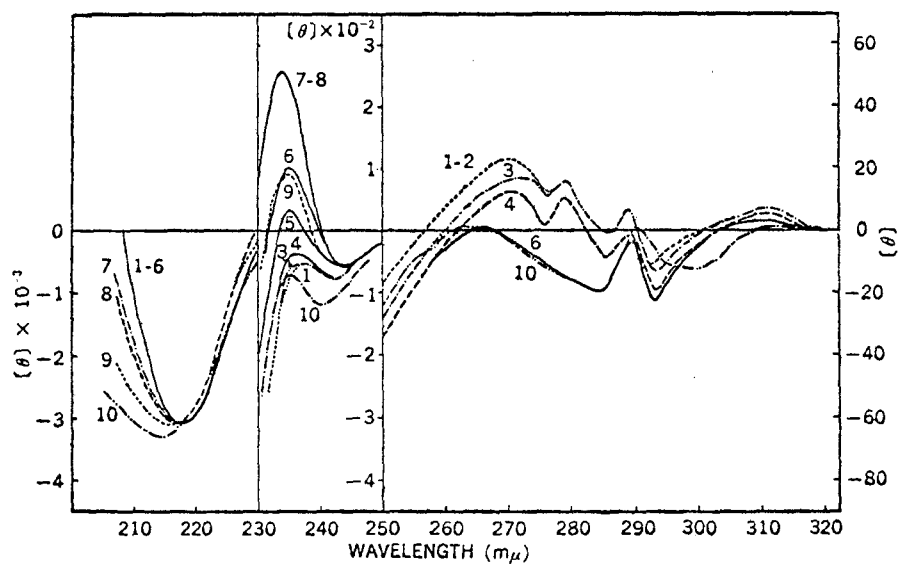


Fig. 43. CD Spectra of Ni protein at various pH values. 25°C, ionic strength 0.15. 1, pH 7.9; 2, pH 7.3; 3, pH 6.0; 4, pH 5.1; 5, pH 4.6; 6, pH 4.1; 7, pH 3.0; 8, pH 2.5; 9, pH 1.8; 10, pH 1.0.

Figure 43 shows the CD spectra of Ni protein at various pH values. The CD spectra at neutral pH values had positive maxima at 310, 290, 280, and 271 nm and negative maxima at 293, 286, 242, and 218 nm.

The changes in the ellipticities at 210, 237-233, and 293 nm are plotted against pH in Fig. 44. The ellipticity at 293 nm changed in the pH range where no change in the ellipticity at 210 nm occurs. The change in the ellipticity at 310 nm, which is not shown in this figure because of small magnitude of ellipticity, was parallel with that at 293 nm. It is very striking that a positive maximum appeared at 237-233 nm when the pH of the solution is lowered below 5.1. The value of $[\theta]$ at 237-233 nm was constant between pH 3.5 and 2.5 and then decreased with decreasing pH. Thus, the changes with pH in the values of $[\theta]$ at 210, 237-233, and 293 nm were not parallel with each other.

Figure 45 shows the CD spectra of Sh protein. The spectrum at pH 6.9 had positive maxima at 300 and 289 nm, negative maxima at 293, 284, and 219 nm and a shoulder at around 228 nm. The shape of this CD spectrum is very similar to that for Fu protein. However, in the case of Sh protein, no change with pH in the spectrum in the region of 250 to 310 nm was observed between pH 6.9 and 5.1. The change in the spectrum below pH 2.8 was very similar to that for Fu protein.

Figure 46 shows the CD spectra of As protein. The shape of the spectra in the region of 250 to 320 nm at pH's between 4.1 and 7.3

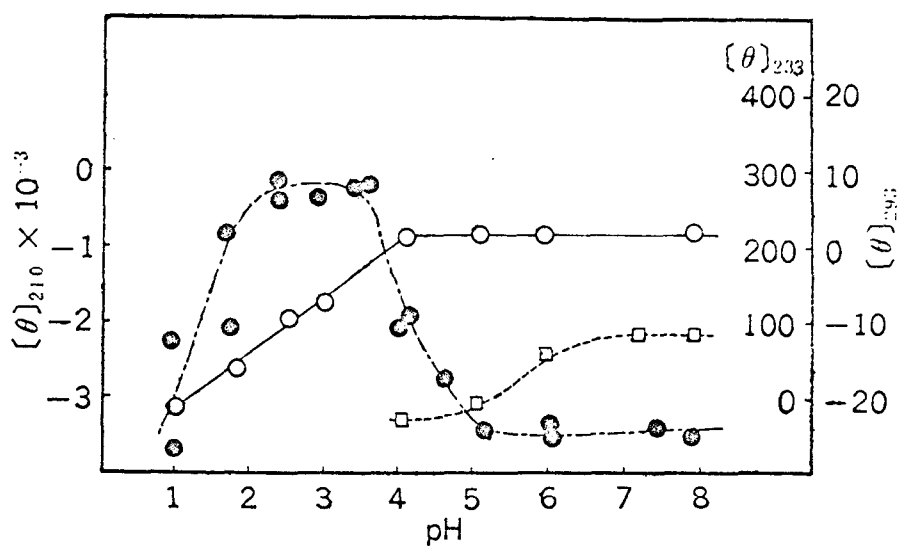


Fig. 44. The pH dependence of the values of $[\theta]$ at 210 nm (\bigcirc), 233 nm (\bullet), and 293 nm (\square) for Ni protein.

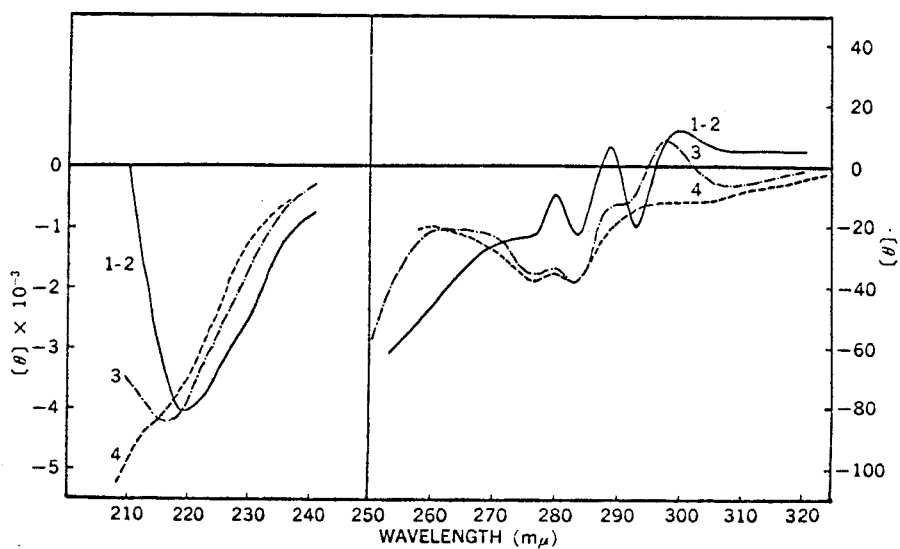


Fig. 45. CD Spectra of Sh protein at various pH values. 25°C, ionic strength 0.15. 1, pH 6.9; 2, pH 5.1; 3, pH 2.8; 4, pH 1.7.

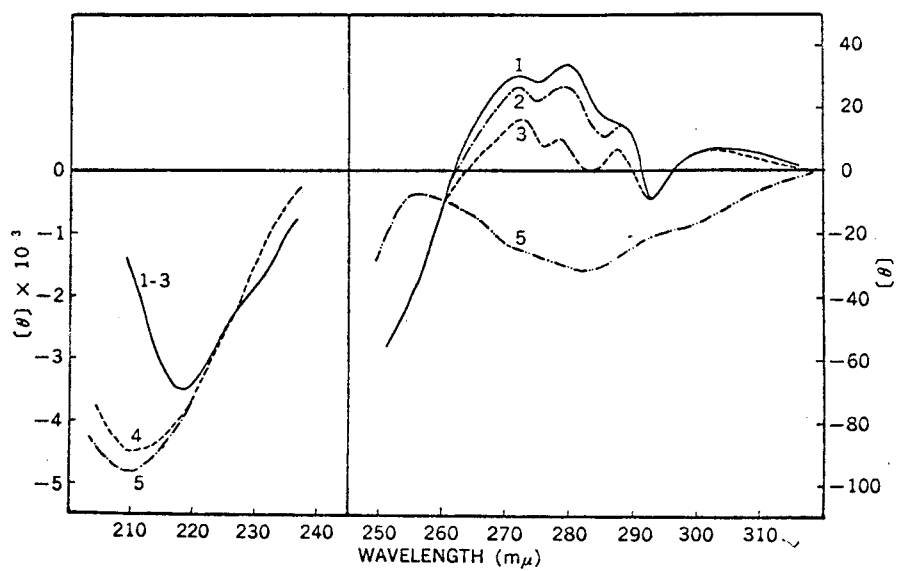


Fig. 46. CD Spectra of As protein at various pH values. 25°C, ionic strength 0.15. 1, pH 7.3; 2, pH 5.1; 3, pH 4.1; 4, pH 3.0; 5, pH 1.9.

resembles that for Ni protein. There were positive maxima at 303, 289, 280, and 272 nm and negative maxima at 293 and 218 nm. While there was no change with pH in the CD spectrum in the region of 205 to 240 nm at pH's between 4.1 and 7.3, the spectrum in the aromatic absorption region changed with pH.

The CD spectrum of To protein at neutral pH value had positive extrema at 302 and 293 nm, a shoulder at 287 nm and negative extrema at 268 and 219 nm (Fig. 47). There was only a slight difference between the CD spectrum at pH 5.1 and that at pH 7.0, in the region of 310 to 270 nm. The CD band at 219 nm was independent of pH in the range of 7.0 to 4.1. At pH 3.0, a great change in the spectrum occurred in the region of 250 to 310 nm.

The shape of the CD spectrum of Ko protein was very similar to that for Fu protein at neutral pH values (Fig. 48). The CD spectra in the pH range of 6.9 to 4.1 had a positive extremum at 293 nm and shoulders at 302 and 283 nm. At pH's below 4.1, the CD spectrum changed and the ellipticities in the region of 295 to 260 nm increased. From Fig. 49, in which the values of $[\theta]$ at 265 and 210 nm are plotted against pH, it is seen that a conformational change occurs below pH 4.

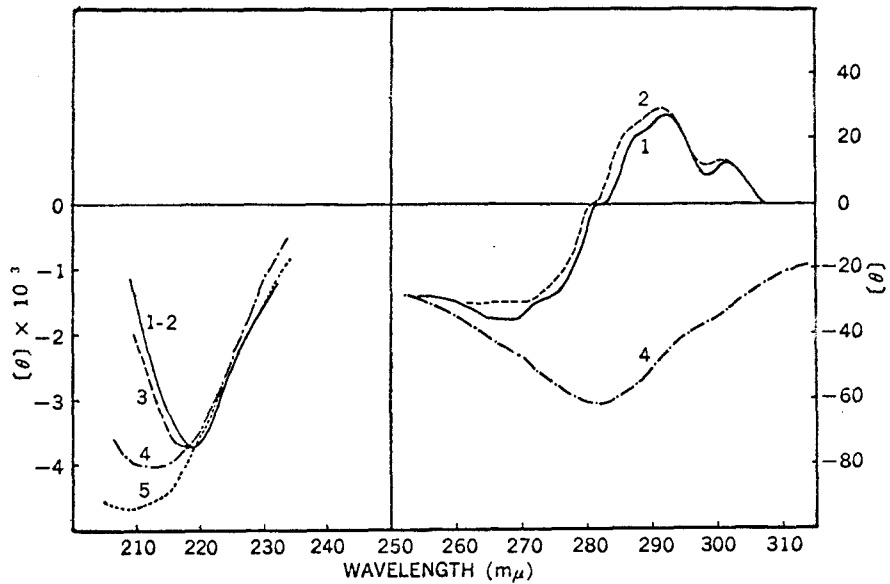


Fig. 47. CD Spectra of To protein at various pH values. 25°C, ionic strength 0.15. 1, pH 7.0; 2, pH 5.1; 3, pH 3.5; 4, pH 3.0; 5, pH 2.0.

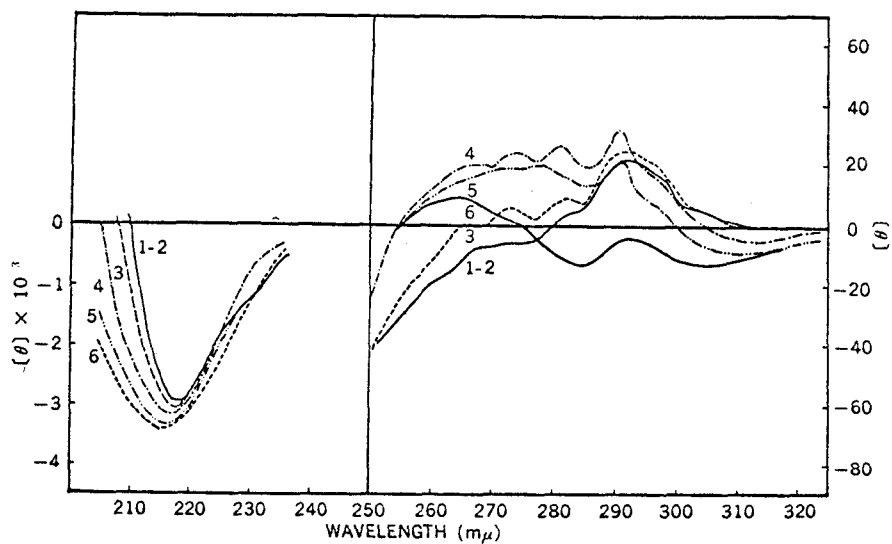


Fig. 48. CD Spectra of Ko protein at various pH values. 25°C, ionic strength 0.15. 1, pH 6.9; 2, pH 4.1; 3, pH 3.5; 4, pH 3.0; 5, pH 2.4; 6, pH 1.8.

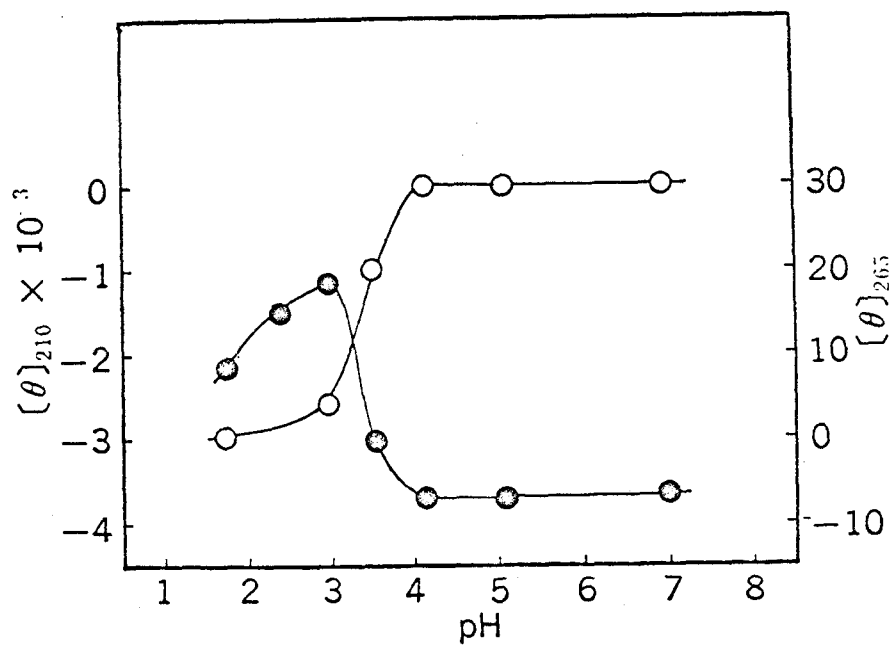


Fig. 49. The pH dependence of the values of $[\theta]$ at 210 nm (○) and 265 nm (●) for Ko protein.

IV DISCUSSION

IV-1 States of Ionizable Groups

As shown in Table I, Bence Jones protein (Ta) contains eighteen carboxyl, two histidyl, one α -amino, ten ϵ -amino, nine tyrosyl and twelve arginyl groups per molecular weight of 22,500.

The titration data for each type of ionization groups were analyzed by plotting them according to the equation of Linderström-Lang (60)

$$\text{pH} - \log \frac{\alpha_i}{1 - \alpha_i} = (\text{pK}_{\text{int}})_i - 0.868w\bar{Z} \quad (3)$$

where α_i is the degree of ionization of the i th type at a given pH, $(\text{pK}_{\text{int}})_i$ is the negative logarithm of the intrinsic dissociation constant of the i th group and $0.868w\bar{Z}$ is a term correcting for any electrostatic interaction between proton and the protein molecule of mean net charge \bar{Z} .

The value of electrostatic interaction factor can be calculated from Eq. (4), assuming the Linderström-Lang model of protein as a sphere with uniform charge distribution of the surface (60).

$$w = \frac{\epsilon^2}{2DkT} \left(\frac{1}{b} - \frac{\kappa}{1 + \kappa a} \right) \quad (4)$$

where ϵ is the electronic charge, D the dielectric constant, k the Boltzmann constant, T the absolute temperature, κ the Debye-Hückel

parameter, b the radius of the sphere which represents the protein molecule, and a the radius of exclusion, taken as $b + 2.5 \text{ \AA}$. The theoretical value of \mathcal{W} for the Bence Jones protein is calculated to be 0.040 at 25°C, ionic strength 0.15, on the basis of a radius of 25.4 \AA which is calculated by assuming partial specific volume to be 0.748 for γ G-immunoglobulin (61) and 20 % hydration. The value of b obtained by small-angle X-ray scattering method (17) was 26.3 \AA . On the basis of this radius, the value of \mathcal{W} is 0.038. The data for eighteen carboxyl groups of Ta protein in 0.15 M KCl were plotted according to Eq. (2) and are shown in Fig. 50. As shown in Fig. 50, the Linderström-Lang plot in the pH range above 4 ($\bar{Z} < 13$) is linear. The values of \mathcal{W} and pK_{int} obtained from this linear portion are 0.030 and 4.50, respectively. The value of \mathcal{W} thus obtained is 21-25 % lower than that theoretical value, as has been generally observed. A value of 4.50 for pK_{int} of the carboxyl groups lie close to the pK_{int} for model compounds (60, 62). A decrease in the slope above $\bar{Z} = 13$ (below pH 4) can be ascribed to a conformational change of the protein molecule. As will be described in followings, it was shown that Ta protein undergoes a conformational change below pH 4.0 from the measurements of ultraviolet absorption spectrum, optical rotation, and circular dichroism.

From the data of amino acid analysis, it was expected that two imidazole groups would be titrated in the neutral pH region but only

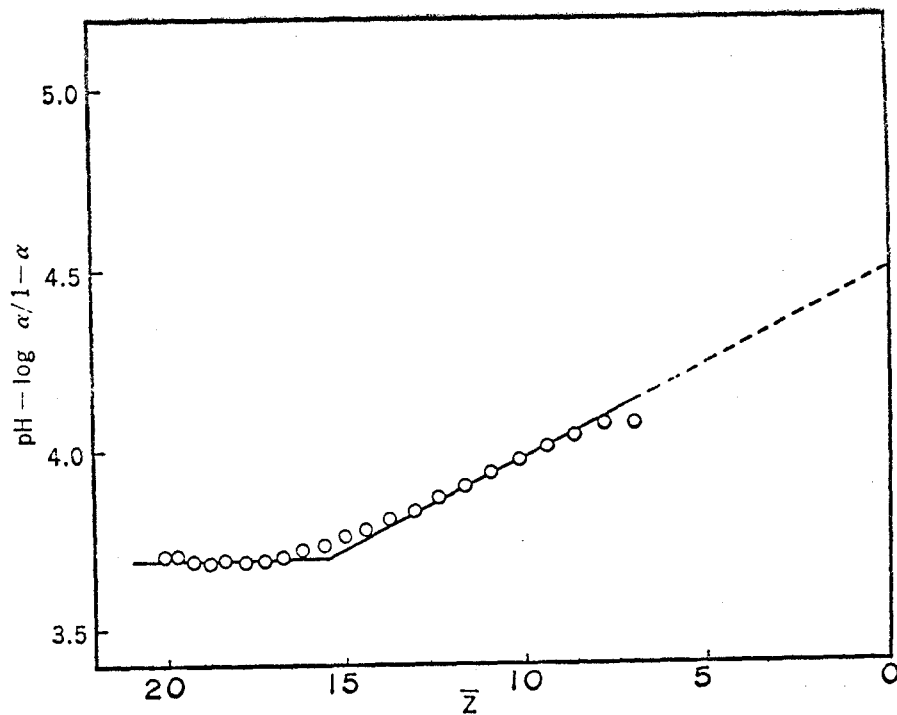


Fig. 50. Plot of the titration data of eighteen carboxyl groups of Ta protein in 0.15 M KCl according to Eq. (3).

one group was actually titrated. We can construct a theoretical titration curve between pH 5.2 and 8.3 which fits the experimental points, assuming that one imidazole and one α -amino groups are titrated with a pK value of 6.45 and 8.15, respectively, and the value of ω is the same as that for carboxyl groups, i.e., 0.030. The pK_{int} value of 6.45 for the imidazole group is normal, but pK_{int} of 8.15 for the α -amino group seems somewhat higher than that of model compounds (60).

At pH's above 8.3, the ϵ -amino groups of the lysyl residues begin to ionize. The number of protons binding to ϵ -amino groups was computed by subtraction of the spectrophotometric titration data shown in Fig. 2, from the potentiometric titration data shown in Fig. 1. Plot of the data according to Eq. (3) for ten lysyl groups is given in Fig. 51.

The plot consists of two linear portions with a break at $\bar{Z} = 0$ which corresponds to pH 10.2. The values of pK_{int} and ω obtained from the linear portion above $\bar{Z} = 0$ were 10.55 and 0.031, respectively. The value of pK_{int} for the lysyl groups is normal and the value of ω is in good agreement with that for carboxyl groups. The change in slope below $\bar{Z} = 0$ (above pH 10.2) reflects a conformational change of Ta protein. As will be shown in the following section, the same conclusion is obtained from the pH dependence of the circular dichroism spectrum.

The result of spectrophotometric titration of tyrosyl groups of

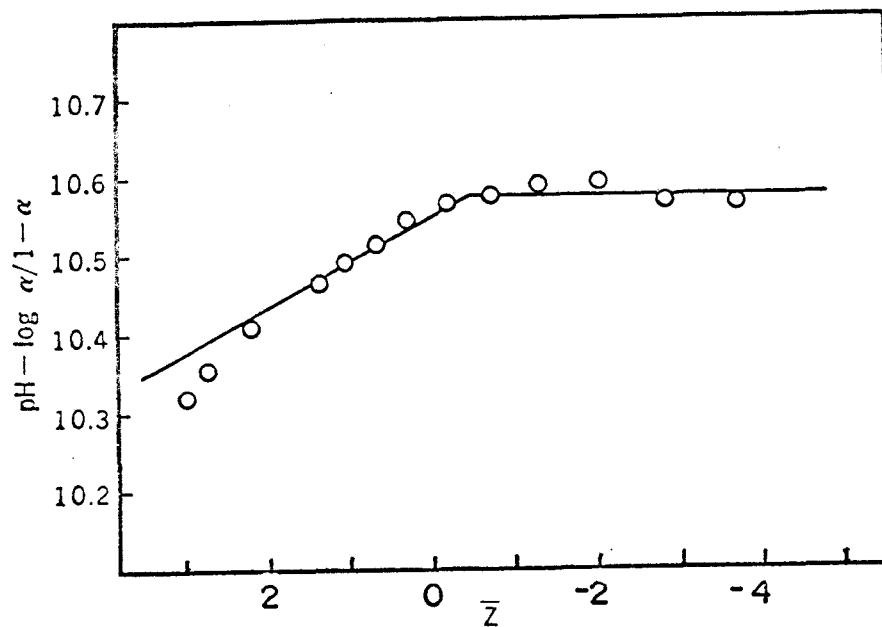


Fig. 51. Plot of the titration data of ten lysyl groups of Ta protein in 0.15 M KCl according to Eq. (3).

Ta protein shown in Fig. 2 is very similar to that of other type \mathcal{K} protein (Lo) reported by Hamaguchi et al.(27). The Linderstrøm-Lang plot for nine tyrosyl groups of Ta protein is shown in Fig. 52, where the points above pH 11.5 are omitted.

A value of 0.005 for w and 11.24 for pK_{int} were obtained from Fig. 52. The value of w for tyrosyl groups is much smaller than that for lysyl or carboxyl groups. However, as shown in Fig. 52, the points deviate from the linear portion above $\bar{Z} = 0$. As described above, Ta protein undergoes a conformational change above pH 10.2 (below $\bar{Z} = 0$). Therefore, the small value of w for the tyrosyl residues below $\bar{Z} = 0$ is due to the conformational change of the protein molecule.

Comparison of the spectrophotometric titration curve (Fig. 2) with the pH dependence of the circular dichroism spectrum (Fig. 40) shows that only one of nine tyrosyl residues of Ta protein ionizes freely without any conformational change. The points deviated from the linear portion of the Linderstrøm-Lang plot for tyrosyl groups (Fig. 52) correspond to those for one tyrosyl residue. A theoretical titration curve of the tyrosyl residue can be constructed, assuming that $pK_{int} = 9.65$ and $w = 0.031$. The value of 9.65 is normal pK_{int} value for tyrosyl groups and the value of w of 0.031 was the same for lysyl groups. The remaining eight tyrosyl residues ionize above pH 10.2 with $pK_{int} = 11.24$ with a conformational change.

Table V summarizes the value of pK_{int} and w for all the ionizable

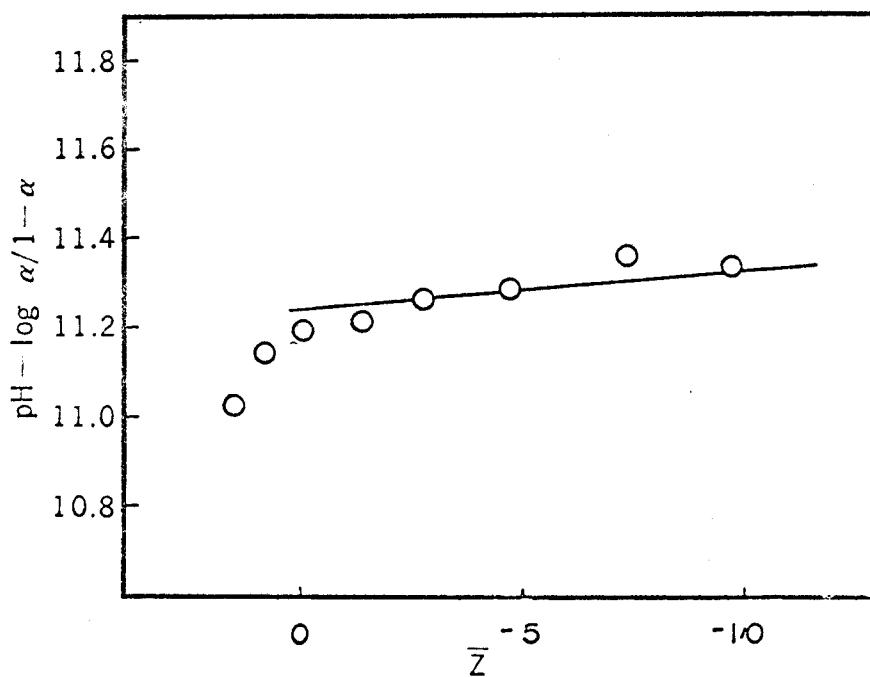


Fig. 52. Plot of the titration data for nine tyrosyl groups of Ta protein at ionic strength of 0.15 according to Eq. (3).

TABLE V. Parameters used to calculate titration curve of Ta protein

Group	Number			
	Analysis	Titration	pK_{int}	w
Carboxyl	18	18	4.50	0.030 ($>pH 4$)
Imidazole	2	1	6.45	0.030
α -Amino	1	1	8.15	0.030
Lysyl	10	10	10.56	0.031 ($<pH 10.2$)
Tyrosyl	9	9	9.55 for 1	0.031 ($<pH 10.2$)
			11.24 for 8	0.005 ($>pH 10.2$)
Arginyl	12			

groups except guanidyl groups of Bence Jones protein (Ta). One of the two imidazole groups is masked and unavailable for titration in the native protein. Only one of the nine tyrosyl residues are located on the surface and ionizes freely.

The conclusion about the state of the tyrosyl and histidyl groups was also confirmed by the experiments of the acetylation of the tyrosyl residues, as described below, and the results of iodination of tyrosyl and histidyl residues of a χ Bence Jones protein by Seon et al.(63). Eighteen carboxyl, one α -amino and ten lysyl groups have normal pK_{int} values. This suggests that at least carboxyl and amino groups are not involved in the dimer formation.

As Tanford et al.(64) had evaluated the value of electrostatic interaction factor \mathcal{W} for serum albumin, the value of \mathcal{W} at each pH was calculated directly by use of Eq. (3), assuming the pK_{int} values of the ionizable groups to be those given in Table V. The results are shown in Fig. 53.

As can be seen from Fig. 53, the value of \mathcal{W} is constant in the region of pH 4.0 to 10.2 and decreases outside of this region. This shows that a conformational change occurs below pH 4.0 and above 10.2. The result shown in Fig. 53 is in good agreement with that obtained by the measurements of circular dichroism, ultraviolet absorption spectra and optical rotation.

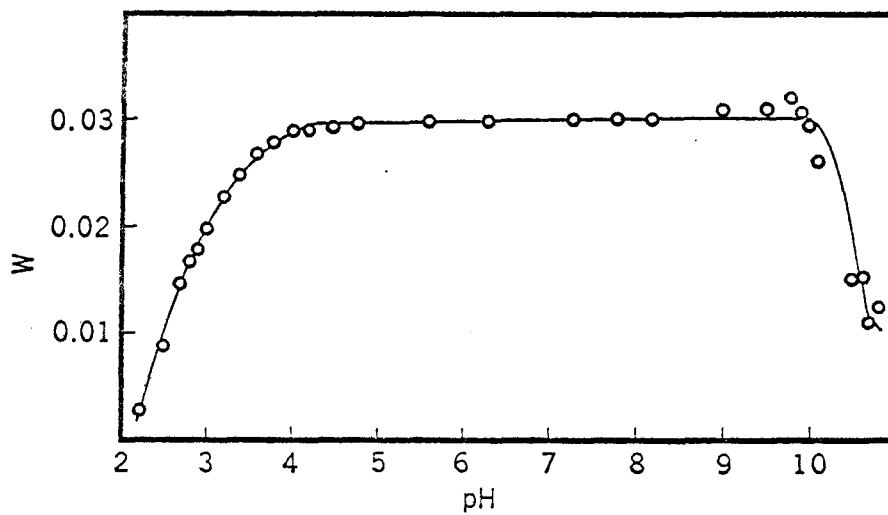


Fig. 53. The empirical electrostatic interaction factor, ω , as a function of pH (see the text).

IV-2 States of Tyrosyl and Tryptophyl Residues

States of Tyrosyl Residues-----Bence Jones proteins contain six to eleven tyrosyl residues per molecular weight of 22,500 (28). These tyrosyl residues may be classified from the reactivity with NAI into three types; (1) 1.5 residues which are readily acetylated at low concentrations of NAI, (2) additional 1.5 residues which are acetylated at higher concentrations of NAI, and (3) the remaining residues which are acetylated after urea denaturation. However, the amount of NAI which is needed for maximal modification is different from protein to protein. In the case of As protein, three tyrosyl residues are acetylated at low concentrations of NAI, whereas 100-fold molar excess of NAI is needed for the modification of three tyrosyl residues of Ya and Ko proteins, and 200-fold molar excess for the three residues of Fu protein. In the case of Ta protein, only 1.5 to 2 tyrosyl residues are acetylated with 300-fold molar excess of NAI, and the reactivity of the tyrosyl residues of Sh protein is exceptional; it has 4.5 NAI-reactive tyrosyl residues. These difference in reactivity have no relation with the antigenic type of Bence Jones proteins.

As described above, one of the nine tyrosyl residues of Ta protein ionizes freely with an intrinsic pK of 9.65. This is in good agreement with the result of acetylation for Ta protein. Hamaguchi et al.(27) have reported the results of the spectrophotometric titration of the tyrosyl groups of Bence Jones proteins at 246 and 296 nm. They showed

that tyrosyl ionization of all the Bence Jones proteins is abnormal. For instance the titration curve of Fu protein at 246 nm has at least four stages. The first stage is the ionization of one tyrosyl residue having an apparent pK value of 9.5. In the second stage, additional two tyrosyl residues ionize accompanying a slight conformational change. The number of tyrosyl residues acetylated at low concentrations of NAI is in agreement with the number of tyrosyl residues with a pK value of 9.5.

Seon et al.(63) showed that Tyr-173 of the constant region of type κ Bence Jones protein is, in general, the most reactive residue toward iodination. The tyrosyl residue of Ta protein which is acetylated at low concentrations of NAI and ionizes freely may therefore be Tyr-173 in the constant region of the molecule. The tyrosyl residue of Ya (type κ) which is readily acetylated may also be Tyr-173. Type λ proteins have a tyrosyl residue at position 174 in place of 173 for type κ (28). This suggests that the most reactive tyrosyl residue of type λ protein (Fu and Ko) may be Tyr-174.

There are additional two tyrosyl residues of Ya, Fu, and Ko proteins which are acetylated at higher concentrations of NAI. These two residues may be less exposed. Seon et al.(63) have found that the next reactive tyrosyl residues toward iodination are Tyr-186 and Tyr-192 in type κ proteins. In the case of As and Sh proteins of type λ , however, the most NAI-reactive tyrosyl residue was not found; three tyrosyl

residues of As protein and four to five tyrosyl residues of Sh protein could not be differentiated into subgroups from the reactivity toward acetylation.

States of Tryptophyl Residues——As shown in Table II, no tryptophyl residue of Ta protein was accessible to HNB bromide. In the presence of 6.3 M urea, however, two tryptophyl residues were modified with the reagent. The value of $\Delta \epsilon$ at 293 nm in the difference spectrum of Ta protein in 6.3 M urea was -3,800. Assuming that all the buried tryptophyl residues (two) are exposed upon urea denaturation and correction for the effect of urea perturbation on the two tryptophyl residues exposed based on the value of $\Delta \epsilon$ for N-acetyl-L-tryptophan ethyl ester in 6.3 M urea, the value of 4,400 was obtained as the change in the molar extinction coefficient at 293 nm accompanying exposure of the two tryptophyl residues from the interior of the protein molecule to aqueous environment. It has been shown for some proteins that the change in the molar extinction coefficient at 293 nm accompanying the transfer of one tryptophyl residue from the interior of the protein molecule to solvent water is about -2,000 to 2,500 (65-67). The value, 2,200, for the transfer of one tryptophyl residue of Ta protein supports the idea that two tryptophyl residues are exposed on urea denaturation. As will be described in the following section, Ta protein undergoes a conformational change at pH's below 4 and one tryptophyl residue is exposed on the acid denaturation. The change in the molar

extinction coefficient at 293 nm for the acid denaturation was -2,050 to -2,100 (Fig. 5 and 37). The addition of 6.3 M urea to the acid-denatured Ta protein solution caused a change in the molar extinction coefficient which corresponds to the exposure of one tryptophyl residue (Table III). These results are summarized as follows: (1) two tryptophyl residues are buried in the native Ta protein molecule, (2) one of these tryptophyl residues is exposed on acid denaturation, (3) the remaining buried tryptophyl residue in the acid-denatured Ta protein is exposed with 6 M urea, and (4) both of the two buried tryptophyl residues in the native molecule are exposed by urea denaturation.

The same analysis was applied to Fu protein (type λ). As shown in Table II, one tryptophyl residue reacts with HNB bromide in 0.15 M KCl at pH 5. In the presence of 6.3 M urea, three tryptophyl residues react with this reagent. These facts show that one of the three tryptophyl residues is located on the surface of the Fu protein molecule and the remaining two are buried in the interior of molecule. The acid difference spectrum of Fu protein showed a value of $\Delta \epsilon = -2,100$ at 293 nm (Table III), which indicates that one tryptophyl residue is exposed from the interior to aqueous environment. The difference spectrum of Fu protein denatured by 6.3 M urea showed a value of $\Delta \epsilon = -4,100$ at 293 nm. Correcting for the effect of 6.3 M urea on three tryptophyl residues, the value of $\Delta \epsilon$ for the exposure of two trypto-

phyl residues from the interior of the protein molecule to solvent water was estimated to be -5,200. This means -2,600 for the exposure of one tryptophyl residue, which is in agreement with the value obtained for Ta protein. The addition of 6.3 M urea to the acid-denatured Fu protein solution caused a change in the molar extinction coefficient corresponding to the exposure of one tryptophyl residue. These facts show that the two tryptophyl residues in Fu protein (type λ), behave similarly to the two buried tryptophyl residues in Ta protein (type χ), upon both acid and urea denaturation.

Human type χ Bence Jones proteins of which amino acid sequences have been determined have tryptophyl residues at positions 35 and 148 (28). It may therefore conclude that the two tryptophyl residues at positions 35 and 148 of Ta protein are buried in the interior of the protein molecule.

In the case of type λ Bence Jones proteins, three tryptophyl residues at positions 34, 150, and 187 are invariant, and a tryptophyl residue at position 90 in some type λ proteins is replaced by a tyrosyl or arginyl residue in other type λ protein (28). Therefore, the three tryptophyl residues of Fu protein may occur at positions 34, 150, and 187. From analogy with Ta protein, the tryptophyl residues at positions 34 and 150 may be inferred to be buried in the interior of the Fu protein molecule and the tryptophyl residue which is located on the surface of the molecule may be Trp-187. In the case of type χ Bence Jones

proteins, Tyr-186 is invariant (28), and Seon et al. (63) have reported that the most reactive tyrosyl residue toward iodination is Tyr-173 and the next reactive ones are Tyr-186 and Tyr-192. Type λ Bence Jones proteins have a tryptophyl residue in place of tyrosyl residue at position 187. These facts also suggest that Trp-187 may be on the surface of Fu protein molecule.

IV Domain Structure

It is known that the extrinsic Cotton effects of dyes attached to a protein reflect sensitively the local environment of the protein molecule (38-41). FMA molecule combined with the sulfhydryl group at the carboxyl terminus in type χ Bence Jones proteins and at the penult in type λ proteins generates characteristic extrinsic Cotton effects. The CD spectra of FMA conjugated with different χ Bence Jones proteins are closely similar to each other (Figs. 7 and 8). The similarity of the position and sign of the CD band observed for FMA conjugated with χ proteins suggests that the local region where FMA is attached has closely similar environment. However, the CD spectra of λ proteins differ one another in intensity and pH dependence. The CD spectra of FMA conjugated with λ Bence Jones proteins differ greatly from specimen to specimen in spectral locations, signs, and magnitudes (Figs. 7 and 9).

Björk et al. (36) and Ghose and Jirgensons (37) have demonstrated

the constant and variable halves of Bence Jones proteins exist as independently folded regions. In view of the similarity of the extrinsic Cotton effects of FMA conjugated with κ proteins, it is suggested that the conformation of the variable portion has no significant effect on the conformation of the constant portion and the environment or conformation of the constant portion is similar to each other in κ proteins.

The difference of CD spectra from specimen to specimen in FMA- λ protein conjugates may be explained in terms of the fact that the constant half of κ proteins has a single amino acid sequence except the residue at position 191 which is related to Inv antigenic specificity, while in the constant half of λ proteins replacements of amino acid residue occur at three positions of 144, 153, and 172 in addition to position 190 which is related Oz antigenic specificity (68). Further variation in 158 to 167 was suggested by the peptide map analysis of some λ Bence Jones proteins. The extrinsic Cotton effects generated by FMA may reflect the difference of local conformation of the constant half in λ proteins. However, the replacements of amino acid residues may not contribute to the conformation of the constant half largely, because the CD spectra of the constant halves of λ proteins calculated are similar to one another as will be described in the following section. Fairclough and Vallee (40) showed that the extrinsic Cotton effects are more sensitive than the side-chain Cotton effects to the

conformational change of proteins. They found the difference of the local conformation between α -chymotrypsin and chymotrypsinogen A by use of extrinsic Cotton effects of arsanilazo-groups, though X-ray diffraction studies show that overall folding of their polypeptide chains is very similar to each other. The CD spectra in the wavelength region between 320 and 240 nm, which are originated from chromophoric side-chains of amino acid residues of these proteins, were very similar to each other.

Another explanation is that the difference of the CD spectra of λ proteins is due to the interaction between the surface of the constant half and that of the variable half. As will be described in the following section, this interaction is suggested from the pH dependence of the CD band at 300 to 310 nm of λ proteins. It may be taken into account the effect of the variable half upon the FMA molecule conjugated with the constant half of λ proteins. In the case of χ proteins, there is no interaction between two halves or, if any, the interaction is more weak than that in the case of λ proteins.

Recently, X-ray crystallographic studies show that the constant and variable halves of χ and λ Bence Jones proteins fold independently (42, 43). Owing to the low resolution of diffraction studies, however, the fine structural features are not apparent yet.

IV-4 Stability toward Denaturants

IV-4-1 Denaturation by GuHCl

The transitions of all the Bence Jones proteins in the present experiments induced by addition of GuHCl begin to occur at 0.8 or 0.9 M. The results presented above also demonstrate that the transitions of Bence Jones proteins consist of two stages. As will be described in the following, in the case of λ proteins, the first transition corresponds to disruption of the constant half and the second to disruption of the variable half. In the case of χ proteins, on the other hand, a conformational change in both the constant half and a portion of the variable half seems to occur in the first transition.

Type λ Bence Jones Proteins——The denaturation of type λ Bence Jones proteins reveals a number of noteworthy features. (1) The denaturation of all the λ proteins studied in the present experiments begins to occur above 0.9 M GuHCl, judging from the optical rotation at 250 nm and from the $[\theta]$ band at 218 nm. (2) Two stages are observed for the change in the optical rotation at 250 nm for Ni and Tod proteins. The first transition occurs between 0.9 and 1.5 M GuHCl and the second above 1.5 M. The GuHCl concentration at which the second transition ends is different from each other. The change in the optical rotation at 250 nm in the first stage is approximately half the total change. In the case of Fu protein, the transition occurs

apparently in one stage. However, the change with GuHCl concentration in the character of the CD spectrum in the aromatic absorption region is very similar to those for Ni and Tod proteins. (3) In the case of the transition of Ni protein, the positive CD band at 233 nm increased and reached a maximum at 1.5 M GuHCl, followed by a decrease with further increase in the GuHCl concentration. Since GuHCl has an ability to randomize the protein molecule (69), this fact suggests that the positive band at 233 nm for Ni protein appears as a consequence of disruption of a part of the Ni protein molecule which, in the native state, has an effect of reducing this positive band. The CD band near 233 nm was not observed for the other two type \mathcal{A} proteins at any GuHCl concentration. These facts suggest that the disruption must have occurred in the constant half of the Bence Jones protein molecule at the GuHCl concentrations up to 1.5 M and the residue which is responsible for the CD band at 233 nm must locate in the variable half. (4) For Ni and Tod proteins, no appreciable difference is observed in the CD spectra between 1.2 and 1.5 M GuHCl. (5) The CD spectra of the three \mathcal{A} proteins in 3.0 or 3.6 M GuHCl are very similar to each other. This suggests that the proteins in these GuHCl solutions are denatured completely and that there was little difference in the CD spectra between the constant and variable half, when they are unfolded completely.

On the basis of these facts, it is assumed that the variable and constant halves are folded independently and that the constant half

of the λ protein molecule is less stable than the variable half in GuHCl solutions. It will be readily accepted that, whereas the constant half has the same stability for all the λ proteins, the stability of the variable half is different from one specimen to another. This is reflected by the fact that while the first transition begins to occur at the same GuHCl concentration (0.9 M) for all the λ proteins, the GuHCl concentration at the end of the transition is different from each other. Thus if it is assumed that the first stage of the transition corresponds to a conformational change of the constant half, the CD spectrum at 1.2 or 1.5 M GuHCl represents the CD of the Bence Jones protein molecule which consists of the constant unfolded and the variable half folded as it is in the native whole molecule.

The observed mean residue ellipticity ($[\theta]_N$) of native Bence Jones protein at any wavelength can be expressed by the following equation,

$$[\theta]_N = \frac{1}{2} [\theta]_N^C + \frac{1}{2} [\theta]_N^V \quad (5)$$

where $[\theta]_N^C$ and $[\theta]_N^V$ are the mean residue ellipticities of the constant half and variable half in the native state, respectively. The number of the residues contained in the both halves is assumed to be identical (107).

Similarly, the mean residue ellipticity of the completely denatured proteins ($[\theta]_D$) is expressed by the equation,

$$[\theta]_D = \frac{1}{2} [\theta]_D^C + \frac{1}{2} [\theta]_D^V \quad (6)$$

where $[\theta]_D^C$ and $[\theta]_D^V$ are the mean residue ellipticities of the completely denatured constant and variable halves, respectively. Since no respective CD spectrum of the constant and variable halves are available, CD spectrum of the whole molecule of the Bence Jones protein in 3.0 or 3.6 M GuHCl was used to estimate the CD of the denatured constant and variable halves with the assumption,

$$[\theta]_D^C = \frac{1}{2} [\theta]_D \quad \text{or} \quad [\theta]_D^V = \frac{1}{2} [\theta]_D \quad (7)$$

This assumption is verified by the fact that all the three λ proteins have the same CD spectrum in the completely denatured state.

At 1.2 or 1.5 M GuHCl, the observed mean residue ellipticity, $[\theta]_D^H$, is expressed by the equation,

$$[\theta]_D^H = \frac{1}{2} [\theta]_D^C + \frac{1}{2} [\theta]_D^V \quad (8)$$

The CD spectra of the native variable half and the native constant half are obtained by the Eqs. (9) and (10), respectively.

$$[\theta]_N^V = 2 \left\{ [\theta]_D^H - \frac{1}{2} [\theta]_D \right\} \quad (9)$$

and

$$[\theta]_N^C = 2 \left\{ [\theta]_N - \left([\theta]_D^H - \frac{1}{2} [\theta]_D \right) \right\} \quad (10)$$

As described in "RESULTS", the presence of 0.6 M GuHCl affects the CD spectra in the region of 230 to 280 of Bence Jones proteins but not the negative band at 218 nm which reflects the conformation of the polypeptide backbone. The reason for this fact is not clear at present but it is not due to an ionic strength effect, since 0.5 M KCl had no effect on the CD spectrum of Tod protein. Since, however, the CD spectrum at GuHCl concentrations higher than 0.6 M may involve the effect of GuHCl on the CD spectrum, the data at 0.6 M GuHCl was used in these calculations instead of the data in the absence of GuHCl for the value of $[\theta]_N$.

The CD spectra of the native variable halves of Ni, Tod, and Fu proteins calculated by using Eq. (9) are shown in Fig. 54. The CD spectra are different from one specimen to another, reflecting different conformations determined by the different amino acid sequence of the variable halves.

Figure 55 shows the CD spectra of the native constant halves of Ni, Tod, and Fu proteins calculated by using Eq. (10). As expected,

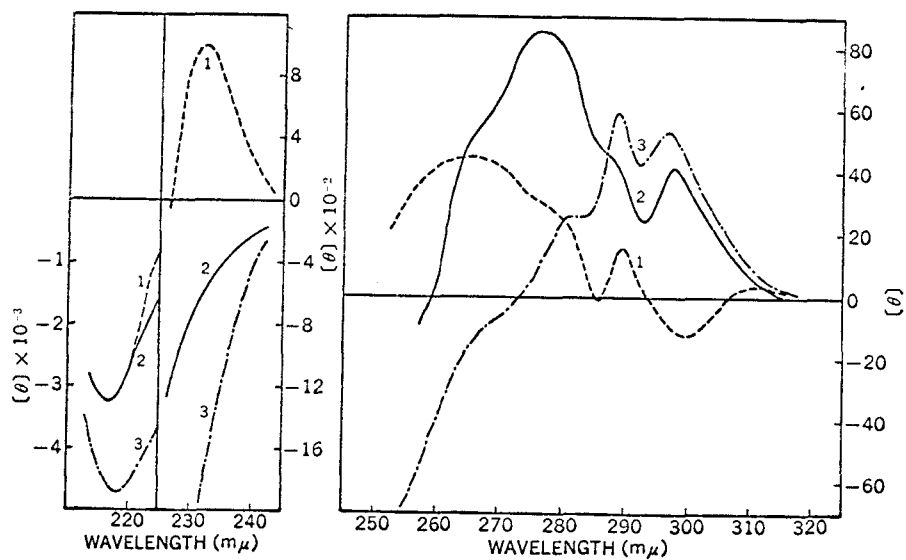


Fig. 54. Calculated CD spectra of variable halves of type A Bence Jones proteins (see the text for detail). 1, Ni protein; 2, Tod protein; 3, Fu protein.

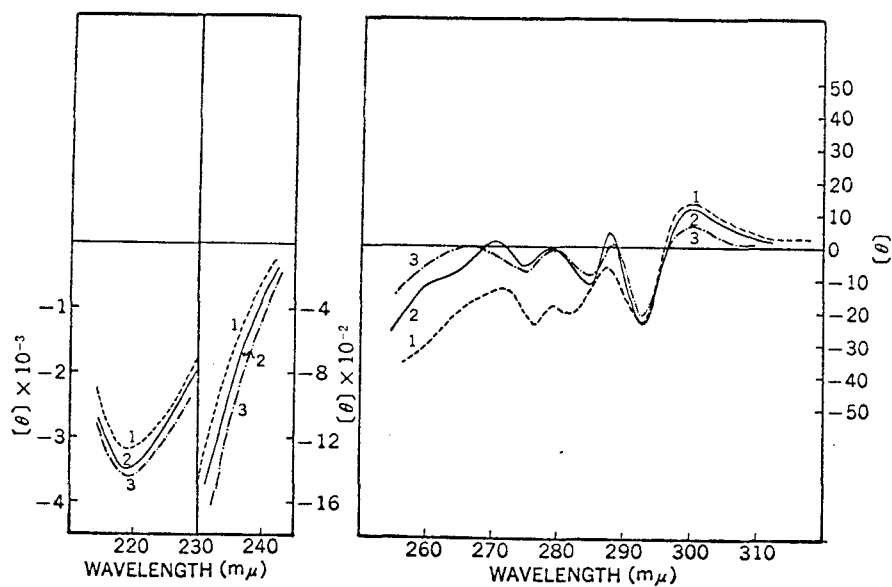


Fig. 55. Calculated CD spectra of constant halves of type λ Bence Jones proteins (see the text for detail). 1, Ni protein; 2, Tod protein; 3, Fu protein.

these spectra are very similar to each other and had a positive maximum at 300 nm and negative maxima at 293 and 218 nm. Several humps observed in the region of 250 to 290 nm also correspond to each other. The value of $[\theta]$ at 218 nm for the three constant halves are approximately the same ($-3.3-3.5 \times 10^3$ degrees $\text{cm}^2 \text{dmole}^{-1}$). These values are compared to a value of -4×10^3 degrees $\text{cm}^2 \text{dmole}^{-1}$ obtained by Björk et al. (36) for the constant half isolated by proteolytic digestion of a λ Bence Jones protein. Recently, the CD spectra of constant and variable halves obtained by limited tryptic digestion of a type λ protein have been reported by Ghose (70). The CD spectrum of the constant half is in quite agreement with the spectrum of the constant half calculated in band positions and sign.

Comparison of the CD spectra in Fig. 54 with those in Fig. 55 reveals that the amplitudes of the CD spectrum in the region of 250 to 320 nm of the variable half are much larger than those for the constant half. The individual variation of the CD spectra of the Bence Jones proteins is thus due to these large amplitudes at different CD positions of the variable half. In the case of χ proteins, the amplitudes of the CD spectrum of the variable half have also been observed to be much larger than those for the constant half (37). The positive CD band at 233 nm observed for Ni protein is originated from tryptophyl or tyrosyl residue (71-73) located in its variable half.

Type χ Bence Jones Proteins——The transitions of the two type χ

proteins (Ta and Ham) induced by addition of GuHCl begin to occur at 0.8 M. The transition curves determined by the measurements of $[m']$ at 250 nm consist of two stages (Fig. 18). Corresponding to this, the CD measurements also confirm the presence of an intermediate (Figs. 19 and 21). The positive CD band for Ta protein and the shoulder for Ham protein appeared around 230 nm suggested to be originated from a tyrosyl or tryptophyl residue located in the constant half, since Ghose and Jirgensons (37) have found that the CD spectra of the constant halves isolated by proteolytic digestion of two χ proteins have also a positive band around 230 nm. As shown in Fig. 19, the positive band at 228 nm for Ta protein decreased steeply above 0.8 M GuHCl. This suggests that, in the case of χ proteins also, the constant half is first disrupted by addition of GuHCl. Unlike the λ proteins described above, however, the first stage of the transition seems to involve not only a conformational change of the constant half but also a conformational change of a part of the variable half. The reason for this is that the change in the value of $[m']$ at 250 nm in the first stage (from 0.8 to about 2 M GuHCl) corresponds to approximately 90 % for Ta protein and 70 % for Ham protein of the total change in the value of $[m']$ (Fig. 18). At the plateau around 2 M GuHCl, the CD spectrum of Ta protein in the region of 250 to 310 nm is very similar to that of Ham protein (Figs. 19 and 21), whereas, in the case of λ proteins, the CD spectra at the plateau around 1.5 M are very different

from each other. This also suggests that in the case of χ proteins, the intermediate does not have a conformation in which only the constant half is unfolded and the variable half remains folded. Attempt to draw CD spectra of the constant and variable halves of χ proteins by use of the same procedure as was done for λ proteins failed.

IV-4-2 Denaturation by Urea

The results of optical rotation measurements indicate that the urea denaturation of Ta protein at neutral pH values proceeds in at least two stages. The first stage corresponds to a steep increase in levorotation between 2 and 4.5 M urea and the second to a gradual increase in levorotation above 5 M urea. The transition is not complete even at 8 M urea. This observation is also confirmed by the CD measurements (Fig. 25).

The Bence Jones protein monomer contains two intrachain disulfide bonds, one in the variable half and the other in the constant half. The reactivity of these disulfide bonds of Ta protein changes in two steps on addition of urea (Fig. 29). Between 2 and 5 M urea, only one intrachain disulfide bond is cleaved and above 5 M urea a further gradual increase in the reactivity is observed. Titani et al.(74) reported that complete reduction of the intrachain disulfide bond in the variable half of a type χ protein does not occur even in 8 M urea solution. Therefore, it is suggested that one disulfide bond of Ta

protein which resists the reduction by DTT at high urea concentrations is located in the variable half.

As described above, Ta protein contains two tryptophyl residues at position 35 in the variable half and at position 148 in the constant half and both tryptophyl residues are buried in the interior of the protein molecule. The change in reactivity of these tryptophyl residues with urea concentration proceeds in a single step (Fig. 29) and all the tryptophyl residues are modified at 4 M urea where only one disulfide bond is reduced. The change in the value of $\Delta \epsilon$ at 293 nm in the difference spectra produced by urea, which originates from the change in the state of the tryptophyl residues, also proceeds in a single step (Fig. 28). Thus, the changes with urea concentration of the reactivity of the intrachain disulfide bonds and that of the tryptophyl residues are not parallel with each other. This difference is not ascribable to the difference in the pH at which these modifications are performed, pH 8 for the disulfide reduction and pH 5.0 for the tryptophyl modification, since no appreciable difference is observed between the change with urea concentration in $[m']$ at pH 5.5 and that at pH 8.0 (Fig. 23). The results of the modification of the tryptophyl residues and disulfide bonds lead us to the conclusion that conformational changes of the constant and variable halves begin to occur simultaneously from the same urea concentration (2 M) and that the constant half is completely unfolded at 4 or 5 M urea while a consid-

erable portion of the variable half remains folded, especially the portion which contains the disulfide bond.

As described above, it was shown that there exists a stable intermediate in the denaturation process of κ and λ proteins by GuHCl. It was demonstrated that the constant half of λ proteins is first disrupted by GuHCl and the intermediate is well characterized as the molecule in which variable half remains folded as it is in the native state and the constant half is completely unfolded. In the case of κ proteins, however, the stable intermediate has not been adequately characterized. The intermediate state observed during the denaturation of κ proteins by GuHCl may be similar to that observed for the urea denaturation described above.

At pH 2.1, where acid denaturation of Ta protein is complete (See, IV-4-3), a further increase in levorotation is observed on addition of urea (Fig. 23). As will be described in a subsequent section, the transition of Ta protein at low pH's reflects a conformational change of the constant half. Thus, the transition curve at pH 2.1 shown in Fig. 23 should mainly represent a conformational change of the variable half.

As can be seen from Figs. 33 and 34, the changes in the values of $[m']$ at 250 nm and $\Delta \mathcal{E}$ at 293 nm for Ni and Fu proteins begin to occur above 2 M urea. In the case of Ni protein, the changes in the values of $[m']$ and $\Delta \mathcal{E}$ occur in more than two stages, and the first stage

appears between 2 and 4 M urea. The CD measurements also confirm the presence of an intermediate in the course of urea denaturation. The CD band at 233-237 nm first increases from 2 to 4 M urea and then decreases. Similar change was also observed for the denaturation of Ni protein by GuHCl. In the case of denaturation by GuHCl, it was demonstrated that the positive CD band at 233 nm of Ni protein is originated from tryptophyl or tyrosyl residue in the variable half. The finding that the CD band at 233 nm increases from 2 to 4 M urea indicates that the constant half of the Ni protein molecule, which has the effect of reducing this CD band in the native state, is disrupted first by urea. However, the change in the value of $[\theta]$ at 233-237 nm on going from 2 to 4 M urea is smaller than that observed for the denaturation by GuHCl. This indicates that a conformational change of the variable half begins to occur prior to completion of the unfolding of the constant half. The change in the reactivity of the disulfide bonds of Ni protein in the presence of urea is quite different from the change in the optical rotation and absorption, and occurs in the urea concentration range where no change is observable in the latter properties (Fig. 33). Similar change is also observed for Fu protein (Fig. 34). This is quite different from the disulfide bond reactivity of type K Ta protein in which the change in the reactivity of the disulfide bonds parallels that of the optical rotation (Figs. 23 and 29). In the case of Ni protein, almost one intrachain disulfide bond is reduced up to

2 M urea. This disulfide bond may be the intrachain bond located in the constant half. Above 3.5 M urea, the number of the disulfide bonds reduced increases again. The change in the reactivity of the disulfide bonds may reflect a small local conformational change in the region where they exist.

In the case of Fu protein, the transition obtained by optical rotation and absorption are sigmoidal and no intermediate is observed (Fig. 34). Both transitions parallel each other. The reactivity of the disulfide bonds increases in the urea concentration range where no changes in the optical rotation and absorption can be observed. These facts indicate that the stabilities of the variable and constant halves are not so different as in the case of Ni protein.

IV-4-3 pH Dependent Conformational Change

All the Bence Jones proteins studied undergo a conformational change at pH's below 4. It is shown that the conformation of immunoglobulin molecules changes below the same pH (75-78). At alkaline side, Ta protein undergoes denaturation above pH 10. The CD spectrum in the region of 230 to 210 nm first becomes deeper at pH 11.9 and then shallower as the pH is raised further, approaching the CD spectrum characteristic of the randomly-coiled polypeptide chain. As described in IV-1, the results of acid-base titration also showed that Ta protein is stable between pH 4 and 10 and conformational changes occur outside of this

region. Similar pH-stability of the conformation was also obtained by other Bence Jones proteins and immunoglobulins. Jirgensons (84) has found that the specific rotation at 589 nm for some Bence Jones proteins and human γ G-immunoglobulin is constant in the region between pH 4 and 10 and becomes more negative outside this region. Hamaguchi et al.(27) have shown that the Moffitt parameter a_0 of ORD of Fu protein (type λ) becomes more negative as pH rises above 10.

As shown in Fig. 35, the acid denaturation of type λ proteins (Fu and Ni) proceeds in two distinct stages. In the case of Ta protein (type κ), the transition obtained by optical rotation is sigmoidal. However, the results of difference spectra showed that the degree of exposure of tyrosyl and tryptophyl residues upon acid denaturation is different depending on pH (Figs. 36 and 37). These facts show that the acid denaturation of Bence Jones proteins of both antigenic types occurs in two or more stages like as GuHCl and urea denaturations. Because the acid denaturation proceeds to a large extent even in the earlier phase of the reaction, it was difficult to measure the rate constant of the denaturation precisely. However, the preliminary kinetic experiments on Ta and Fu proteins suggest the acid denaturation does not obey a first order reaction. The fact also suggests that there exists a stable intermediate in the acid transition of the Bence Jones proteins.

The results of difference absorption spectra show that one of the

two tryptophyl residues buried in the interior of the Bence Jones protein (Ta) molecule is exposed on acid denaturation. A complete exposure of the other tryptophyl residue is accomplished only after addition of urea. As has been described in the section of urea denaturation, the further change in the value of $[m']$ at 250 nm was observed by addition of urea to the solution at pH 2.1, where the transition by acid had been completed. Therefore, the acid-denatured Bence Jones protein molecules are not in the completely disordered state. Recently, Ghose (70) has studied the stabilities at pH 2.1 of the constant and variable halves obtained by limited tryptic digestion of a type κ protein, and shown that the constant half undergoes drastic unfolding whereas no unfolding is observed for the variable half. Thus, the transition curve of Ta protein in Fig. 35 should represent a conformational change of the constant half. Therefore, the tryptophyl residue which is exposed on acid denaturation should be located in the constant half of Ta protein.

As shown in Fig. 44, while the values of $[\theta]$ at 210 nm change below pH's 4, the values of $[\theta]$ at 233 nm first increase from pH 5 to 3.5, become constant and decrease below pH's 2.5 in the denaturation of Ni protein. The change in the ellipticity at 233 nm on going from pH 5.4 to 3.5 was about $300 \text{ degrees cm}^2 \text{ dmole}^{-1}$. The similar change of this CD band was observed in the course of denaturation of Ni protein by GuHCl and urea. In the case of denaturation by GuHCl, it was suggested

that the CD band at 233 nm was originated from a tryptophyl or tyrosyl residue in the variable half, and the increase of this band was a consequence of disruption of the constant half. Therefore, it may be concluded that the constant half of λ proteins is first disrupted in the acid denaturation as well as in the GuHCl denaturation.

The CD spectra obtained in the present study and those obtained by Ikeda et al.(20) show that, while the CD spectra of type χ proteins have a positive extremum between 293 and 297 nm and have no CD band at around 300 nm, the CD spectra of type λ proteins have a positive extremum between 300 and 310 nm in addition to an extremum at around 295 nm. This reflects the difference in the state of tryptophyl residues between type χ and type λ proteins. A CD band at 300 to 310 nm has been observed for some proteins such as chymotrypsin (79), ovalbmin (80), bromelain (81), and lysozyme (82, 83) and has been attributed to tryptophyl residues. As described above (See, IV-2), it was suggested that Trp-187 in type λ proteins is exposed on the protein molecule and Trp-34 and 150 in type λ protein and Trp-35 and 148 in type χ proteins are buried in the interior of the protein molecules. These two buried tryptophyl residues for type χ and type λ proteins behave quite similarly in acid denaturation. The fact that type λ proteins have a CD band at 300 to 310 nm while type χ proteins have no CD band in this wavelength region, suggests that Trp-187 of type λ proteins is responsible for the presence of the CD band at 300 to 310 nm. This

conclusion was supported by the results of GuHCl denaturation of type λ proteins. The calculated CD spectra of the constant halves in the three type λ proteins have a CD band at 300nm. The CD band at 300 to 310 nm of Ni and Fu proteins change with pH in the region where no conformational change occurs (Fig. 41). This fact suggests that the exposed tryptophyl residue at position 187 interacts with closely spaced ionizable group. The replacements of amino acid which concern ionizable groups in the constant region is that of Lys and Asn at position 172 and Lys and Arg at position 190 which related to Oz factor. It is difficult to interpret the pH dependence of the CD band at 300 to 310 nm for Fu and Ni proteins in terms of the interaction of a tryptophyl residue and lysine or arginine residue, since the midpoint of the pH dependence lies near pH 6. Therefore, the pH dependence of the CD band would be interpreted in terms of Trp-187 and an ionizable groups which exist in the variable region. In the case of other type λ proteins, Sh and Ko, no change with pH was observed for the CD band at 300 to 310 nm. This fact suggests that Trp-187 of these proteins does not interact with ionizable group. However, it can not be overlooked that the replacements of amino acid residues in the constant half of λ proteins cause the local conformational change of this half, as was discussed in IV-3.

(1) Potentiometric and spectrophotometric titrations of a type χ Ta protein show that eighteen carboxyl, one α -amino and ten ϵ -amino groups have normal pK_{int} values. One of two imidazole groups has a normal pK_{int} value but the remaining one is masked in the interior of the protein molecule. Only one of the nine tyrosyl residues ionizes freely without any conformational change. From the change in the electrostatic interaction factor of the Linderström-Lang equation with pH, it was found that a conformational change occurs below pH 4.0 and above 10.2.

(2) Modification of the tyrosyl residues with N-acetylimidazole (NAI) shows that two type χ proteins and two of four type λ proteins had a tyrosyl residue which is acetylated at low concentrations of NAI. At higher concentrations of NAI, additional two tyrosyl residues were acetylated. Other two type λ proteins were exceptional; one had three and the other had five NAI-reactive tyrosyl residues. In the native state, no tryptophyl residue in a type χ protein (Ta) was modified with 2-hydroxy-5-nitrobenzyl bromide (HNB bromide). A type λ protein (Fu) had one HNB-bromide-reactive tryptophyl residue. In 6 M urea, all the tryptophyl residues (two for Ta protein and three for Fu protein) were modified. Difference absorption spectra showed that one of two buried tryptophyl residues of these proteins was exposed upon acid

denaturation and the other was exposed on further treatment of acid-denatured protein with 6 M urea. It was suggested that the tryptophyl residue which is located on the surface of the Fu protein molecule is Trp-187.

(3) Extrinsic Cotton effects of fluorescein mercuric acetate (FMA) conjugated with the cysteine residue produced by reduction of the interchain disulfide bond of Bence Jones protein were investigated. The extrinsic Cotton effects of FMA attached to κ Bence Jones proteins were similar to each other. In the case of λ Bence Jones proteins, however, the extrinsic Cotton effects were greatly different from specimen to specimen, reflecting difference in the environment of the COOH-terminal half of λ proteins.

(4) In the case of λ proteins, the constant half is first disrupted in the course of denaturation by GuHCl and the presence of an intermediate, in which the constant half is completely unfolded and the variable half remains to be folded, is observed. The results of urea denaturation of Ni protein also show that the variable half is more stable than the constant half in urea solution. On the other hand, for another type λ protein, Fu, no distinct difference is observed in the stabilities of the variable and constant halves in the denaturations by GuHCl and urea. In the acid denaturation of Fu protein, however, it was shown that one of two buried tryptophyl residues exposed.

In the case of χ proteins, an intermediate which appears in the course of the denaturation by GuHCl , has not been characterized as the state in which the constant half is completely unfolded and the variable half is completely folded. The results of urea denaturation of χ proteins suggest that in the intermediate which appears in the course of urea denaturation, both the constant and variable halves are disrupted by urea but the region in which the intrachain disulfide bond in the variable half is located remains intact. Acid denaturation of type χ proteins accompanies exposure of one of the two buried tryptophyl residues. The tryptophyl residue which is exposed on acid denaturation should be located in the constant half. Therefore, it may conclude that the variable halves both χ and λ proteins so far studied are more stable against denaturing agents than the constant halves. (See Fig's 56 and 57).

A schematic representation of the denaturation of type λ Bence Jones proteins

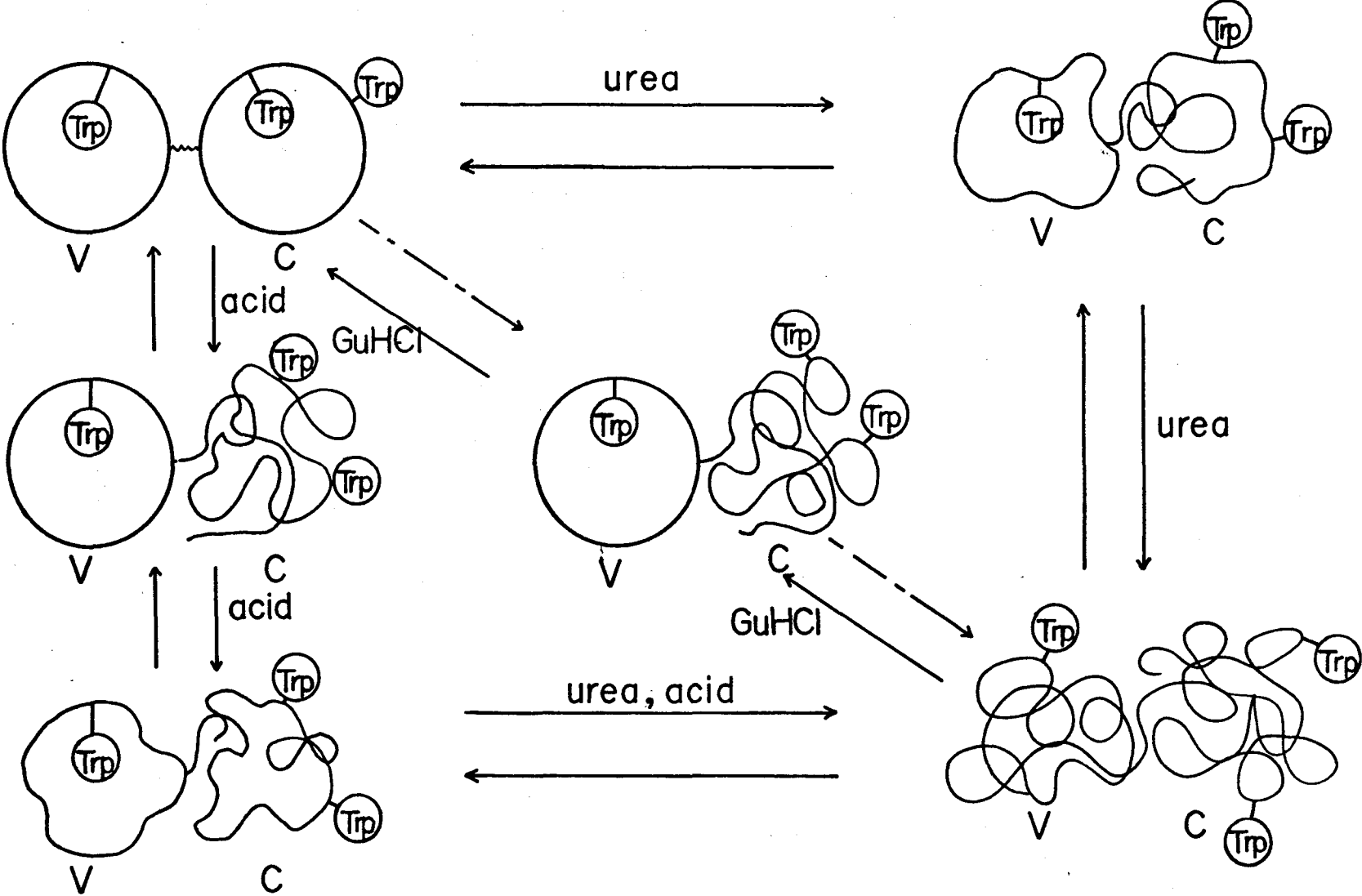


Figure 56

A schematic representation of the denaturation of type κ Bence Jones proteins

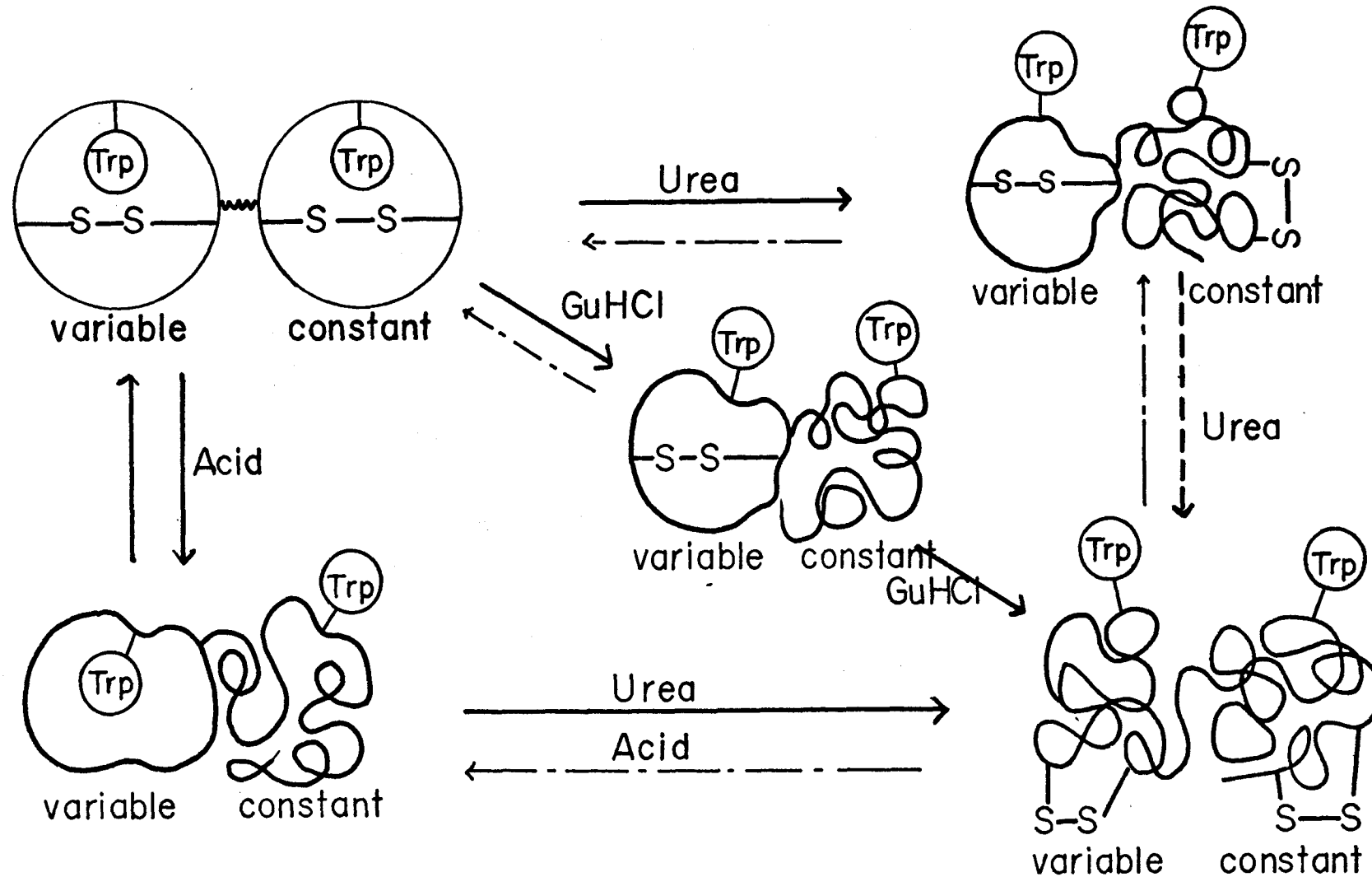


Figure 57

ACKNOWLEDGEMENT

The author would like to express appreciation to Professor Kozo Hamaguchi, Osaka University, for his kind guidance, many valuable suggestions and continuous encouragement during the course of this work. The author is greatly indebted to Professor Shunsuke Migita, Kanazawa University, for providing Bence Jones proteins and to Dr. Kiyoshi Ikeda, Osaka University, for many valuable discussions.

The author would like to acknowledge the continuous encouragement of Professor Jiro Koyama, Hokkaido University. The author also thanks to Professor Katsuya Hayashi, Kyushu University, and to Professor Junzo Noguchi, Hokkaido University, for kind guidance in preparing subpapers.

REFERENCES

- (1) G.M. Edelman, J. Am. Chem. Soc., 81, 3155 (1959)
- (2) H.B. Jones, Phil. Trans. (London), 138, 55 (1848)
- (3) G.M. Edelman and J.A. Gally, J. Exptl. Med., 116, 207 (1962)
- (4) M. Mannik and H.G. Kunkel, J. Exptl. Med., 116, 859 (1962)
- (5) S. Migita and F.W. Putnam, J. Exptl. Med., 117, 81 (1963)
- (6) L. Korngold and R. Lipari, Cancer, 9, 262 (1956)
- (7) J.F. Heremans, M.T. Heremans, and H.F. Schultze, Clin. Chem. Acta, 4, 96 (1959)
- (8) M. Heiderberger and K.D. Pederson, J. Exptl. Med., 65, 393 (1937)
- (9) D.S. Rowe and J.L. Fahey, J. Exptl. Med., 121, 171 (1965)
- (10) K. Ishizaka and T. Ishizaka, J. Immun., 99, 1187 (1967)
- (11) F.M. Putnam, K. Titani, M. Wikler, and T. Shinoda, Cold. Spring Harbor Symp. Quant. Biol., 32, 9 (1967)
- (12) F.M. Putnam and A. Miyake, J. Biol. Chem., 227, 1083 (1957)
- (13) J.A. Gally and G.M. Edelman, J. Exptl. Med., 119, 817 (1964)
- (14) Van Eijk, H.G. Monfoort, and H.G.K. Westenbrink, Koninkl. Ned. Akad. Wetenschap. Proc. Series C., 66, 363 (1963)
- (15) F.W. Putnam and P. Stelos, J. Biol. Chem., 203, 347 (1953)
- (16) A. Holasek, I. Pascher, and H. Hauser, Monatsch. Chem., 92, 463 (1961)

- (17) A. Holasek, O. Kratky, P. Mittelbach, and H. Wawra, *J. Mol. Biol.*, 7, 321 (1963)
- (18) K. Hamaguchi and S. Migita, *J. Biochem.*, 56, 512 (1964)
- (19) B. Jirgensons, S. Saine, and D.L. Ross, *J. Biol. Chem.*, 241, 2314 (1966)
- (20) K. Ikeda, K. Hamaguchi, and S. Migita, *J. Biochem.*, 63, 654 (1968)
- (21) B. Jirgensons, *J. Biol. Chem.*, 240, 1064 (1965)
- (22) M. Winkler and P. Doty, *Biochim. Biophys. Acta*, 54, 448 (1961)
- (23) P.K. Sarker and P. Doty, *Proc. Natl. Acad. Sci. U.S.*, 55, 981 (1968)
- (24) R.E. Cathou and T.C. Werner, *Biochemistry*, 9, 3149 (1970)
- (25) K.E. Neet and F.W. Putnam, *J. Biol. Chem.*, 241, 2320 (1966)
- (26) K. Hamaguchi and S. Migita, *J. Biochem.*, 56, 512 (1964)
- (27) K. Hamaguchi, H. Sakai, and S. Migita, *J. Biochem.*, 62, 46 (1967)
- (28) G.M. Edelman and W.E. Gall, *Ann. Rev. Biochem.*, 38 415 (1969)
- (29) G.M. Edelman, B.A. Cunningham, W.E. Gall, P.D. Gottlieb, U. Rutishauser, and M.J. Waxdal, *Proc. Natl. Acad. Sci. U.S.*, 63, 78 (1969)
- (30) H.F. Deutsch, *Science*, 141, 435 (1969)
- (31) D. Cioli and C. Baglioni, *J. Mol. Biol.*, 15, 385 (1966)
- (32) H.G. Van Eyk and K. Myszkowska, *Clin. Chim. Acta*, 18, 101 (1967)

- (33) M. Tan and W. Epstein, *J. Immunol.*, 98, 568 (1967)
- (34) A. Solomom, J. Killander, H.M. Grey, and H.G. Kunkel, *Science*, 151, 1237 (1966)
- (35) A. Solomon and C.L. McLaughlin, *J. Biol. Chem.*, 244, 3393 (1969)
- (36) I. Björk, F.A. Karlsson, and I. Berggard, *Proc. Natl. Acad. Sci. U.S.*, 68, 1707 (1971)
- (37) A.C. Ghose and B. Jirgensons, *Biochim. Biophys. Acta*, 251, 14 (1971)
- (38) A. Conway-Jacobs, B. Schechter, and M. Sela, *Biochemistry*, 9, 4870 (1970)
- (39) G.F. Fairclough, Jr. and B.L. Vallee, *Biochemistry*, 9, 4087 (1970)
- (40) G.F. Fairclough, Jr. and B.L. Vallee, *Biochemistry*, 10, 2470 (1971)
- (41) V. Reid, M. Glaser, R. Kennett, and S.J. Singer, *Proc. Natl. Acad. Sci. U.S.*, 68 1184 (1971)
- (42) A.B. Edmundson, M. Schffer, K.R. Ely, and M.K. Wood, *Biochemistry*, 11, 1822 (1972)
- (43) O. Epp, W. Dalm, H. Fehlhammer, A. Ruhlman, W. Steigeman, P. Schwager, and R. Huber, *J. Mol. Biol.*, 69, 315 (1972)
- (44) Y. Nozaki and C. Tanford, *J. Am. Chem. Soc.*, 89, 736 (1967)
- (45) D.E. Spackman, W.H. Stein, and S. Moore, *Anal. Chem.*, 30, 1190, (1958)

- (46) T.W. Goodwin and R.A. Morton, *Biochem. J.*, 40, 628 (1946)
- (47) G. Fasman, "Methods in Enzymology" ed. by S.P. Colowick and N.O. Kaplan, Academic Press Inc., New York, Vol. VI, p.928 (1963)
- (48) W. Kielly and W.F. Harrington, *Biochim. Biophys. Acta*, 41, 401 (1960)
- (49) D. Urry and J.W. Pettegrew, *J. Am. Chem. Soc.*, 89, 5276 (1967)
- (50) J.Y. Cassim and J.T. Yang, *Biochemistry*, 8, 1947 (1969)
- (51) J.F. Riordam, W.E.C. Wacker, and D.L. Vallee, *Biochemistry*, 4, 1758 (1965)
- (52) D.E. Koshland, Jr., Y.D. Karkhanis, and H.G. Latham, *J. Am. Chem. Soc.*, 86, 1448 (1964)
- (53) H.R. Horton and D.E. Koshland, Jr., *J. Am. Chem. Soc.*, 87, 1126 (1965)
- (54) N.B. Oza and C.J. Martin, *Biochem. Biophys. Res. Commun.*, 26, 7 (1967)
- (55) G.L. Ellman, *Arch. Biochem. Biophys.*, 82, 70 (1959)
- (56) I.M. Klotz and J. Avers, *J. Am. Chem. Soc.*, 79, 4078 (1957)
- (57) F. Karush, N.R. Klinman, and R. Marks, *Anal. Biochem.*, 9, 100 (1964)
- (58) R.M. Dowben and S.H. Orkin, *Proc. Natl. Acad. Sci. U.S.*, 58, 2051 (1967)

- (59) O.H. Lowry, N.J. Rosebrough, A.L. Farr, and R.J. Randall, J. Biol. Chem., 193, 265 (1951)
- (60) C. Tanford, Advances in Protein Chem., 17, 69 (1962)
- (61) M.E. Noelken, C.A. Nelson, C.E. Buckley, and C. Tanford, J. Biol. Chem., 240 218 (1965)
- (62) Y. Nozaki and C. Tanford, J. Biol. Chem., 242, 4731 (1967)
- (63) B.K. Seon, O.A. Roholt, and D. Pressman, Biochim. Biophys. Acta, 200, 81 (1970)
- (64) C. Tanford, S.A. Swanson, and W.S. Shore, J. Am. Chem. Soc., 77, 6414 (1955)
- (65) M.J. Kronman, L. Cerankowski, and L.G. Holmes, Biochemistry, 4, 518 (1965)
- (66) J.W. Donovan, Biochemistry, 3, 67 (1964)
- (67) K. Ogasahara and K. Hamaguchi, J. Biochem., 61, 199 (1967)
- (68) D. Gibson, M. Levanon, and O. Smithies, Biochemistry, 10, 3114 (1971)
- (69) C. Tanford, Advances in Protein Chem., 23 121 (1968)
- (70) A.C. Ghose, Biochim. Biophys. Acta, 278, 337 (1972)
- (71) E.R. Simons and E.R. Blout, J. Biol. Chem., 243, 218 (1968)
- (72) A. Cosani, E. Peggion, A.S. Verdini, and M. Terbojevichi, Biopolymers, 6, 963 (1968)
- (73) M. Shiraki, Sci. Papers College of Gen. Education, Univ. of Tokyo, 19, 151 (1969)

- (74) K. Titani, E.J. Whitley, Jr., and F.W. Putnam, *J. Biol. Chem.*, 244, 3521 (1969)
- (75) R.A. Phelps and J.R. Carn, *Biochim. Biophys. Acta*, 23, 149 (1957)
- (76) J.T. Yang and J.F. Foster, *J. Am. Chem. Soc.*, 77, 2374 (1955)
- (77) H. Edelhoch, R.E. Lippoldt, and R.F. Steiner, *J. Am. Chem. Soc.*, 84, 2133 (1962)
- (78) H.J. Gould, T.J. Gill, III, and P. Doty, *J. Biol. Chem.*, 239, 2842 (1964)
- (79) G.D. Fasman, R.J. Foster, and S. Beychok, *J. Mol. Biol.*, 19, 240 (1966)
- (80) M.J. Gorbunoff, *Biochemistry*, 8, 2591 (1969)
- (81) T. Sakai, K. Ikeda, K. Hamaguchi, and T. Murachi, *Biochemistry*, 9, 1939 (1970)
- (82) K. Ikeda and K. Hamaguchi, *J. Biochem.*, 71, 265 (1972)
- (83) K. Ikeda, K. Hamaguchi, S. Miwa, and T. Nishina, *J. Biochem.*, 71, 371 (1972)
- (84) B. Jirgensons, *Arch. Biochem. Biophys.*, 48, 154 (1954)